

MODEL BASED CONTROL OF AMINE SWEETENING UNIT

A THESIS IN MECHATRONICS

Presented to the faculty of the American University of Sharjah
School of Engineering
in partial fulfillment of
the requirements for the degree

MASTER OF SCIENCES

By
JASIM AL HAMMADI
B.S. 1999

Sharjah, UAE
June, 2005

© 2005

JASIM AL HAMMADI

ALL RIGHTS RESERVED

MODEL BASED CONTROL OF AMINE SWEETENING UNIT

Jasim AL Hammadi, Candidate for the Master of Science Degree

American University of Sharjah, 2005

ABSTRACT

Many industrial processes often exhibit significant non-linear behavior, and amine sweetening unit comprising absorption and regeneration towers is a typical example of such chemical processing plants. Conventional linear control schemes based on rigorous mathematical models, implemented in sweetening units, show poor performance and lead to off-specification products. Therefore, the need for advanced controls based on non-linear model structure is required. The black-box approach of modeling and control an amine system using Artificial Neural Networks (ANNs) is studied in this thesis. As a first step, a rigorous model for steady state simulation of an amine unit in Abu Dhabi Gas Liquefaction Company (ADGAS) is developed. This model is used to study the effect of varying system operating and sizing parameters on H_2S and CO_2 sweet gas concentrations. Desired H_2S specification in the sweet gas can be maintained by operating the plant with low DEA concentration and/or low DEA solution temperature. In contrast, high solution concentration and/or high DEA temperature tends to increase CO_2 removal from the process gas. Then, dynamic analysis of amine sweetening plant is

conducted on the developed rigorous simulation model. It aims to prioritize the system controlling variables, namely; DEA solution flow rate, DEA solution temperature, and reboiler duty as per their speed of response on sweet gas quality. Dynamic profiles of H_2S sweet gas composition show that steam flow rate gives the shortest time constant among other controlling parameters. On the other side, CO_2 pick up is experienced to increase faster with the increase of DEA solution flow rate.

Non-linear amine process needs to be operated under tight performance specifications to meet product quality and satisfy environmental considerations. Non-linear predictive control appears to be a well suited approach for this kind of problems. Because Artificial Neural Networks (ANNs) can provide good empirical models of complex nonlinear processes, dynamic data extracted from HYSYS are used to model amine plant applying ANN technique. Two NN models are developed for H_2S and CO_2 separately because they expose different dynamic behavior when reacting with DEA solution. Feed-Forward Neural Networks (FNNs) are found to give very good match with rigorous plant data.

In this work, the MPC model based control strategy was applied to amine absorption plant with view to control H_2S and CO_2 composition in sweet gas. The FNN model is augmented in the MPC control structure as the plant model leads to NN-MPC. The performance of the proposed MPC structure under different model uncertainties has been investigated. The closed-loop performance and stability of the proposed NN-MPC depend on setting prediction and control horizons. Accordingly, it is desirable to minimize the performance objective determined by the cost functional using long horizons. However, from computational point of view using short horizons is preferred. The shorter the horizon, the less costly the solution of the on-line optimization problem.

CONTENTS

ABSTRACT	III
CONTENTS	V
FIGURES	VII
ACRONYMS	XII
ACKNOWLEDGMENTS	XIII
1.0 INTRODUCTION	1
1.1 OVERVIEW	1
1.2 RESEARCH OBJECTIVES	3
1.3 METHODOLOGY	4
1.7 STRUCTURE OF THE THESIS:	7
1.0 BACKGROUND	9
2.1 MODELING OF AMINE ABSORPTION UNIT:	9
2.2 MODEL PREDICTIVE CONTROL:	14
2.3 NON-LINEAR SYSTEM MODELING AND PREDICTION USING NEURAL NETWORKS:	18
2.4 NEURO-MPC CONTROLLERS FOR MIMO NON-LINEAR SYSTEMS:	21
3.0 SIMULATION OF AMINE SWEETENING UNIT	26
3.1 DESCRIPTION OF AMINE SWEETENING UNIT:	26
3.2 SIMULATION STRATEGY:	31
3.3 SENSITIVITY ANALYSIS OF STEADY STATE MODEL:	32
3.4 DYNAMIC SIMULATION:	47
4.0 NEURAL NETWORK MODELING FOR AMINE SWEETENING UNIT	59

4.1 INTRODUCTION:	59
4.2 OVERVIEW OF ARTIFICIAL NEURAL NETWORKS (ANNs):	59
4.3 TRAINING OF A NEURAL NETWORK	60
4.4 TRAINING AND VALIDATION OF ANN MODELS:	64
5.0 NEURO-MPC CONTROL OF AMINE SWEETENING UNIT MANIPULATOR.....	68
5.1 THE PRINCIPLES OF NON-LINEAR MODEL PREDICTIVE CONTROL:	74
5.2 MATHEMATICAL FORMULATION OF NON-LINEAR MPC:	76
5.3 SIMULINK MODEL OF THE AMINE SWEETENING UNIT:	77
5.4 TRAINING OF THE NN PREDICTIVE MODEL:	80
5.5 SIMULATION RESULTS OF NN-MPC:	90
6.0 CONCLUSION AND RECOMMENDATIONS	113
6.1 SUMMARY AND CONCLUSIONS:	113
6.2 RECOMMENDATIONS:	114
REFERENCES	116
APPENDICES	120
MATLAB CODE FOR FNN MODELING	120
ADGAS PROCESS FLOW DIAGRAMS (PFDs)	122
VITA	123

FIGURES

FIGURE 1.1 METHODOLOGY OF RESEARCH	5
FIGURE 2.1 EQUILIBRIUM BASED APPROACH OF TWO-FILM THEORY	9
FIGURE 2.2 MODEL COMPLEXITY WITH REGARD TO DESCRIPTION OF MASS TRANSFER AND CHEMICAL REACTION	10
FIGURE 2.3 RATE-BASED APPROACH OF TWO FILM THEORY	11
FIGURE 2.4 BASIC STRUCTURE OF MPC	16
FIGURE 2.5 SIMPLIFIED MPC SCHEME.....	23
FIGURE 3.1 DEA ABSORPTION SYSTEM.....	27
FIGURE 3.2 DEA REGENERATION SECTION	28
FIGURE 3.3 AMINE SYSTEM PARAMETERS.....	32
FIGURE 3.4 STEADY STATE MODEL DEVELOPED USING CHEMSHARE SIMULATOR	33
FIGURE 3.50 EFFECT OF H ₂ S/CO ₂ RATIO ON SWEET GAS QUALITY	43
FIGURE 4.1 STRUCTURE OF A NEURON	60
FIGURE 4.2 ONE HIDDEN LAYER FEED-FORWARD NETWORK.....	62
FIGURE 4.3 MULTILAYER FEED-FORWARD NETWORK.....	63
FIGURE 4.4 FEED-FORWARD BACK-PROPAGATION NETWORK.....	65
FIGURE 4.5 RIGOROUS Vs. ANN PLOT: NN MODEL OF 6 PLANT INPUTS AND 1 PLANT OUTPUT (CO ₂).....	72
FIGURE 5.1 BASIC PRINCIPLE OF MPC.....	74
FIGURE 5.2 SIMULINK MODEL OF PROPOSED MPC CONTROLLING H ₂ S OUTLET	78
FIGURE 5.3 SUB-BLOCK OF AMINE SWEETENING UNIT	78

FIGURE 5.4 SUB-BLOCK OF NN-MPC.....	79
FIGURE 5.5 SIMULINK MODEL OF PROPOSED MPC CONTROLLING CO ₂ OUTLET	79
FIGURE 5.6 LEARNING CURVE: NN MODEL RELATING DEA FLOW & H ₂ S	81
FIGURE 5.7 TRAINING DATA: NN MODEL RELATING DEA FLOW & H ₂ S	81
FIGURE 5.8 VALIDATION DATA: NN MODEL RELATING DEA FLOW & H ₂ S	82
FIGURE 5.9 NN MODEL RELATING DEA TEMPERATURE & H ₂ S	82
FIGURE 5.10 TRAINING DATA: NN MODEL RELATING DEA TEMP & H ₂ S	83
FIGURE 5.11 VALIDATION DATA: NN MODEL RELATING DEA TEMP & H ₂ S	83
FIGURE 5.12 LEARNING CURVE: NN MODEL RELATING REBOILER DUTY & H ₂ S	84
FIGURE 5.13 TRAINING DATA: NN MODEL RELATING REBOILER DUTY & H ₂ S.....	84
FIGURE 5.14 VALIDATION DATA: NN MODEL RELATING REBOILER DUTY & H ₂ S	85
FIGURE 5.15 LEARNING CURVE: NN MODEL RELATING DEA FLOW & CO ₂	85
FIGURE 5.16 TRAINING DATA: NN MODEL RELATING DEA FLOW & CO ₂	86
FIGURE 5.17 VALIDATION DATA: NN MODEL RELATING DEA FLOW & CO ₂	86
FIGURE 5.18 LEARNING CURVE: NN MODEL RELATING DEA TEMPERATURE & CO ₂	87
FIGURE 5.19 TRAINING DATA: NN MODEL RELATING DEA TEMPERATURE & CO ₂	87
FIGURE 5.20 VALIDATION DATA: NN MODEL RELATING DEA TEMP & CO ₂	88
FIGURE 5.21 LEARNING CURVE: NN MODEL RELATING REBOILER DUTY & CO ₂	88
FIGURE 5.22 TRAINING DATA: NN MODEL RELATING REBOILER DUTY & CO ₂	89
FIGURE 5.23 VALIDATION DATA: NN MODEL RELATING REBOILER DUTY & CO ₂	89
FIGURE 5.24 DYNAMIC PROFILE OF DEA FLOW RATE IN RESPONSE TO STEP CHANGE IN FEED FLOW RATE (SHORT HORIZON OF H ₂ S NN-MPC)	93
FIGURE 5.25 DYNAMIC PROFILE OF DEA TEMPERATURE IN RESPONSE TO STEP CHANGE IN FEED FLOW RATE (SHORT HORIZON OF H ₂ S NN-MPC)	93

FIGURE 5.26 DYNAMIC PROFILE OF REBOILER DUTY IN RESPONSE TO STEP CHANGE IN FEED FLOW RATE (SHORT HORIZON OF H ₂ S NN-MPC)	94
FIGURE 5.27 DYNAMIC PROFILE OF H ₂ S SWEET GAS CONCENTRATION IN RESPONSE TO STEP CHANGE IN FEED FLOW RATE FOR NN-MPC WITH SHORT HORIZON	95
FIGURE 5.28 DYNAMIC PROFILE OF DEA FLOW RATE IN RESPONSE TO STEP CHANGE IN FEED FLOW RATE (LONG HORIZON OF H ₂ S NN-MPC)	95
FIGURE 5.29 DYNAMIC PROFILE OF DEA TEMPERATURE IN RESPONSE TO STEP CHANGE IN FEED FLOW RATE (LONG HORIZON OF H ₂ S NN-MPC)	96
FIGURE 5.30 DYNAMIC PROFILE OF REBOILER DUTY IN RESPONSE TO STEP CHANGE IN FEED FLOW RATE (LONG HORIZON OF H ₂ S NN-MPC)	96
FIGURE 5.31 DYNAMIC PROFILE H ₂ S SWEET GAS CONCENTRATION IN RESPONSE TO STEP CHANGE IN FEED FLOW RATE FOR NN-MPC WITH LONG HORIZON	97
FIGURE 5.32 DYNAMIC PROFILE OF DEA FLOW RATE IN RESPONSE TO STEP CHANGE IN H ₂ S FEED MOLE FRACTION (SHORT HORIZON OF H ₂ S NN-MPC)	98
FIGURE 5.33 DYNAMIC PROFILE OF DEA TEMPERATURE IN RESPONSE TO STEP CHANGE IN H ₂ S FEED MOLE FRACTION (SHORT HORIZON OF H ₂ S NN-MPC)	98
FIGURE 5.34 DYNAMIC PROFILE OF REBOILER DUTY IN RESPONSE TO STEP CHANGE IN H ₂ S FEED MOLE FRACTION (SHORT HORIZON OF H ₂ S NN-MPC)	99
FIGURE 5.35 DYNAMIC PROFILE OF H ₂ S SWEET GAS CONCENTRATION IN RESPONSE TO STEP CHANGE IN H ₂ S FEED MOLE FRACTION (SHORT HORIZON OF H ₂ S NN-MPC)	99
FIGURE 5.36 DYNAMIC PROFILE OF DEA FLOW RATE IN RESPONSE TO STEP CHANGE IN H ₂ S FEED MOLE FRACTION (LONG HORIZON OF H ₂ S NN-MPC)	100
FIGURE 5.37 DYNAMIC PROFILE OF DEA TEMPERATURE IN RESPONSE TO STEP CHANGE IN H ₂ S FEED MOLE FRACTION (LONG HORIZON OF H ₂ S NN-MPC)	101
FIGURE 5.38 DYNAMIC PROFILE OF REBOILER DUTY IN RESPONSE TO STEP CHANGE IN H ₂ S FEED MOLE FRACTION (LONG HORIZON OF H ₂ S NN-MPC)	101

FIGURE 5.39 DYNAMIC PROFILE OF H ₂ S SWEET GAS CONCENTRATION IN RESPONSE TO STEP CHANGE IN H ₂ S FEED MOLE FRACTION (LONG HORIZON OF H ₂ S NN-MPC)	102
FIGURE 5.40 DYNAMIC PROFILE OF DEA FLOW RATE IN RESPONSE TO STEP CHANGE IN FEED FLOW RATE (SHORT HORIZON OF CO ₂ NN-MPC)	103
FIGURE 5.41 DYNAMIC PROFILE OF DEA TEMPERATURE IN RESPONSE TO STEP CHANGE IN FEED FLOW RATE (SHORT HORIZON OF CO ₂ NN-MPC)	103
FIGURE 5.42 DYNAMIC PROFILE OF REBOILER DUTY IN RESPONSE TO STEP CHANGE IN FEED FLOW RATE (SHORT HORIZON OF CO ₂ NN-MPC)	104
FIGURE 5.43 DYNAMIC PROFILE OF CO ₂ SWEET GAS CONCENTRATION IN RESPONSE TO STEP CHANGE IN FEED FLOW RATE (SHORT HORIZON OF CO ₂ NN-MPC)	104
FIGURE 5.44 DYNAMIC PROFILE OF DEA FLOW RATE IN RESPONSE TO STEP CHANGE IN FEED FLOW RATE (LONG HORIZON OF CO ₂ NN-MPC)	105
FIGURE 5.45 DYNAMIC PROFILE OF DEA TEMPERATURE IN RESPONSE TO STEP CHANGE IN FEED FLOW RATE (LONG HORIZON OF CO ₂ NN-MPC)	106
FIGURE 5.46 DYNAMIC PROFILE OF REBOILER DUTY IN RESPONSE TO STEP CHANGE IN FEED FLOW RATE (LONG HORIZON OF CO ₂ NN-MPC)	106
FIGURE 5.47 DYNAMIC PROFILE OF CO ₂ SWEET GAS CONCENTRATION IN RESPONSE TO STEP CHANGE IN FEED FLOW RATE (LONG HORIZON OF CO ₂ NN-MPC)	107
FIGURE 5.48 DYNAMIC PROFILE OF DEA FLOW RATE IN RESPONSE TO STEP CHANGE IN CO ₂ FEED MOLE FRACTION (SHORT HORIZON OF CO ₂ NN-MPC)	108
FIGURE 5.49 DYNAMIC PROFILE OF DEA TEMPERATURE IN RESPONSE TO STEP CHANGE IN CO ₂ FEED MOLE FRACTION (SHORT HORIZON OF CO ₂ NN-MPC)	108
FIGURE 5.50 DYNAMIC PROFILE OF REBOILER DUTY IN REPOSE TO STEP CHANGE IN CO ₂ FEED MOLE FRACTION (SHORT HORIZON OF CO ₂ NN-MPC)	109
FIGURE 5.51 DYNAMIC PROFILE OF CO ₂ SWEET GAS CONCENTRATION IN RESPONSE TO STEP CHANGE IN CO ₂ FEED MOLE FRACTION (SHORT HORIZON OF CO ₂ NN-MPC)	109

FIGURE 5.52 DYNAMIC PROFILE OF DEA FLOW RATE IN RESPONSE TO STEP CHANGE IN CO ₂ FEED MOLE FRACTION (LONG HORIZON OF CO ₂ NN-MPC).....	110
FIGURE 5.53 DYNAMIC PROFILE OF DEA TEMPERATURE IN RESPONSE TO STEP CHANGE IN CO ₂ FEED MOLE FRACTION (LONG HORIZON OF CO ₂ NN-MPC).....	111
FIGURE 5.54 DYNAMIC PROFILE OF REBOILER DUTY IN RESPONSE TO STEP CHANGE IN CO ₂ FEED MOLE FRACTION (LONG HORIZON OF CO ₂ NN-MPC).....	111
FIGURE 5.55 DYNAMIC PROFILE OF CO ₂ SWEET GAS CONCENTRATION IN RESPONSE TO STEP CHANGE IN CO ₂ FEED MOLE FRACTION (LONG HORIZON OF NN-MPC)	112

ACRONYMS

AGRU	Acid Gas Removal Unit
ANN	Artificial Neural Networks
BP	Back-Propagation
CMAC	Cerebellar Model Articulation Control
DAE	Differential and Algebraic Equations
DEA	Diethanolamine
DMC	Dynamic Matrix Control
FNN	Feed-Forward Neural Network
GMDH	Group Method of Data Handling
LNG	Liquefied Natural Gas
LVQ	Learning Vector Quantisation
MBC	Model Based Control
MPC	Model Predictive Control
MLP	Multi-Layer Perceptron
MIMO	Multi Input Multi Output
NN	Neural Network
NNMPC	Model Predictive Control Based on a Neural Network Predictor
ODE	Ordinary Differential Equations
RNN	Recurrent Neural Network

ACKNOWLEDGMENTS

I would like to express my sincere thanks to my supervisors Dr. Nabeel Abdel Jabbar & Dr. Mohamed Jarrah for their patient supervision, concrete direction and instructive suggestion. Their enthusiasm, understanding and cheerful manner have made this work possible.

Many thanks are also given to Abu Dhabi Gas Liquefaction Company (ADGAS) for their approval on confidential plant data release and encouragement.

1.0 INTRODUCTION

1.1 Overview

According to the International Energy Agency (IEA), natural gas will have a major share in the future energy supply of the world. Crude (sour) natural gas contains, in addition to CH_4 and higher hydrocarbons, various amounts of H_2S , CO_2 and N_2 , as well as small amounts of gases such as He , O_2 , Ar , H_2 and H_2O vapor. The concentration of H_2S and CO_2 in natural gases and associated gases varies from a few percent to as high as 70-80 percent in certain reservoirs, particularly those with enhanced oil recovery (EOR). In these processes, H_2S and CO_2 are considered to be impurities that must be removed from industrial gases. The removal of H_2S from natural gas, known as gas sweetening, must be maximized to meet with pipeline specifications prior to its use in combustion applications. In addition, the removal of CO_2 from industrial gas streams has become important in the recent years. This has resulted from the environmental concern for a reduction of greenhouse gas emissions from industrial sources. Here, CO_2 is considered to be the largest contributor to the global warming problem, and is thus the major target for reduction.

The aqueous solutions of alkanolamines are considered the most commonly used sweetening agents in industrial plants. The amine process has been used commercially, since the early thirties. Monoethanolamine (MEA), diethanolamine (DEA), methyldiethanolamine (MDEA), diglycolamine (DGA), and diisopropanolamine (DIPA) are nowadays the most important alkanolamines used in absorption units for the removal of undesirable acid gases. Many industrial processes often exhibit significant non-linear

behavior, and amine sweetening unit comprising absorption and regeneration towers is a typical example in chemical processing plants. Because amine processes make transitions over the equilibrium points of the system, conventional linear control schemes cannot cope with system's non-linearity resulting in poor control performance.

Abu Dhabi Gas Liquefaction Company (ADGAS) is reportedly experiencing some opportunity losses of its main product (LNG) contributed by mal-performance of Acid Gas Removal Units (AGRUs). An alternative method to overcome problems associated with those linear controllers is to implement model-based control algorithms. Indeed, developing a valid dynamic model of a process is often the major part of the work required to implement advanced control strategies. A traditional approach to modeling is to develop a model from first principles and estimate the values of the model parameters from process data. However, this procedure is often difficult and/or costly because the process may not be well understood or is too complex to model. Furthermore, the developed model may be based on simplifying assumptions that degrade in accuracy, but is necessary in order to make it solvable for a real time application. An alternative approach to modeling is to identify the model non-parametrically from input/output data. Several non-parametric methods have been proposed to model non-linear systems. Artificial Neural Network (ANN) is one of the most commonly used non-parametric techniques in modeling and process control.

ANNs have been used widely in the area of chemical mass transfer processes. A packed distillation column was used to demonstrate the use of an ANN for MPC in a pilot plant at the University of Texas at Austin by J. C. MACMURRAY and D. M. HIMMELBLAU

in 1994. The column had the interesting feature of multiple changes in the sign of the process gains as the operating conditions changed. In addition, ANNs were used by R. Barrati, G. Vacca and A. Servida for modeling and control applications on two actual distillation columns: the butane splitter tower and the gasoline stabilizer. The two distillation columns are in operation at the SARAS refinery, Italy. In both applications, significant improvement in the operation of columns was recorded.

The main objective of this thesis is to utilize the concept of Neural Networks Model Predictive Controller (NN-MPC) in maintaining H_2S and CO_2 composition in the sweet gas stream exiting the amine absorption unit within desired specifications. Due to the difference in reaction rates of H_2S and CO_2 , separately, with DEA solution, two adaptive controllers are to be designed to cope with varying feed gas quality. Moreover, the controlling operating parameters of ADGAS amine absorption unit are to be scheduled as per their speed of response. This can be achieved by building steady state and dynamic models using adequate process flow sheet simulators.

1.2 Research Objectives:

1.2.1 Sensitivity Analysis of Operating & Sizing Parameters:

- The effect of varying system operating & sizing parameters on sweet gas quality is to be inspected on a steady state model of ADGAS Acid Gas Removal Unit. The model is to be developed using Cheshire Design II simulator
- Study cause-and-effect relationships between the input and output variables (i.e. effect of feed flow rate variation on sweet gas quality)
- Detect operating behavior of the system
- Re-sizing columns & existing packing characteristics

1.2.2 Modeling:

- Neural Network Modeling (NNM) technique is to be applied for obtaining a data-driven model of Amine sweetening unit
- Compare different frameworks & learning rules of Artificial Neural Networks to find out the best model representing the system
- Data is to be extracted from ASPENTECH chemical simulation software (HYSYS-Version 3.2)

1.2.3 Control:

- Designing Neural Networks- Model Predictive Controller (NN-MPC) utilizing data extracted from HYSYS dynamic model
- Due to the difference in the rate of reaction of H_2S and CO_2 , separately, with DEA solution, two adaptive controllers are to be designed to cope with varying feed gas quality

1.3 Methodology:

The general steps that will be used to navigate through this research, as demonstrated by Fig 1.1, are as follows:

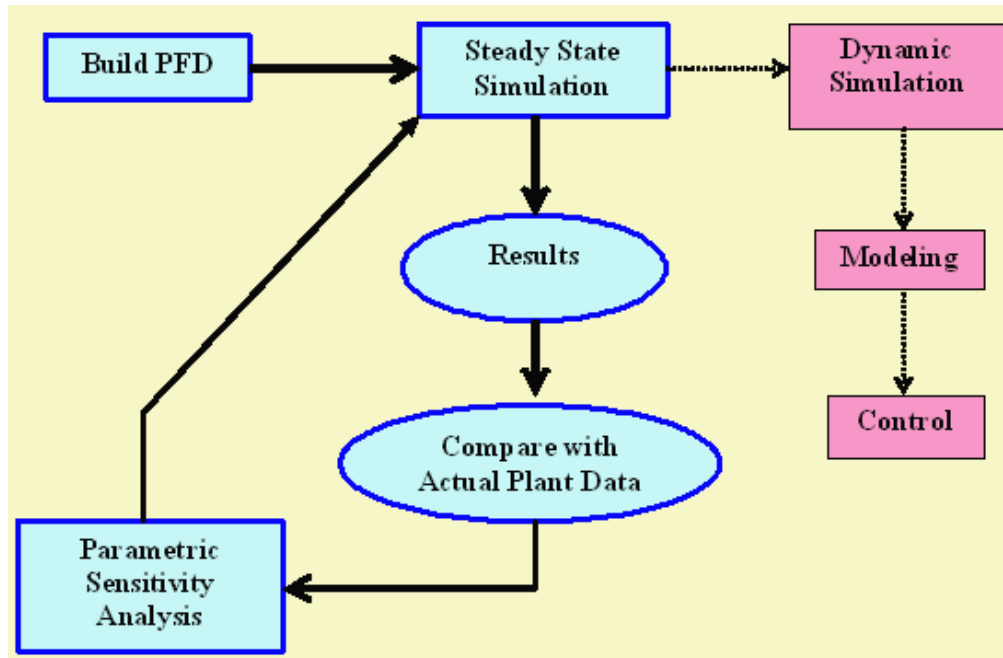


Figure 1.1 Methodology of research

1.3.1 Build Process Flow Diagram (PFD):

Process Flow Diagram (PFD) of ADGAS Train-3 Acid Gas Removal Unit is to be developed in the workspace of CHEMSHARE DESIGN II

1.3.2 Steady State Simulation:

A steady state model of the foregoing PFD is used to extract data. Those simulated data are compared with corresponding design data in order to minimize the error between them via tuning the steady state model

1.3.3 Sensitivity Analysis of Operating & Sizing Parameters:

Once the error between simulated & design data is minimized, the steady state model is used to inspect the effect of varying operating & sizing system parameters on sweet gas quality

1.3.4 Dynamic Simulation:

Because CHEMSHARE DESIGN II has only a steady state simulator, the dynamic simulation was carried out using ASPENTECH simulator (HYSYS-Version 3.2). The conditions of the converged model from step-2 were transferred into Process Simulation Diagram (PSD) of Amine unit in HYSYS. The steady state case was converted into dynamic one as follows:

1. Converting From Steady State:

To prepare the case for dynamic simulation, values will be installed to define pressure flow relations and PF specifications will be added to selected streams. The tray sizing utility will be implemented for sizing tray sections; all other unit operations will be sized.

2. Adding Controllers:

In this step, appropriate controllers will be installed and defined manually

3. Preparing the Dynamic Simulation:

In the last step, the Databook will be set-up. Changes will be made to key variables in the process and the dynamics behavior of the model will be observed.

1.3.5 Modeling & Control:

The Amine sweetening Unit is to be modeled using data-driven modeling technique (i.e. Artificial Neural Networks), and this model will be used to design a Non-linear Model Predictive Controller (NMPC) to adaptively re-schedule the system varying control gains

1.7 Structure of the Thesis:

This thesis is organized into six chapters. Chapter 1 presents a brief overview and outlines the proposed objectives of this research. The methodology applied in this report is introduced as well.

In Chapter 2, the fundamental aspects of neural networks are detailed. The general characteristics of a neural network have been summarized. This progresses on to listing the applications of ANNs in the area of chemical mass transfer processes to describe the extent of previous research on the topic. In addition, the theory of model predictive control is given. Because there is a colossal amount of intricate details within the fields of neural networks and model predictive control, this chapter aimed to give only overview of these two fields. In this chapter, physical modeling principles of chemical absorption processes are explained and the feasibility of applying model predictive controllers based on these linear models is given.

Chapter 3 deals with the setting up of an amine absorption simulation model. To investigate the parameters affecting directly the proposed control scheme, different system parameters are tested on a steady state model developed using a chemical process simulator (CHEMSHARE DESIGN-II) on data extracted from Abu Dhabi Gas Liquefaction Company (ADGAS) plant. The sensitivity analysis carried out on this steady state model will filter out those parameters with neglected effect on sweet gas

quality. In chapter 3, a dynamic model built in (HYSYS) is analyzed to prioritize those controlling parameters as per their speed of response. The outcome of this analysis will offer a zero-investment option to ADGAS in dealing with their mal-performance of their sweetening units.

In Chapter 4 the method of constructing an NN model of amine absorption dynamics for the MPC control is discussed. One approach of using an FNN for modeling the system forward dynamics is also provided. The FNN model is trained by using the data obtained from the amine unit's dynamic responses to a set of step changed inputs within specific operational ranges. The NN models relating sweet gas constituents and controlling parameters are introduced as well.

In chapter 5, the model-based control of amine sweetening process is performed by using the MPC method discussed in Chapter 2, based on the neural network modeling technique developed in Chapter 3. Two MPC controllers maintaining sweet gas quality at desired levels are designed by developing NN models relating plant outputs namely, H_2S and CO_2 with DEA solution flow rate, DEA temperature, and the regeneration reboiler duty. Finally in Chapter 6 the conclusions of this thesis are given and some recommendations are offered.

2.0 BACKGROUND

2.1 Modeling of Amine Absorption Unit:

Two physical modeling approaches for absorption processes are in common use: the equilibrium-based approach and the rate-based approach:

2.1.1 Equilibrium-Based Approach:

The equilibrium-based approach, as shown in Fig 2.1, is suitable for non-reactive systems. It assumes a theoretical stage in which the liquid and gas phases attain equilibrium. The performance of this stage is then adjusted by applying a tray efficiency correction factor. As, in practice, equilibrium is rarely attained since mass and heat transfer are actually rate processes that are driven by gradients of chemical potential and temperature, traditional equilibrium stage models and efficiency approaches are mostly inadequate for the description of chemisorption processes.

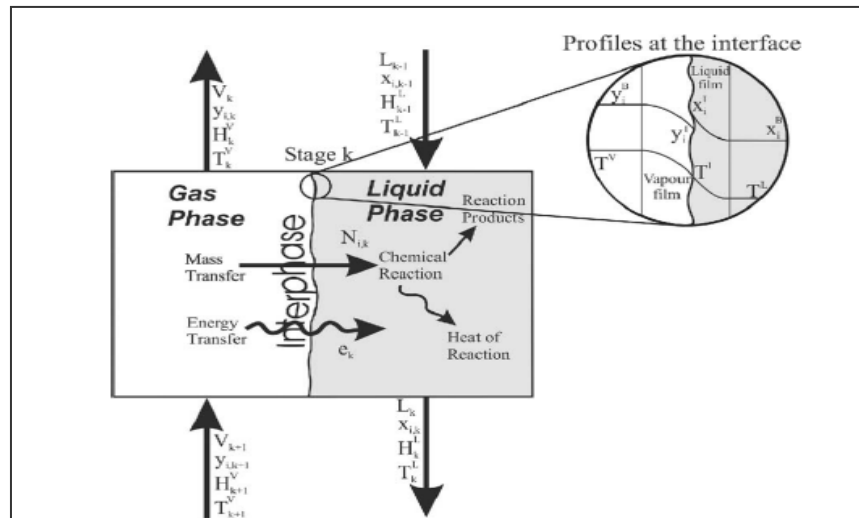


Figure 2.1 Equilibrium Based Approach of Two-Film Theory

2.1.2 Rate-Based Approach:

Accurate dynamic models for industrial reactive absorption processes have to be both rigorous enough in order to reflect the process complexity and simple enough to ensure feasibility of process simulations.

Fig 2.2 shows different modeling approaches representing different complexities concerning the description of mass transfer and chemical reaction are presented. A comparison among these modeling approaches revealed that traditional equilibrium stage models and efficiency approaches are inadequate in this context. Therefore, rigorous models describing multi-component mass transfer accompanied by chemical reactions in reactive separation processes have been developed which are based on the Maxwell_ Stefan equations [31]

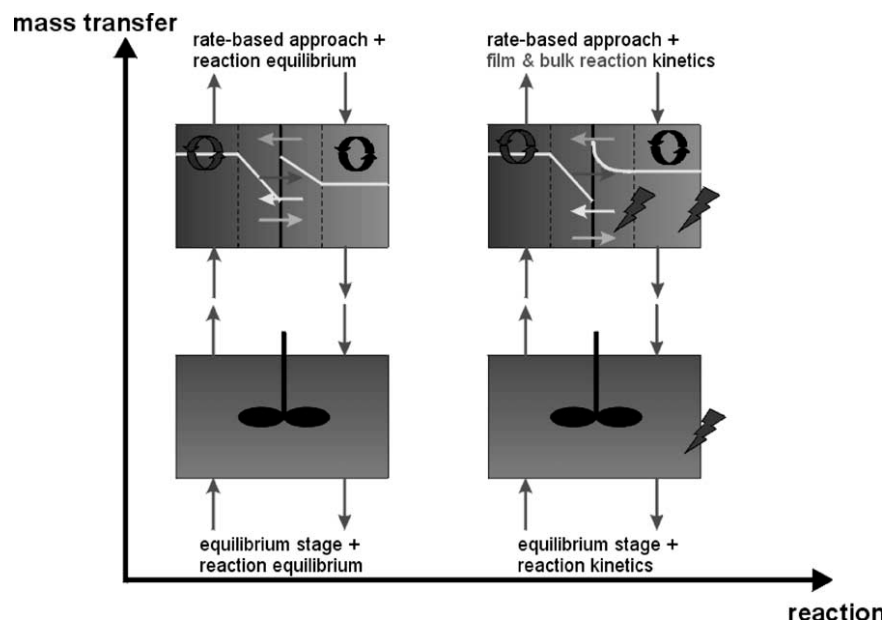


Figure 2.2 Model complexity with regard to description of mass transfer and chemical reaction

The two-film theory, as demonstrated in Fig 2.3, which is suitable for the description of mass transfer in complex reactive absorption processes [30] has been applied for the dynamic simulation of different systems of components [31]

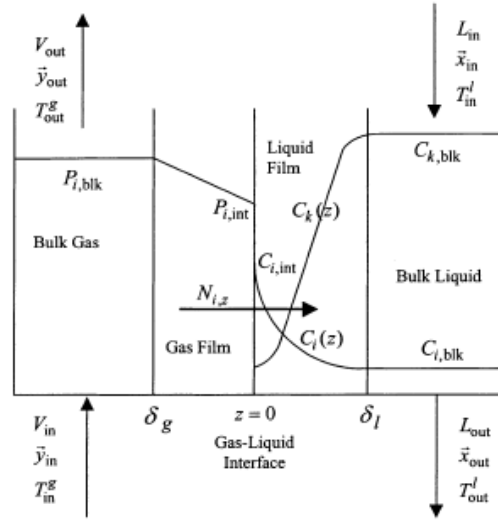


Figure 2.3 Rate-based approach of two film theory

This model takes into account diffusional interactions, the direct influence of chemical reactions on mass transfer and thermodynamic non-idealities and considers the impact of particular column internals on hydrodynamics. In contrast to classical two-film models, the chemical reaction kinetics and mass action laws are taken into account in the differential equations describing the liquid film region in order to avoid un-predictive correction parameters like enhancement factors. Although recent publications present approaches of enhancement factors for reversible and multi-step reactions, a general analytical expression could not be obtained and numerical techniques are required as well as simplifications such as irreversibility of reaction steps, equal diffusivities or limited reaction. The differential mass balance for the liquid film region leads to non-linear

concentration profiles and considers changing mass transfer rates along the film coordinate [30]:

$$\frac{1}{\delta^{lf}} \frac{dn_i^{lf}}{d\eta} - R_i^{lf} = 0; i = 1, \dots, m \quad (2.1)$$

Where:

n molar flux ($mol / m^2 s$)
 R gas constant ($8.3144 J / mol K$)
 δ film thickness (m)
 η film coordinate

Subscripts

i component index

Superscripts

lf liquid film

Additional driving forces in electrolyte systems are accounted for by the Nernst_ Planck equation including electrical potential gradients [30]:

$$n_i^{lf} = - \frac{c_i^{lf} D_{i,eff}^{lf}}{\delta^{lf}} \left(\frac{dx_i^{lf}}{d\eta} + x_i^{lf} z_i \frac{F}{RT} \frac{d\varphi}{d\eta} \right) + x_i^{lf} n_m^{lf}; \quad (2.2)$$

$i = 1, \dots, m$

Where:

c molar concentration (mol / m^3)
 D_{eff} effective diffusion coefficient (m^2 / s)
 F Faraday's constant ($9.65 \times 10^4 C / mol$)
 n molar flux ($mol / m^2 s$)
 R gas constant ($8.3144 J / mol K$)

T	temperature (K)
x	liquid mole fraction (mol / mol)
z_i	ionic charge of component i
η	film coordinate

Subscripts

i	component index
m	solvent
t	total

Superscripts

lf	liquid film
------	-------------

The condition of electro neutrality which has to be satisfied everywhere in the liquid phase is used for the determination of the electrical potential. All mass and energy balances, e. g. the component material balance for the liquid bulk phase, are dynamic and consider the relevant hold-ups in the liquid phase for dynamic simulations and control issues which leads to a system of partial differential equations [30].

Although recent publications present approaches of enhancement factors for reversible and multi-step reactions, a general analytical expression could not be obtained and numerical techniques are required. The investigation of the dynamic column behavior requires some model reductions as well as simplifications such as reversibility of reaction steps, equal diffusivities or limited reaction orders [34]. Those model reductions will limit the calculation time allowing simple dynamic model, but the full dynamic behavior of chemisorption system will not be reflected via those simplified models.

Obtaining numerical solution of the simplified dynamic model equations is considered the current technique in limiting the calculation time. A chemisorption process will result in a system of differential and algebraic equations (DAE), which its solution requires initial values for the differential variables. This DAE system has to be implemented into a numerical solver which converts the DAE system into ordinary differential equations (ODE) by differentiating all algebraic expressions. The necessary number of differentiations to get a set of differential equations defines the index of this DAE system. There are two obstacles encountered in applying numerical solution technique pertaining to reducing high index problems; Firstly, a careful analysis of the whole system of equations with the choice of suitable initial conditions is required. Secondly, numerical solution solvers require the DAE system to be represented in state space, and accordingly, preventing exclusive appearance of algebraic variables in differential equations. Therefore, the need for dynamical representative technique has risen to overcome the above mentioned disadvantages of rate-based modeling approach.

2.2 Model Predictive Control:

The incipient interest in the applications of MPC can be dated back to the late 1970s. In 1978, Richalet *et al* [27] presented the Model Predictive Heuristic Control (MPHC) method in which an impulse response model was used to predict the effect at the output of the future control actions. The control actions to be exerted on the system are determined by minimizing the error between the predicted and the desired outputs of the system, subject to the operation restriction [27]. In 1980, Culter and Ramaker proposed

the Dynamic Matrix Control (DMC) method in which a step response model was used [6]. During 1980s, MPC quickly became popular particularly in chemical process industry due to the simplicity of the algorithm and to the use of the impulse or step response model, which is preferred, as being more intuitive and requiring no previous information for its identification [13]. MPC has been used in over 2,000 industrial applications in the refining, petro-chemical, pulp and paper, and food processing industries [35]

The basic structure of the MPC is illustrated in Fig 2.4, in which a model is used to predict the future plant outputs, based on past and current values of plant status and on the proposed optimal future control actions. These control actions are calculated by the optimizer by taking into account the cost function (where the future tracking error is considered) as well as the constraints. The objective of the MPC is minimization of the predicted output errors by adjusting control actions over a given horizon.

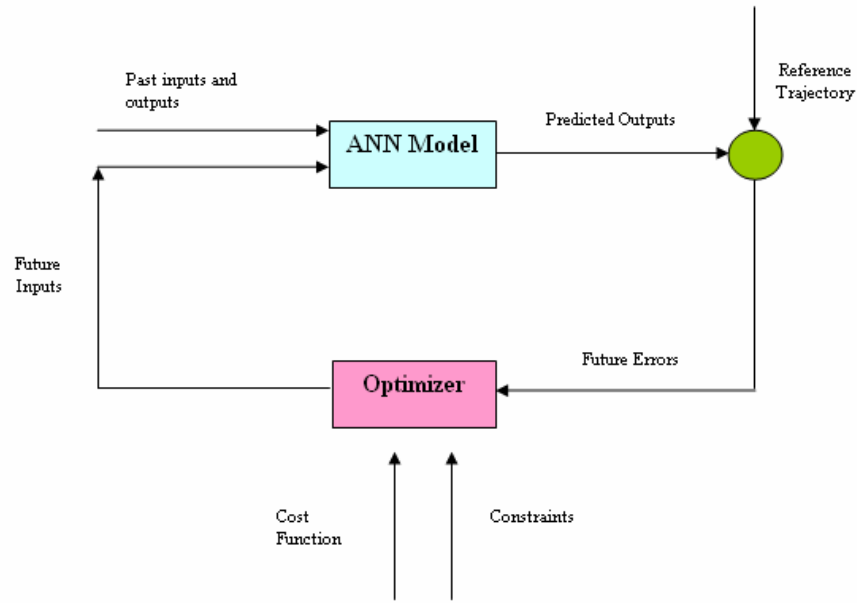


Figure 2.4 Basic Structure of MPC

As a consequence, the predictive model plays a decisive role in determining the optimal control actions. Therefore the chosen model must be capable of capturing the system's basic dynamic modes, so as to precisely predict the future outputs of the system. In addition, the model has to be simple enough to be implemented practically.

Many systems are, however, in general inherently nonlinear. This, together with higher product quality specifications and increasing productivity demands, tighter environmental regulations and demanding economical considerations in the process industry require operating systems closer to the boundary of the admissible operating region. In these cases, linear models are often inadequate to describe the process dynamics and nonlinear models have to be used. This motivates the use of nonlinear model predictive control. Until recently, most industrial applications have relied on linear dynamic models. These dynamic models have been developed using empirical data obtained from plant testing.

Linear, rather than non-linear, models have been used because of the difficulty in developing a generic non-linear model from empirical data and also because of the computational expense involved in using non-linear models in the MPC formulation.

2.2.1 Why Non-linear Model Predictive Control?

Several factors have contributed to the widespread use of MPC in the process industries:

- **Multivariate Control:** Industrial processes are typically coupled MIMO systems. The number of inputs and outputs can be large and the coupling can be significant. The MPC approach is well suited for MIMO applications.
- **Constraints:** Constraints on the inputs and outputs of a process due to physical constraints and safety considerations are common in the process industries. An example of a physical constraint is the upper limit of an actuator. An example of a safety constraint is an upper limit on the temperature in an exothermic reactor. These constraints can be directly integrated into the control calculation using MPC.
- **Sampling Period:** Unlike systems in other industries, such as automotive or aerospace, the open-loop settling time for most industrial processes is typically tens of minutes or hours rather than milliseconds. This relatively slow settling time translates to sampling periods measured in minutes. Because the sampling period is sufficiently long, the complex optimization calculations required to implement MPC can be solved at each sampling period.
- **Commercial Tools:** Commercial tools that facilitate model development and controller implementation have allowed the proliferation of MPC in the process industries. These tools allow the user to build dynamic models based on empirical data, tune the controller for robustness in a simulation environment, and implement the controller on

the process in real time. In addition to these tools, service organizations that implement these MPC solutions have proliferated.

2.3 Non-linear System Modeling and Prediction using Neural Networks:

Artificial Neural Network is a computational structure capable of representing the nonlinear functional relationship between input and output variables. There are a number of configurations of the network available, with many training algorithms for each representation. There are several reasons for the growing use of (ANNs) in the field of chemical engineering [19]. First, recent advances in computer technology and parallel processing have made the use of ANNs more economically feasible than in the past. Second, since ANNs are composed of nets of nonlinear basis functions, they have the ability to evolve good process models from example data and require little or no a priori knowledge of the task to be performed. Third, ANNs allow many of the ideas of system identification and adaptive control originally applied to linear (or linearized) systems to be generalized to cope with more severe non-linearity because they have an inherent ability to approximate any arbitrary non-linear function. Thus, ANNs provides a possible way to identify the model of a non-linear system effectively.

Based on their ability to learn sophisticated non-linear relationships, the effectiveness of ANNs has been successfully demonstrated by previous studies when employed to model complex non-linear systems [4,5,25,36,37,42]

ANNs generally consist of a number of interconnected processing elements called neurons. These processing elements are functions consisting of a summing junction and a non-linear operation (also known as activation function). How the neuron connections are arranged and the nature of the connections determine the structure of a network. How the strengths of the connections are adjusted or trained to achieve a desired overall behavior of the network, is governed by its learning algorithm. Thus ANNs can be classified according to their structures and learning algorithms.

In terms of their structures, ANNs can be divided into two major categories: feed-forwarded NNs (FNNs) and recurrent NNs (RNNs). FNN is the structure in which signals flow from the input layer to the output layer via unidirectional forward connections. The neurons are connected from one layer to the next, but not within the same layer. The most commonly used FNN is the Multi-layer Perceptrons (MLP) [26]. Others are the Cerebellar Model Articulation Control (CMAC) network [1], the Learning Vector Quantisation (LVQ) network [15], the Group Method of Data Handling (GMDH) network [15], Radial Basis Function (RBF) network [14]. It has been proven that a multilayer feed-forward network can approximate any non-linear relationship between the inputs and the outputs to any predefined accuracy. FNN will be discussed in more details in Chapter 4

RNN is another network structure in which the outputs of some neurons are fed back to the same neurons or to neurons in preceding layers. Signals can flow in both forward and

backward directions. The most notable RNN is the Hopfield network [16]. Some others are the Jordan network [21], the Elman network [8], and the time-lag network [41].

Good process models are essential for the implementation of most advanced control algorithms. Indeed, developing a valid dynamic model of a process is often the major part of the work required to implement advanced control strategies. A traditional approach to modeling is to develop a model from first principles and estimate the values of the model parameters from process data. However, this procedure is often difficult and/or costly because the process may not be well understood or is too complex to model. Furthermore, the developed model may be based on simplifying assumptions that degrade in accuracy, but is necessary in order to make it solvable for a real time application. An alternative approach to modeling is to identify the model non-parametrically from input/output data. Several non-parametric methods have been proposed to model non-linear systems. ANN is one of the most commonly used non-parametric techniques in modeling and process control.

Narendra and Parthasarathy (1990) and Hunt (1992) both present an overview of the issues pertaining to the use of ANNs for process modeling, identification, and control. There are two general approaches have been evolved in using ANNs for process modeling, identification, and control. One centers on using neural networks as the process controller. The network is trained to identify the inverse dynamics of the process to be controlled, and is then used to directly control the process. The other, and preferred, approach is to develop an ANN model of the process that in turn is then used for some

type of model based control such as model predictive control. This latter methodology is the more commonly reported application of neural networks for control of chemical processes.

Neural networks have the remarkable capability of capturing system dynamics and approximating the behavior of the plant under different operating conditions. They are used to estimate the unknown non-linear dynamics and to compensate for them [39]. They are cost-effective, easy to implement and data-driven. They have been implemented successfully in different modeling areas where non-linearity and complexity are major issues.

2.4 Neuro-MPC Controllers for MIMO Non-linear Systems:

To overcome the problems resulting from using linear models in the MPC, some researchers have tried to extend MPC to use non-linear models. The technique Joseph *et al.* used is to obtain a non-linear model through system analysis to help the control calculation arrive at an appropriate action [22]. The predictive methods using such non-linear models have also been made adaptive by estimating the parameters of the model that are most likely to change [22]. This requires the model to be of the correct structure, otherwise steady state offsets from the set points may result despite parameter adaptation. Selecting such an accurate structure requires significant analysis and a prior knowledge of the system. However, due to the complexity of the practical systems, or lack of knowledge of critical parameters of the systems, in many cases it is impossible to obtain a suitable physically founded system model in an analytical way.

An alternative method to overcome the above problems is to use ANNs as non-linear black box models to predict the dynamic behavior of the systems. There have also been many reports on using ANNs for non-linear system control. Psaltis *et al.* proposed general learning architectures to learn the plant inverse dynamics for the FNN based feed-forward controller [26]. Narendra and Parthasarathy developed generalized ANN models for both identification and control of non-linear systems. Hunt and Sbarbaro used ANNs for non-linear internal control [20]. Fang and Dissanayake used an NN in time-optimal trajectory planning [11]. An extensive review on applying ANNs to control has also been given by Hunt *et al.* [20]

2.4.1 Properties, Advantages, and Disadvantages of NMPC:

In general, using an infinite prediction and control horizon, i.e. T_p and T_c is desirable to minimize the performance objective determined by the cost. However, the open-loop optimal control is often formulated in a finite horizon manner and the input function is parameterized finitely, in order to allow a (real-time) numerical solution of the nonlinear open-loop optimal control problem. It is clear, that the shorter the horizon, the less costly the solution of the on-line optimization problem. Thus it is desirable from a computational point of view to implement MPC schemes using short horizons. But, when a finite prediction horizon is used, the actual closed-loop input and state trajectories will differ from the predicted open-loop trajectories, even if no plant models mismatch and no disturbances are present [34, 35]. This fact is depicted in Figure 6 where the system can only move inside the shaded area as state constraints of the form $x(\tau) \in X$ are assumed.

This makes the key difference between standard control strategies, where the feedback law is obtained a priori and

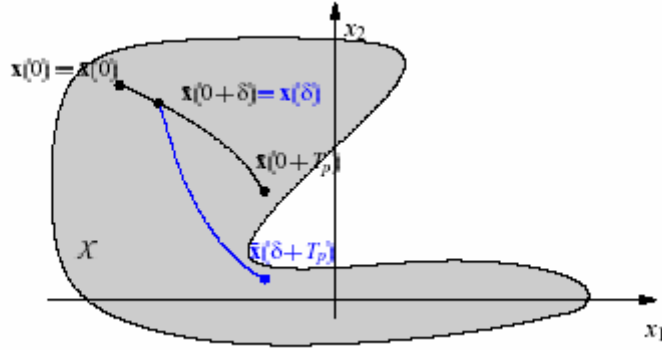


Figure 2.5 Simplified MPC Scheme

NMPC where the feedback law is obtained on-line and has two immediate consequences. Firstly, the actual goal to compute a feedback such that the performance objective over the *infinite horizon* of the closed loop is minimized is not achieved. In general it is by no means true that a repeated minimization over a *finite horizon objective* in a receding horizon manner leads to an optimal solution for the infinite horizon problem [29]. In fact, the two solutions differ significantly if a short horizon is chosen. Secondly, if the predicted and the actual trajectories differ, there is no guarantee that the closed-loop system will be stable. It is indeed easy to construct examples for which the closed-loop becomes unstable if a (small) finite horizon is chosen. Hence, when using finite horizons in standard NMPC, the stage cost cannot be chosen simply based on the desired physical objectives.

From the remarks given so far and from the basic NMPC setup, one can extract the following key characteristics of NMPC:

- NMPC allows the use of a nonlinear model for prediction.
- NMPC allows the explicit consideration of state and input constraints.
- In NMPC a specified performance criteria is minimized on-line.
- In NMPC the predicted behavior is in general different from the closed loop behavior.
- The on-line solution of an open-loop optimal control problem is necessary for the application of NMPC.
- To perform the prediction the system states must be measured or estimated.

The Non-linear Model Predictive Controller (NMPC) has been successfully applied on a packed column used for absorption process with partial state reference model, of an absorption packed column. The absorption column, being experimented, used a solution of Diethanolamine (DEA) as the absorbent to decrease the concentration of CO_2 in a gas mixture below a desired value. It is to be emphasized that MPC based on linear models is acceptable when the process operates at a single set point and the primary use of the controller is the rejection of disturbances. Because Amine absorption process make transitions over the non-linearity of the system, linear MPC often results in poor control performance. To properly control this process, a non-linear model is needed in the MPC algorithm.

In addition, there is on going PHD research at the University of Newcastle Upon Tyne-UK on absorption and de-sorption of Carbon Dioxide from Monoethanolamine (MEA) solutions using Higee Technology.

3.0 SIMULATION OF AMINE SWEETENING UNIT

This chapter describes ADGAS amine sweetening unit along its operating conditions. Steady state analysis of the process is conducted on the developed rigorous model. The effect of system operating parameters on H_2S and CO_2 sweet gas concentrations is inspected. Then, this steady state model is converted into dynamic model using process flow sheet simulator (HYSYS). Dynamic analysis of the process results in prioritizing the amine unit controlling parameters, namely; DEA solution flow rate, DEA solution temperature, and reboiler duty as per their speed of response. This offers ADGAS a viable alternative to maintain throughput across their facilities at desired rate despite any feed disturbance.

3.1 Description of Amine Sweetening Unit:

The general process flow for an amine sweetening plant is demonstrated in the simplified process schematics released from ADGAS plant. Fig 3.1 shows the absorption section, whereas Fig 3.2 shows the regeneration section. The process flow scheme varies little, regardless of the aqueous amine solution used as the sweetening agent. The Diethanolamine, due to its reactivity and availability at low cost, is the most generally accepted and widely used of the many available alkanolamines solvents for removal of H_2S and CO_2 from natural gas streams. The primary pieces of equipment of concern are the absorber column and stripper column, together with the associated piping, heat exchange, and separation equipment.

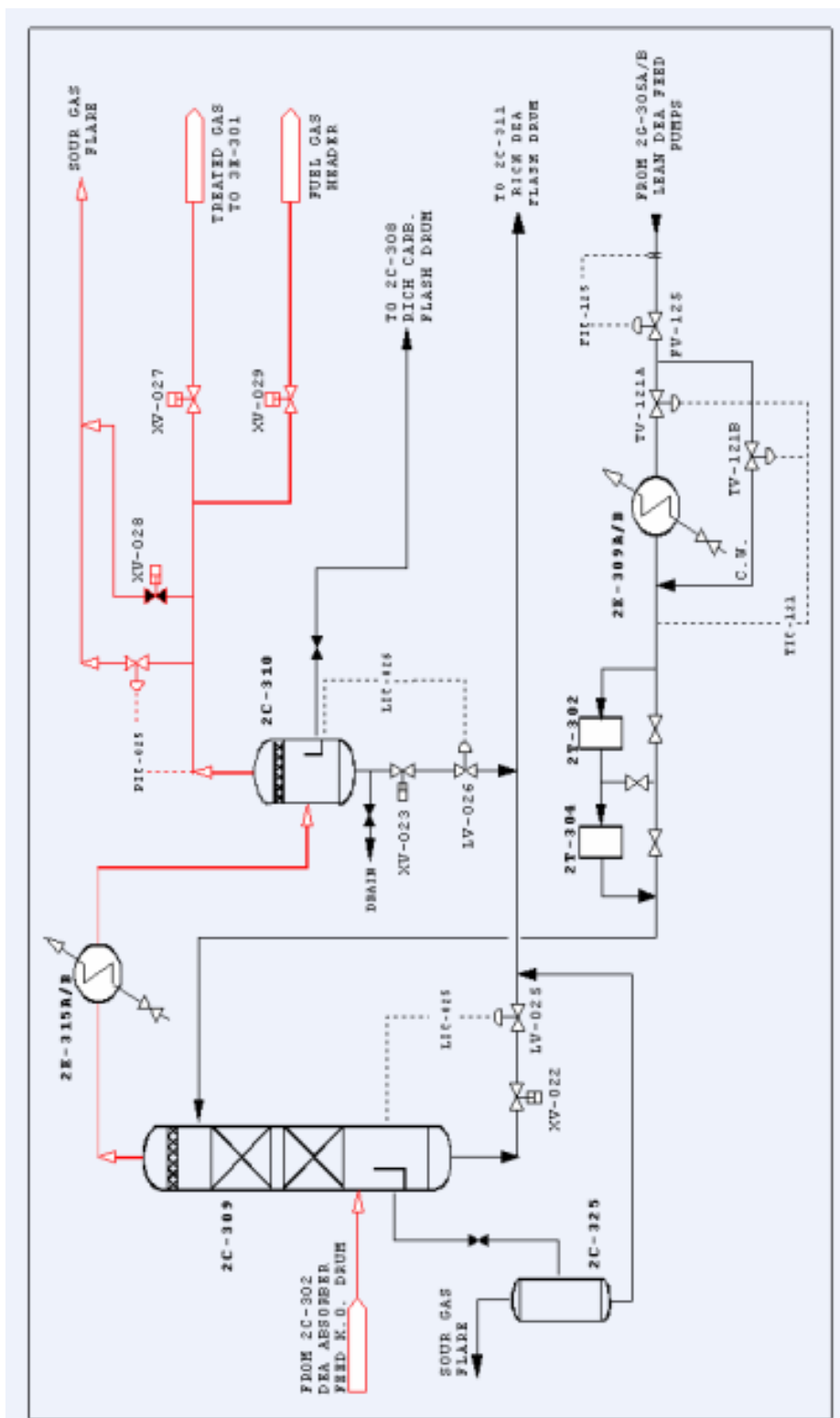


Figure 3.1 DEA absorption system

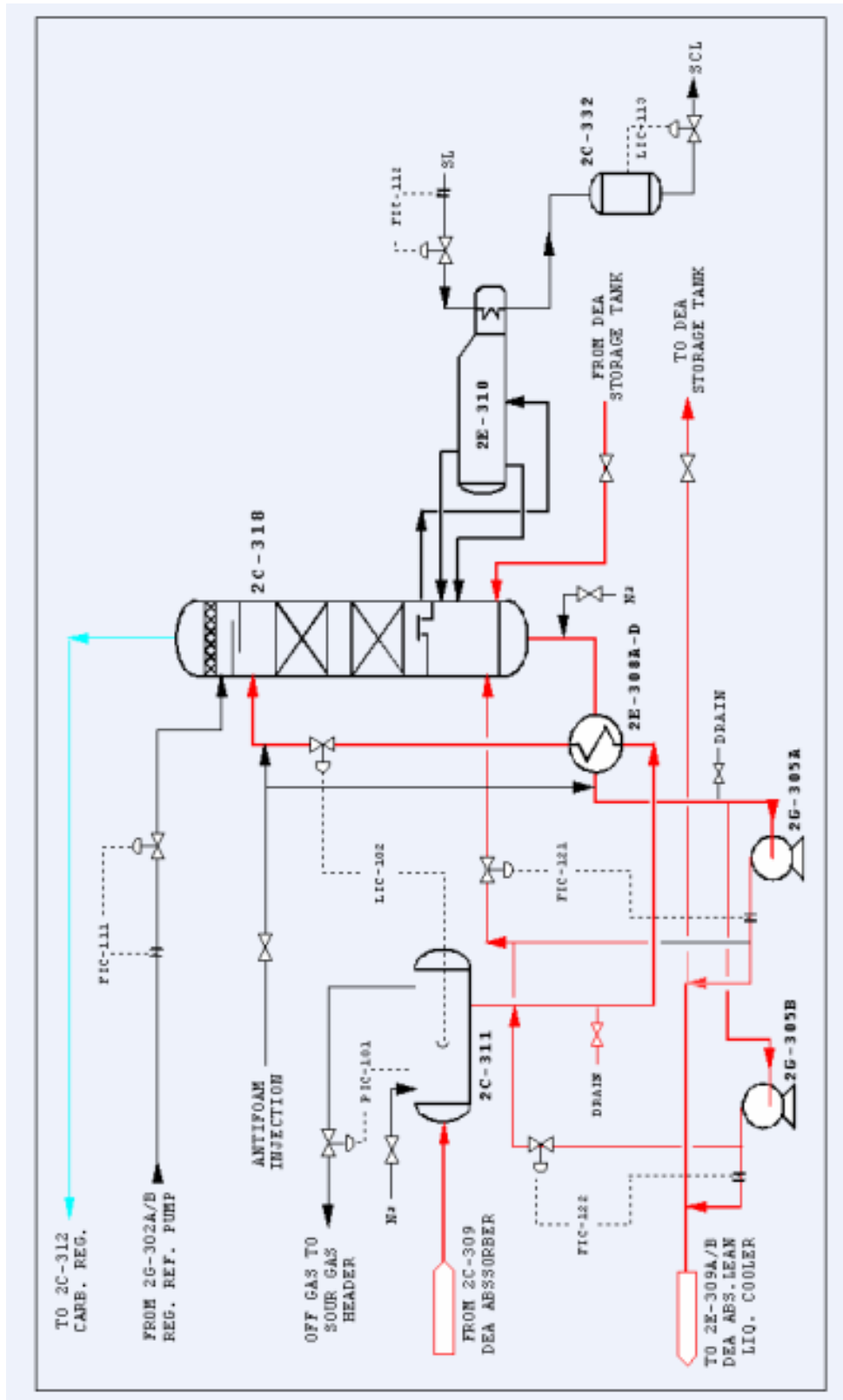


Figure 3.2 DEA regeneration section

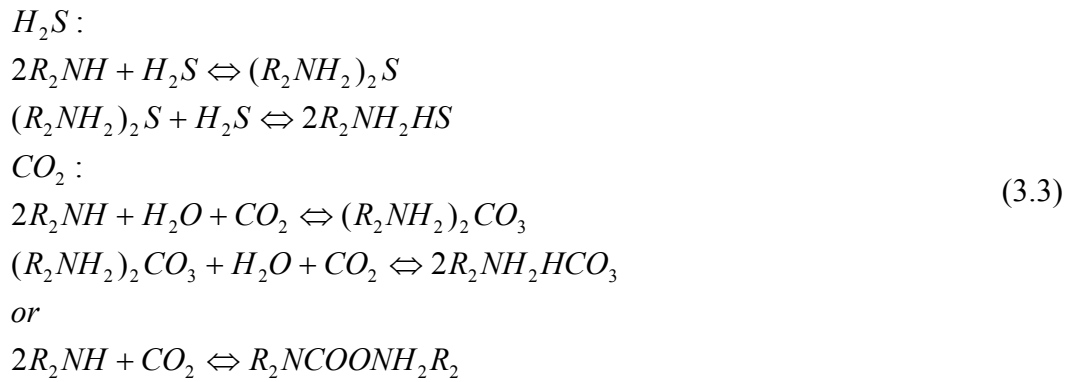
The sour gas containing H_2S and/or CO_2 will nearly always enter the plant through a scrubber to remove any free liquids and/or entrained solids. The sour gas then enters the bottom of the absorber column and flows upward through the absorber in intimate counter-current contact with the aqueous amine solution. Sweetened gas leaves the top of the absorber and flows to a dehydration unit before being considered ready for sale.

Lean amine solution from the bottom of the stripper column is pumped through an amine-amine heat exchanger and then through a water or air-cooled exchanger before being introduced to the top of the absorber column. The amine moves downward through the absorber counter-current to the sour gas, and absorbs acid gas constituents from the gas stream. Rich amine solution flows from the bottom of the absorber through the amine-amine heat exchanger and then to the top of the stripper column.

The amine-amine heat exchanger serves as a heat conservation device and lowers total heat requirements for the process. A part of the absorbed acid gases will be flashed from the heated rich solution on the top of the stripper. The remainder of the rich solution flows downward through the stripper in counter-current contact with vapor generated in the reboiler. The reboiler vapor (primarily steam) strips the acid gases from the rich solution. The acid gases and the steam leave the top of the stripper and pass overhead through a condenser, where the major portion of the steam is condensed and cooled. The acid gases are separated in a separator and sent to the flare or to processing. The condensed steam is returned to the top of the stripper as reflux.

Rich amine solution leaves the bottom of the absorber at an elevated temperature due to the heat of reaction released when acid gases react with the amine. For this reason heat exchange on the lean amine solution in the amine-amine exchanger does not cool it sufficiently for many processes. The amine cooler serves to lower the lean amine temperature to the 100°F range. Higher temperatures on the lean amine solution will result in excessive amine losses through vaporization and also lower acid gas carrying capacity in the solution because of temperature effects

The primary reactions of the diethanolamine with H_2S and CO_2 are:



Important to note is the presence of water or steam on the left-hand side of both the carbon dioxide reactions. This presence of water undoubtedly accounts for the fact that carbon dioxide is much more difficult to strip from the alkanolamine solutions by steam than is H_2S .

The reactions shown above proceed to the right at low temperatures and to the left at higher temperatures. This is the reason that hydrogen sulfide and carbon dioxide can be absorbed by alkanolamine solutions at ambient temperatures. At elevated temperatures

(as exist in the stripper column) the reactions are reversed with the sulfide and carbonate salts being decomposed and the acid gases released in the stripper column

3.2 Simulation Strategy:

Steady-state simulation has been a useful tool for the design and rating of single process equipment, as well as for complete plants. Even for day-to-day plant operations, steady state simulation has been stretched to its maximum by applying it to extract process information and operating conditions that might be evolving with time.

Dynamic simulation is the tool of choice to reproduce the expected behavior of still-to-be-built plants, as well as to match the operating conditions of already functioning assets. Notwithstanding, the immediate advantage that can be anticipated in implementing a dynamic simulation in real plants is the testing and checking of process control strategies. That is the reason why the first process industries that have incorporated dynamic simulation as a common working tool have been the oil-and-gas and refining ones, where controlling and maintaining the productive processes inside a very thin operating interval ensures a continuous flow of on-spec product, crucial aspect of such low added value type of industries. In this section, analysis is conducted on developed steady state and dynamic rigorous models of ADGAS amine sweetening unit. The controlling parameters are the DEA solution flow rate, DEA solution temperature, and reboiler duty. The disturbing parameters are the feed flow rate, H_2S and CO_2 mole fractions in the feed gas.

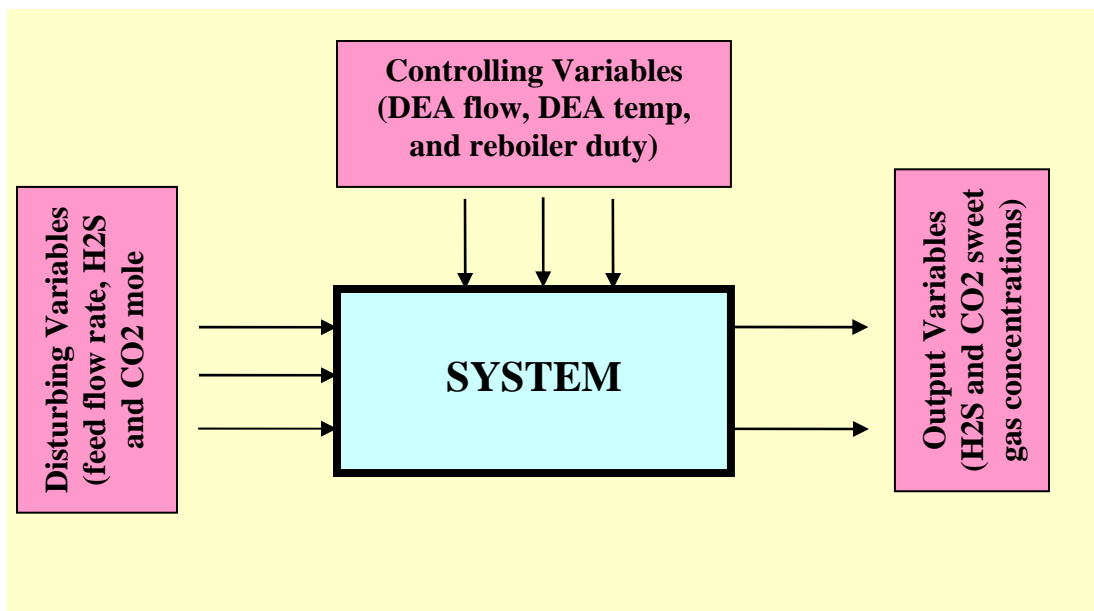


Figure 3.3 Amine system parameters

3.3 Sensitivity Analysis of Steady State Model:

Sensitivity analysis is carried out on steady state model developed using process flow sheet simulator (CHEMSHARE DESIGN-II). The effect of varying operating and sizing parameters on H_2S and CO_2 sweet gas composition is studied. The operating parameters are those mentioned-above disturbing and controlling parameters. The sizing parameters are the number of trays in absorption column, and number of trays in regeneration column. The outcome of this analysis is to visualize the effect of those parameters on sweet gas quality and deleting non-effecting controlling parameters before designing model-based control in Chapter 5

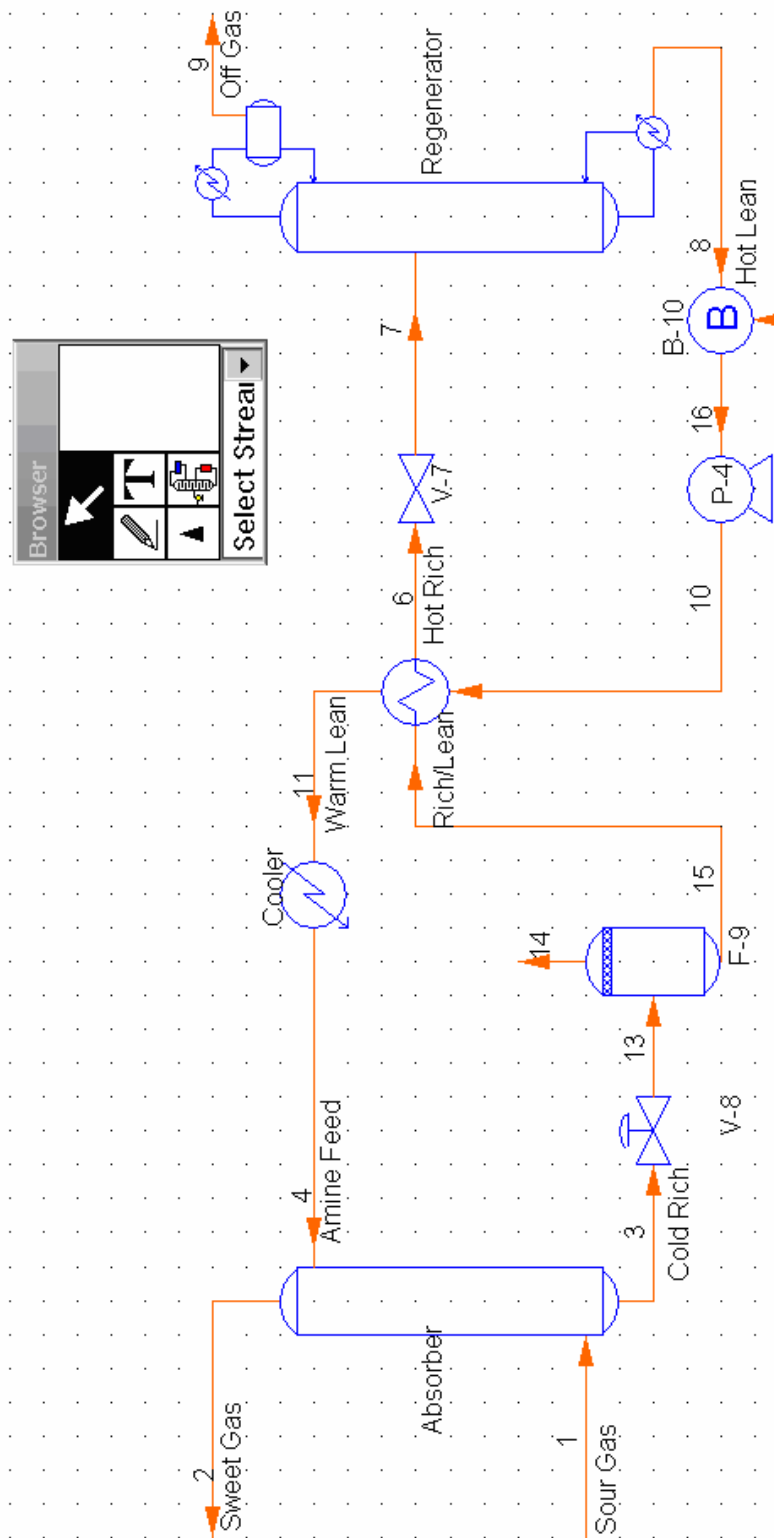


Figure 3.4 Steady state model developed using CHEMSHARE simulator

3.3.1 Sensitivity Analysis of Operating Parameters:

- Amine Concentration:

From operational aspect, the simplest variable to explore is increasing the amine concentration. However, this is not always feasible because it will adversely affect mass and heat transfer efficiency due to viscosity increase. In addition, it will increase DEA solution boiling point causing higher heat duty for the regeneration system. Moreover, the system will be exposed to severe corrosion problems in the lean/rich exchanger and reboiler caused by rich acid gas loadings after increasing solution concentration. Fig 3.5 shows the sweet gas quality as a function of weight percent amine. It can be seen that both H_2S and CO_2 concentrations decreased with increasing amine concentration. Based on Fig 3.5, DEA higher than 24 weight percent or greater is required to achieve the specified acid gas removal. At that concentration, DEA tends to pick up a large amount of acid gases and may cause corrosive conditions. Accordingly, increasing the amine concentration is not a viable option in this case.

Table 0.1 Effect of lean DEA solution strength on sweet gas quality

Lean DEA Strength (wt%)	H ₂ S (ppmv) Ex. DEA Absorber	CO ₂ (ppmv) Ex. DEA Absorber
15	5.19	56.86
16	5.09	56.04
17	5.18	56.04
18	5.12	56.03
19	5.04	55.45
20	4.92	54.68
21	4.55	52.97
22	4.7	53.45
23	4.56	52.97
24	4.39	52.6
25	4.22	52.29

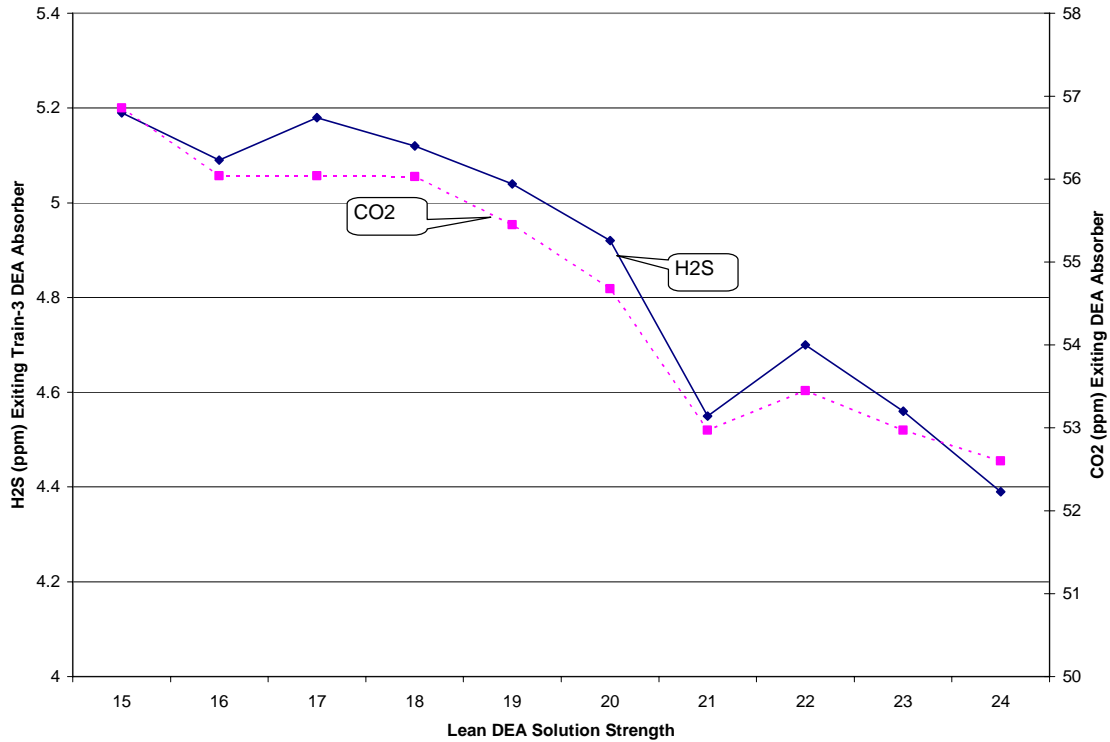


Figure 3.5 Effect of lean DEA solution strength on sweet gas quality

- DEA Solution Temperature:

The simulator was used to study how lean amine temperature affects the H_2S and CO_2 composition of the sweet gas while holding all other process variables constant. Obviously, the duty in the lean amine cooler and the amine and water makeup are adjusted to account for increases in lean amine temperature.

Fig 3.6 Shows the acid gas concentration in the sweet gas on a per volume inlet gas flow rate basis for 20 weight percent DEA solution. In investigating the effect of trim cooler temperature, the competition between thermodynamic equilibrium and kinetically limited absorption may be exploited. Concerning CO_2 sweet gas concentration, it starts decreasing as the lean amine temperature increases. The higher temperature increases the kinetic effect to a greater extent relative to the decrease in solubility. However, the

solubility dominates the kinetics and the H_2S sweet gas concentration increases with corresponding increase of lean solution temperature.

Table 3.2 Effect of DEA solution temperature on sweet gas quality

Effect of Lean DEA Solution Temperature on Train-3 DEA Absorber Performance		
Lean DEA Solution Temperature (Deg. C)	H ₂ S (ppmv) Ex. DEA Absorber	CO ₂ (ppmv) Ex. DEA Absorber
40	4.26	55.85
41	4.36	55.65
42	4.47	55.44
43	4.57	55.27
44	4.7	55.04
45	4.81	54.85
46 (Base)	4.92	54.68
47	5.05	54.49
48	4.91	53
49	5.03	52.82
50	5.16	52.65
51	5.29	52.51
52	5.42	52.27
53	5.55	52.08
54	5.7	51.93
55	5.82	51.7
56	5.96	51.53
57	6.1	51.36
58	6.29	51.29
59	6.4	51.04

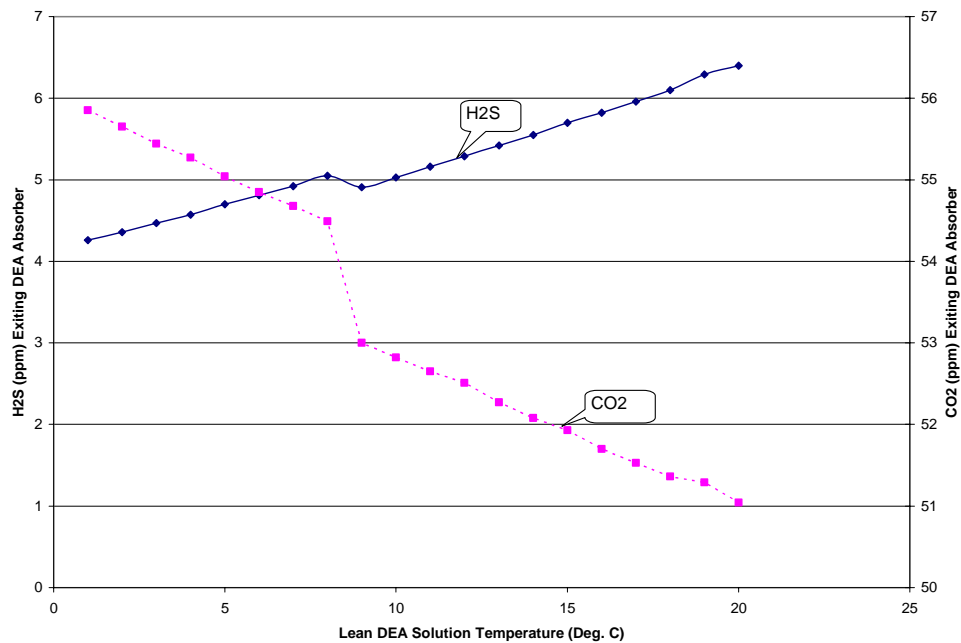


Figure 3.6 Effect of DEA solution temperature on sweet gas quality

Temperature variation of the lean amine appears to have an effect on the amount of CO_2 absorbed. This may be important for removing significant amounts of CO_2 from the inlet stream. Accordingly, the lean amine temperature is to be varied based on acid gas concentration in the sour gas to meet desired specification.

- Steam Flow Rate:

The regeneration heat requirement of the amine sweetening unit can be assessed via two variables: steam flow rate and reboiler duty. In the steady state model, the steam flow rate was varied to study the effect of regeneration heat input on sweet gas quality.

Table 3.3 Effect of reboiler duty on sweet gas quality

Train-3 DEA Regenerator Performance				
DEA Regenerator Reboiler's Steam Rate (tons)/ Reboiler Duty (KW)	H ₂ S (wt%) in Lean DEA solution	H ₂ S (ppmv) Ex. DEA Absorber	CO ₂ (wt%) in Lean DEA Solution	CO ₂ (ppmv) Ex. DEA Absorber
15 / 8730	0.382	11.1	0.451	56.95
16 / 9312	0.355	9.84	0.429	56.3
16.5 / 9600	0.344	9.3	0.418	56.02
17 / 9890	0.333	8.76	0.411	55.93
18 / 10476	0.362	8.21	0.446	55.85
19 / 11058	0.341	7.4	0.429	55.81
20 / 11640	0.322	6.72	0.413	55.78
21 / 12222	0.317	6.52	0.414	55.74
21.5 / 12513	0.297	5.83	0.393	55.28
22 / 12804	0.29	5.6	0.386	55.11
22.5 / 13095	0.283	5.36	0.38	54.96
23 / 13386	0.276	5.13	0.374	54.82
23.5 / 13677 (Base)	0.269	4.92	0.368	54.68

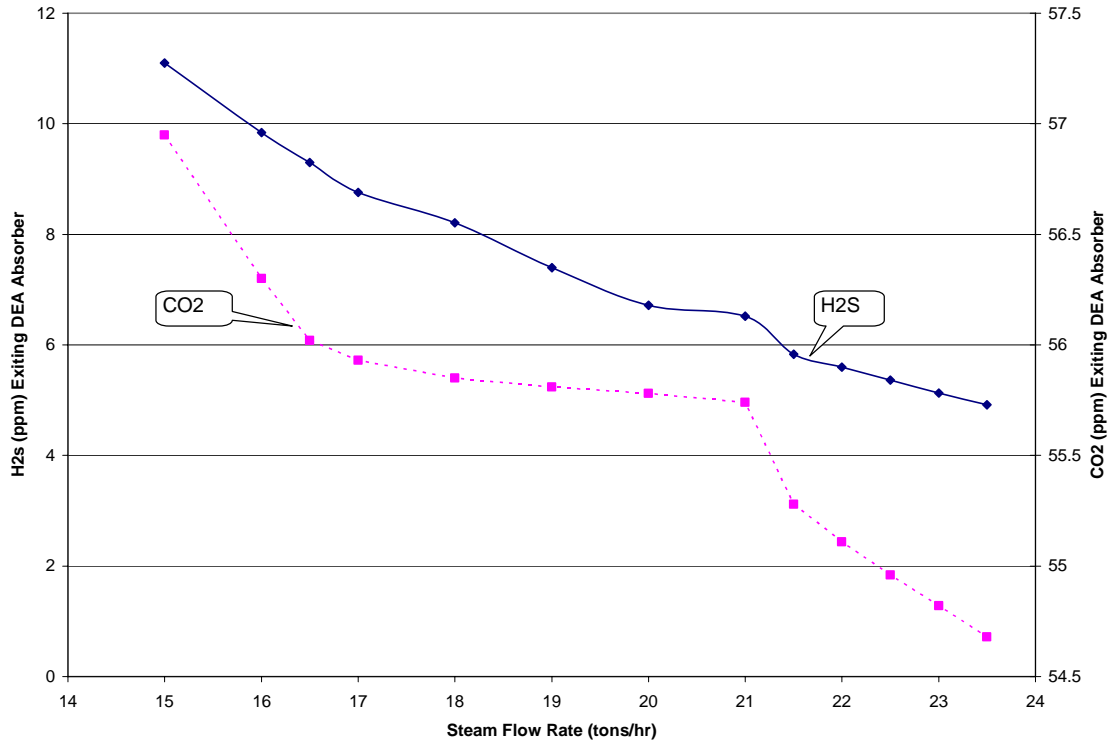


Figure 3.7 Effect of reboiler duty on sweet gas quality

From Fig 3.7, it can be clearly seen that increasing steam flow rate decreases the acid gas concentration in the sweet gas. The more steam the greater heat input into the regeneration column and, subsequently, the more acid gases released out from the rich amine solution. It is to be mentioned that Train-3 regeneration reboiler in ADGAS is currently operating at 20 tons of steam per hour. Based on simulation results, the design steam flow rate of 23.5 tons/hr corresponds to H_2S and CO_2 sweet gas concentrations of 1ppm and 54.7ppm, respectively. It can be concluded that the design reboiler duty could be utilized to reduce H_2S slip in the sweet gas, whereas no room available for further improvement in CO_2 pickup

- DEA Solution Flow Rate:

The effect of manipulating DEA solution flow rate on acid gas concentrations in the sweet gas is inspected using CHEMSHARE DESIGN-II.

Table 3.4 Effect of DEA solution flow rate on sweet gas quality

Percentage of Lean DEA Solution Rate (%)	DEA Solution Flow Rate (m3/hr)	H2S (ppmv) Ex. Train-1 DEA Absorber	CO2 (ppmv) Ex. Train-1 DEA Absorber
80	100	5.35	80.41
85	106.25	5.24	75.59
90	112.5	5.13	61.11
95	118.75	5.03	57.90
100	125	4.92	54.68
105	131.25	4.88	52.27
110	137.5	4.85	49.86
115	143.75	4.81	47.44
120	150	4.78	45.03

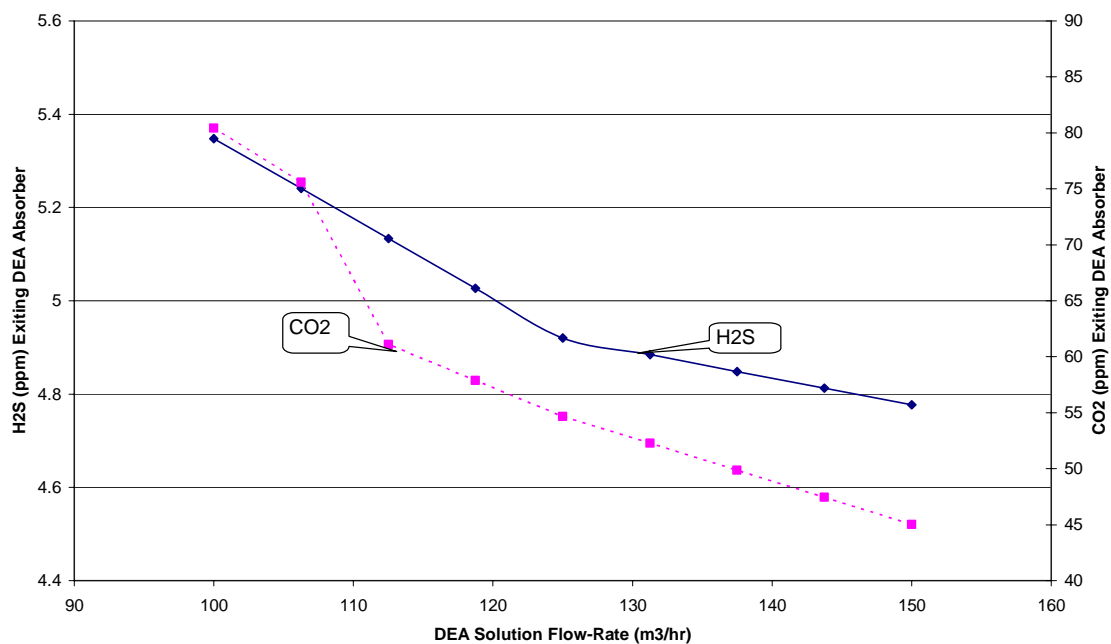


Figure 3.8 Effect of DEA solution flow rate on sweet gas quality

Fig 3.8 shows the acid gas concentration in the sweet gas as a function of lean amine rate for 20 weight percent DEA. Obviously, increasing DEA solution flow rate contributes positively in improving acid gas quality. This contribution varies among the two acid gas constituents based on their rate of reaction with DEA. The faster rate of reaction of CO_2 contributes to more efficient removal of this constituent from rich amine solution. In contrast, slight improvement was observed in H_2S sweet gas concentration. This operating variable accounts for reducing acid gas concentration in the sweet gas. However, it can be used mainly to remove significant amounts of CO_2 from the inlet sour stream.

- Sour Feed Flow Rate:

While holding process variables unchanged, absorption removal of H_2S and CO_2 is a function of inlet stream conditions. These conditions can be visualized from two versions: quantitative and qualitative. The quantitative part can be located in stream's rate, whereas the qualitative side is represented by stream's composition. Concerning to inlet sour stream's rate, the steady state model developed using CHEMSHARE DESIGN-II is used to investigate its effect on concentrations of H_2S and CO_2 in the sweet gas. Fig 3.9 demonstrates the simulation results where it can be stated that increasing inlet acid load would reduce acid gas quality. The difference in reaction rate with DEA reflects on the corresponding concentrations of H_2S and CO_2 in the sweet gas. Accordingly, with the same acid load applied into the system, there was 40 percent increase in CO_2

concentration from its initial value. In contrast, only 15 percent difference was observed with H_2S concentration.

Table 3.5 Effect of acid gas rate on sweet gas quality

Percentage of Feed Flowrate (%)	Acid Gas Rate	H ₂ S (ppmv) Ex. DEA Absorber	CO ₂ (ppmv) Ex. DEA Absorber
-10%	21735.207	10.6	48.28
-5%	22942.7185	10.83	52.64
100 (Base)	24150.23	11.01	54.68
5%	25357.7415	11.74	62.83
10%	26565.253	11.58	65.39
15%	27772.7645	12.26	71.46
20%	28980.276	12.09	73.48
25%	30187.7875	12.3	77.31
30%	31395.299	12.54	81.08

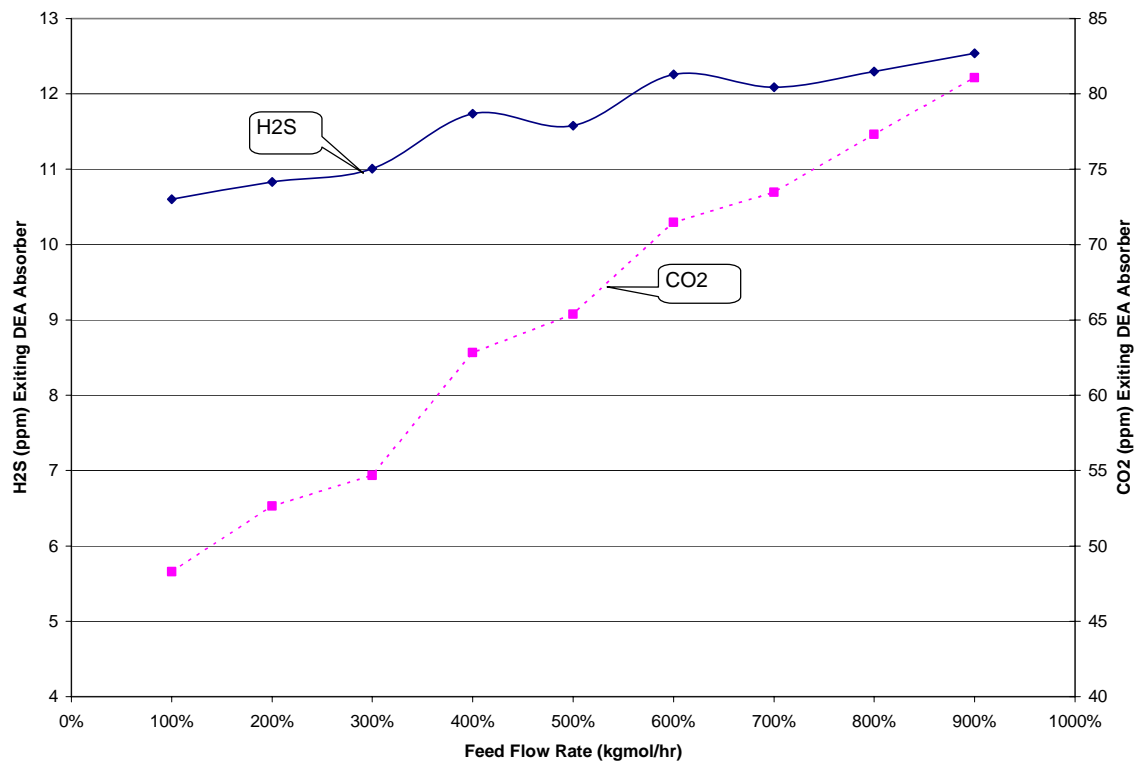


Figure 3.9 Effect of acid feed rate on sweet gas quality

- H₂S/CO₂ Ratio:

The qualitative aspect of inlet sour stream is inspected by varying H_2S to CO_2 ratio while holding all other variables unchanged. Fig 3.10 shows the interaction between inlet feed composition and sweet gas quality. The higher H_2S to CO_2 ratio, the higher H_2S slip in the sweet gas. The concentration of CO_2 decreased monotonically by almost 80 percent after increasing c to CO_2 from 0.5 to 3

Table 3.6 Effect of H₂S/CO₂ Ratio on sweet gas quality

Effect of H ₂ S/CO ₂ Ratio on Train-3 DEA Absorber Performance				
H ₂ S / CO ₂ Ratio	H ₂ S (ppmv) Feed To DEA Absorber	CO ₂ (ppmv) Feed To DEA Absorber	H ₂ S (ppmv) Ex. DEA Absorber	CO ₂ (ppmv) Ex. DEA Absorber
0.5	600	1200	2.41	83.78
1	600	600	3.31	41.4
1.5	900	600	4.45	41.06
2	800	400	4.56	27.28
2.5	750	300	4.98	20.49
3	750	250	4.81	16.95

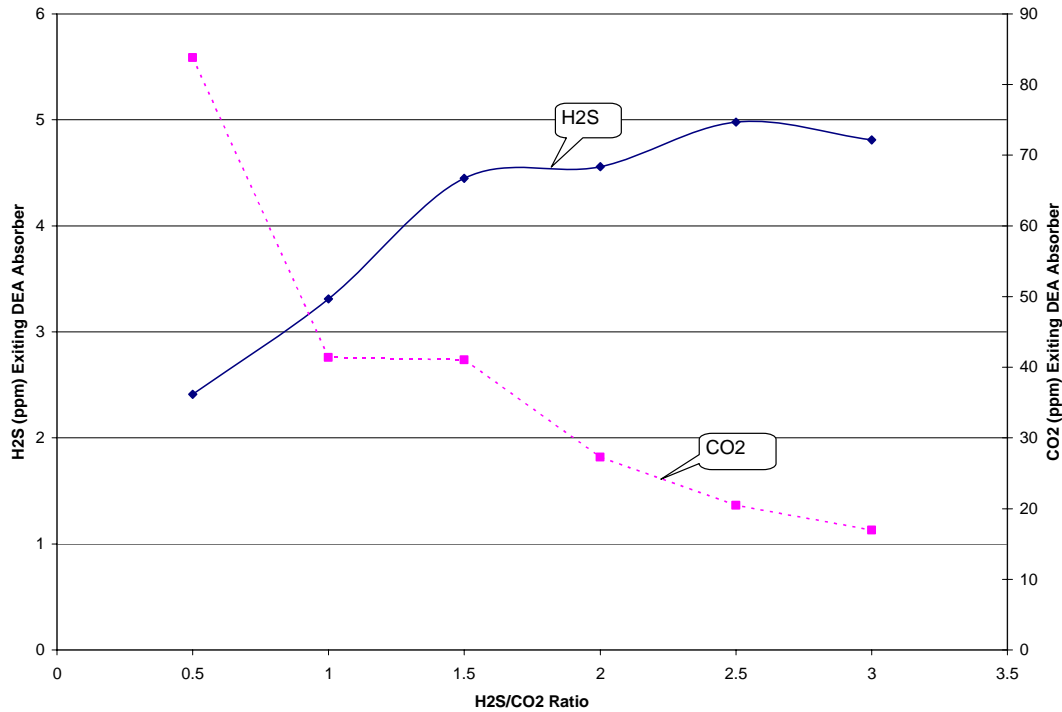


Figure 3.10 Effect of H₂S/CO₂ ratio on sweet gas quality

3.3.2 Sensitivity Analysis of Sizing Parameters:

Amine sweetening unit is a typical example of mass transfer operation accompanied by reaction. Therefore, inspecting the effect of mass transfer rate on sweet gas specification can be done by varying the number of equilibrium stages in each of the two packed columns.

Based on simulation results, the number of equilibrium stages required to meet sweet gas specification are 15.5 and 17.5 for H_2S and CO_2 , respectively. On the other hand, 8 equilibrium stages in the regenerator column are required versus a corresponding double figure for CO_2 (please refer to Figs 3.11 & 3.12). Increasing number of regenerator equilibrium stages will reduce H_2S composition in the sweet gas. It can be concluded that the regeneration section of Amine sweetening unit has the dominant effect on H_2S specification.

Table 3.7 Effect of number of DEA absorber trays on sweet gas quality

No. Trays in DEA Absorber / No. Trays in DEA Regenerator	H ₂ S (ppmv) Ex. Train-1 DEA Absorber	CO ₂ (ppmv) Ex. Train-1 DEA Absorber
14 / 8	5.05	87.59
15 / 8	5.03	74.82
16 / 8	4.97	63.94
17 / 8	4.92	54.68
18 / 8	4.9	45.58
19 / 8	4.87	40
20 / 8	4.86	34.24
21 / 8	4.83	29.32
22 / 8	4.83	25.14

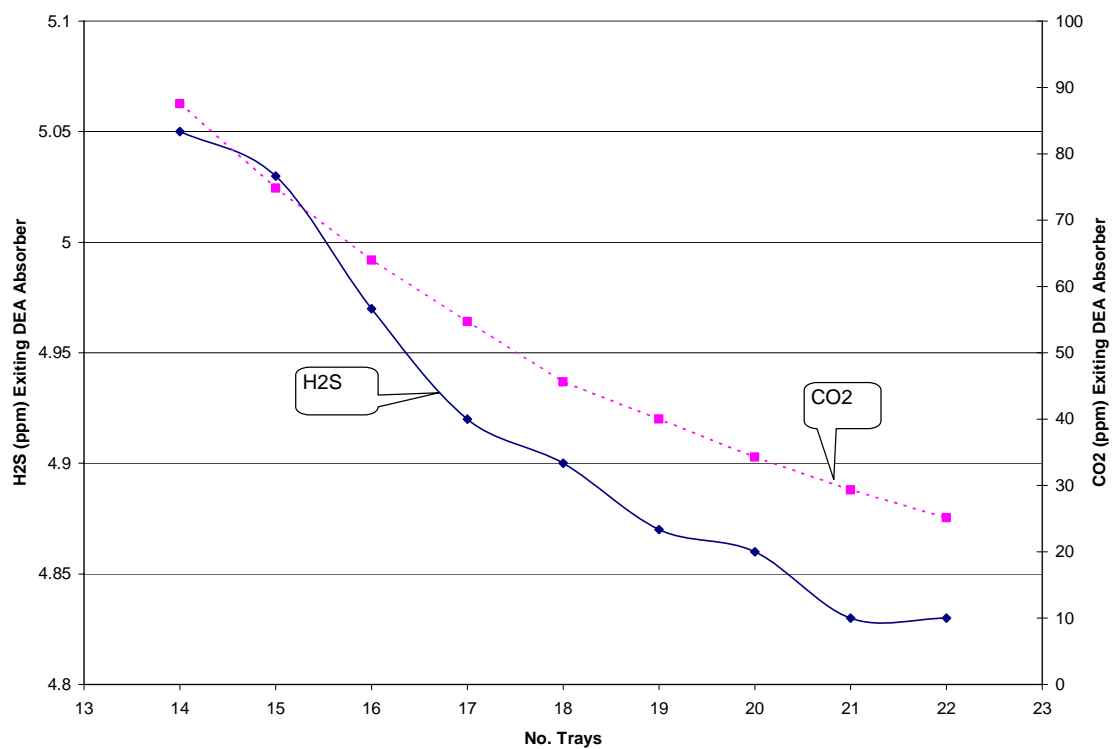


Figure 3.11 Effect of number of DEA absorber trays on sweet gas quality

Table 3.8 Effect of number of DEA regenerator trays on sweet gas quality

No. Trays in DEA Absorber / No. Trays in DEA Regenerator	H ₂ S (ppmv) Ex. Train-1 DEA Absorber	CO ₂ (ppmv) Ex. Train-1 DEA Absorber
17 / 5	7.25	55.91
17 / 6	6.57	55.63
17 / 7	5.49	54.97
17 / 8	4.92	54.68
17 / 9	4.53	54.43
17 / 10	4.22	54.24
17 / 11	3.97	54.12
17 / 12	3.5	52.7

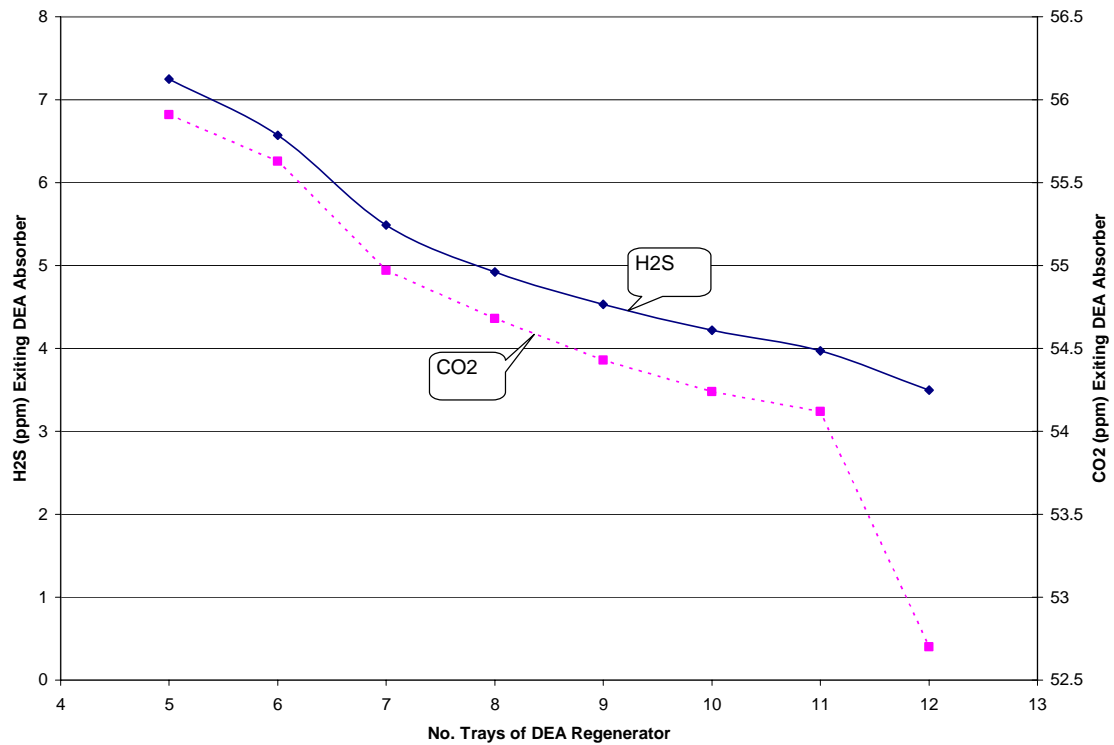


Figure 3.12 Effect of number of DEA regenerator trays on sweet gas quality

3.3.3 Discussion of Sensitivity Analysis Results:

ADGAS facility discussed here should not be thought of as being representative of general conditions since, in gas processing; there really is no general case. Each case must be considered on an individual basis due to a wide range of conditions and requirements for gas processing units. However, a few generalities or guidelines can be inferred for other facilities. If the objective is to slip as much CO_2 as possible while meeting the H_2S specification, use Diethanolamine (DEA) at low concentration and flow rate. In addition, use as few theoretical equilibrium stages as possible and operate the absorber at the lowest temperature possible. Because CO_2 absorption is kinetically controlled, decreasing the contact time and temperature tends to increase the amount of CO_2 slip. The limits of solution concentration, flow rate and equilibrium stages depend on the H_2S specification. The cold absorber temperature also enhances H_2S solubility. Facilities with this objective tend to be fairly stable as the inlet gas composition increases in CO_2 concentration.

If the objective is to achieve a certain CO_2 concentration, then the problem is more complicated. Attempts should be made to increase the amine concentration. Moreover, increasing the lean amine temperature increases CO_2 pickup; however, there is a limit to the maximum temperature. This temperature depends on amine concentration, inlet gas composition, and the amount of CO_2 pickup. Increasing the lean amine temperature decreases H_2S pickup and increases amine and water losses.

3.4 Dynamic Simulation:

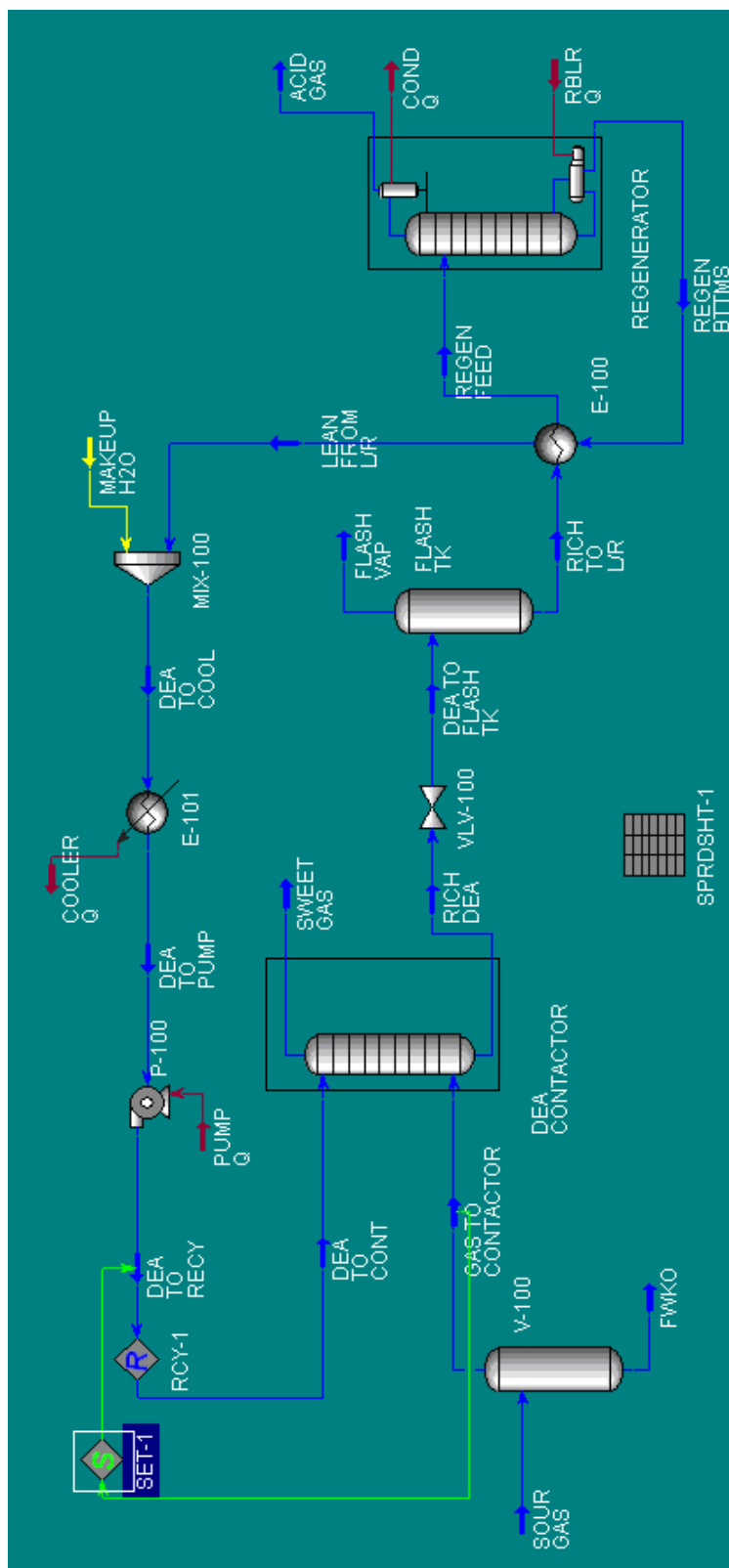
One obvious limitation of steady state modeling is that it tells us nothing about the dynamic response of the system undergoing change in its operating conditions. Accordingly, it is difficult to compare the dynamic disturbance rejection capability of different system variables.

In this thesis, step response system identification is not of interest. The main target is to obtain dynamic input-output data that can be used for neural network modeling. Training data for the ANN model are extracted from HYSYS rigorous dynamic model of amine sweetening unit. The system is excited by varying its disturbing and controlling variables with reference to design values listed in Table 3.9. Due to HYSYS convergence problems, the manipulated variables will not be fixed at their nominal design values. Increasing the fidelity of the neural network model is coincided with enriching its dynamics data. Accordingly, a small sampling interval time of 20 msec is selected. In addition, 15 percent of static values obtained at the end of each run are added to those collected dynamic data. A total of 48 runs to the dynamic model are used to excite the amine absorption system and 21,000 data sets are collected.

HYSYS process simulator is used also to address the dynamic behavior of the operating variables in amine sweetening unit. The operating conditions being investigated are the disturbing and control variables affecting sweet gas quality. This will setup the basis to prioritize the operating parameters as per their dynamic response, and eventually provide the panel operator with fast tracking hints in capturing system upsets.

Table 3.9 Design conditions of amine sweetening plant

Component	Design Value	Unit
SOUR GAS - Molar Flow	1245.18	kgmole/h
SOUR GAS - Comp Mole Frac (H ₂ S)	0.0172	
SOUR GAS - Comp Mole Frac (CO ₂)	0.04	
DEA TO CONT - Std Ideal Liq Vol Flow	43.41	m ³ /h
DEA TO CONT - Temperature	35.12	C
Reboiler - Duty	10986810.29	kcal/h
SWEET GAS - Comp Mole Frac (H ₂ S)	0.000004400	
SWEET GAS - Comp Mole Frac (CO ₂)	0.000000131	



3.4.1 Dynamic Simulation of Disturbing Variables:

The disturbing parameters are those parameters affecting sweet gas quality. They include the sour gas flow rate and the acid load represented by H_2S & CO_2 feed gas concentrations. A dynamic analysis of disturbing variables will help in visualizing their effect on the system and accordingly give better explanations on the general performance of the plant. The disturbing variables being experimented are namely; sour gas flow rate, H_2S and CO_2 mole fractions in the feed gas. Fig 3.14 shows the dynamic profile of amine plant variables due to changing the feed flow rate from 1245 to 1260 kmoles/hr. Dynamic profile of system variables after increasing the H_2S mole fraction in the feed gas from 0.0172 to 0.01978 weight percent is shown in Fig 3.15. The dynamic data in response to increasing CO_2 feed gas composition from 0.0413 to 0.047495 are shown in Fig 3.16. It can be observed that HYSYS adjust the manipulated variables to cope with changing the system disturbing variables.

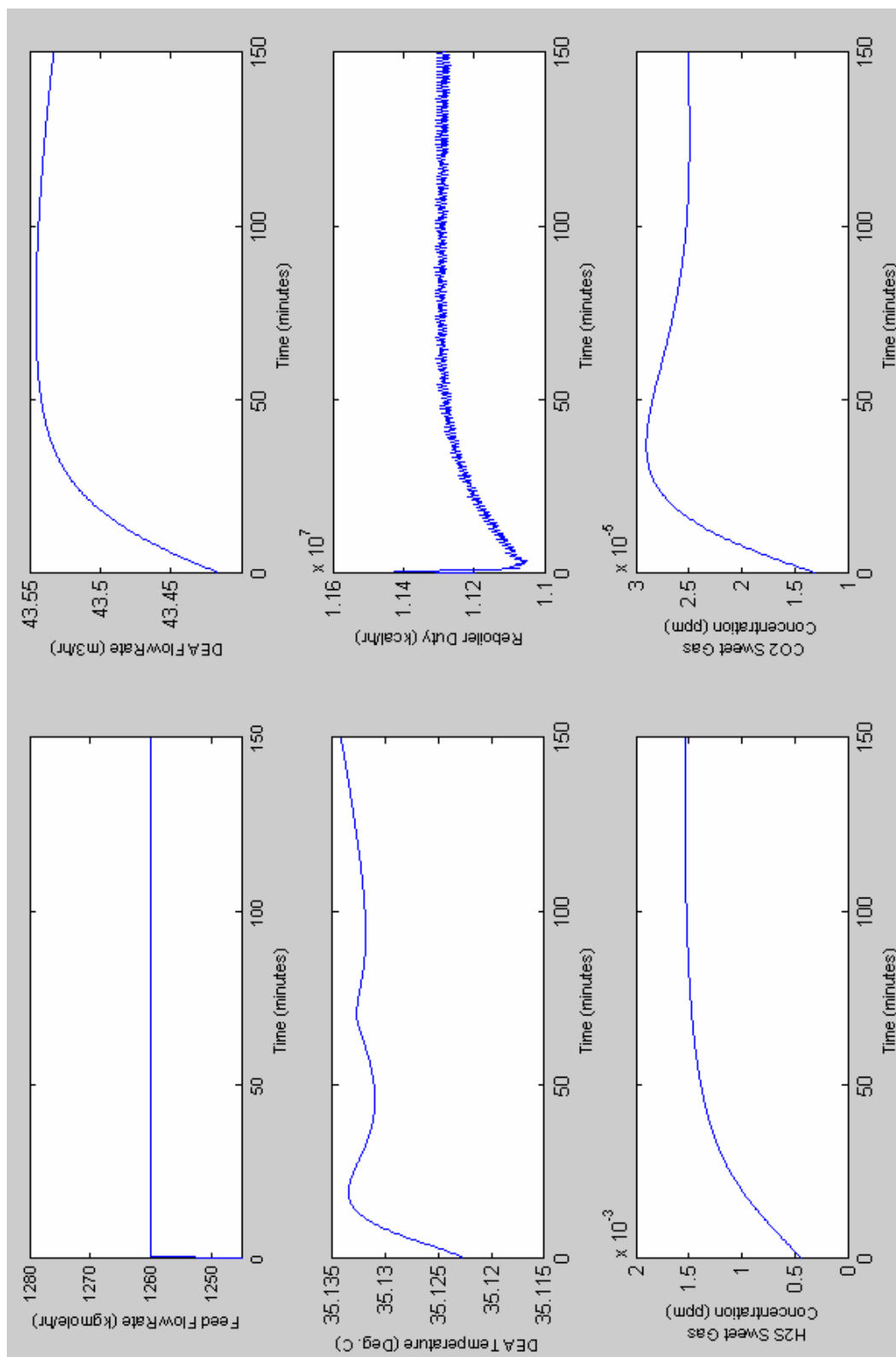


Figure 3.14 Dynamic data in response to changing feed flow in feed flow from 1245 to 1260 kgmoles/hr

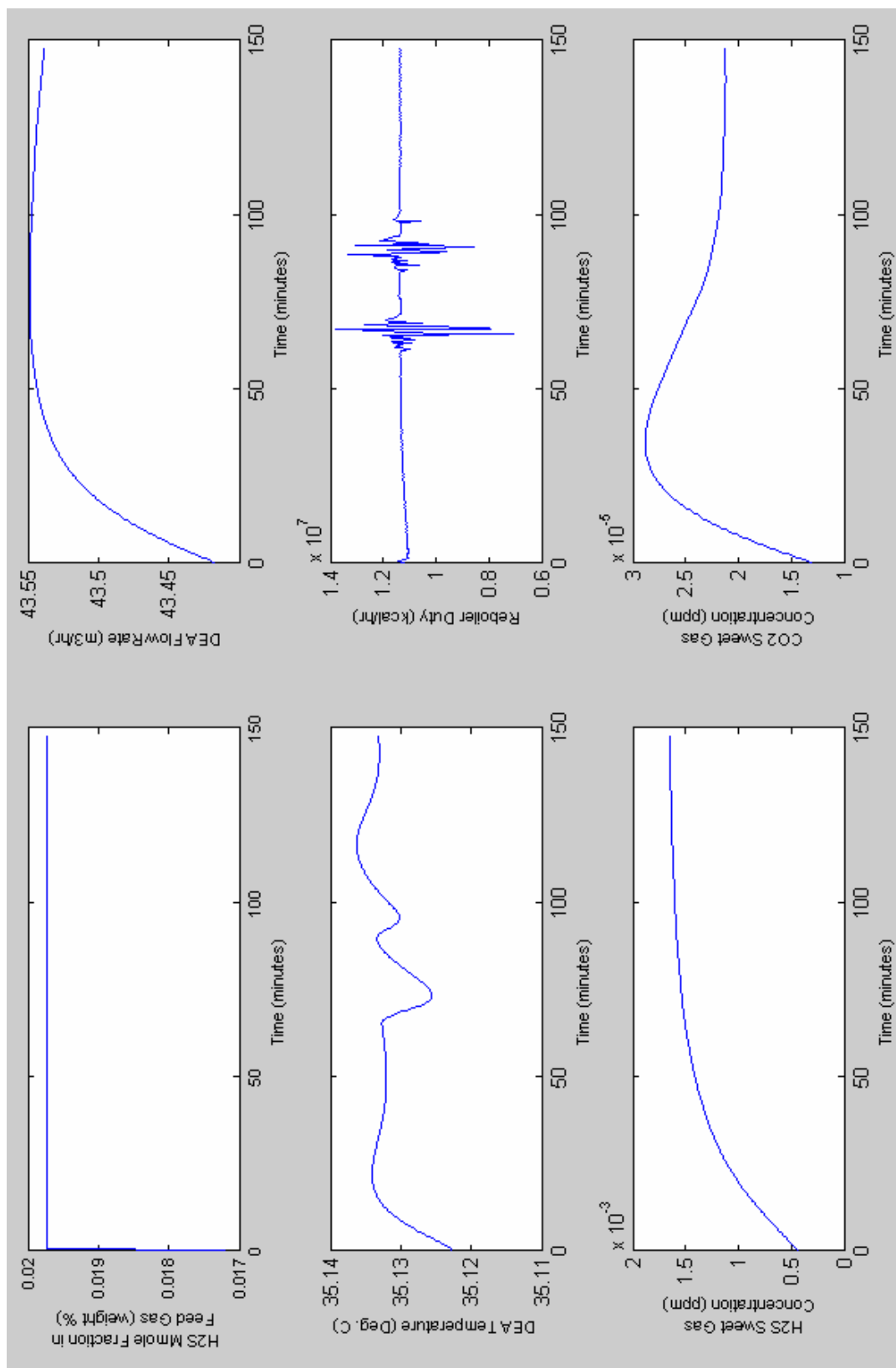


Figure 0.15 Dynamic data in response to changing H2S mole fraction in the feed gas from 0.0172 to 0.0198 weight percent

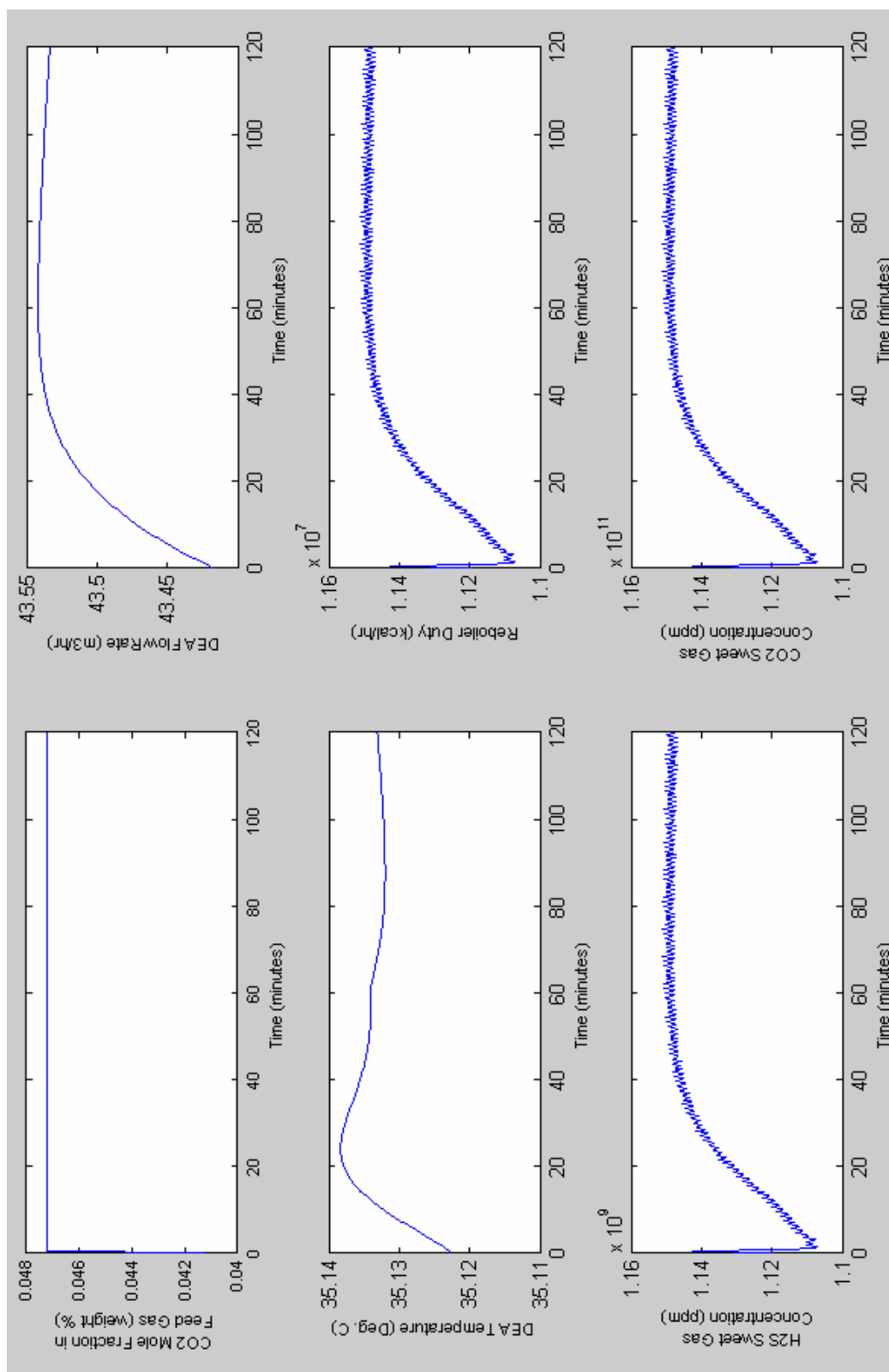


Figure 3.16 Dynamic data in response to changing CO₂ mole fraction in the feed gas from 0.04 to 0.047 weight percent

3.4.2 Dynamic Simulation of Manipulated Variables:

Manipulated parameters are those control variables used in maintaining sweet gas quality at desired specifications. They include DEA solution flow rate, temperature of DEA solution and regeneration heat input represented by reboiler duty.

Fig 3.17 shows the dynamic profile of amine plant variables due to changing the DEA solution flow rate from 43.4 to 49.9 m^3/hr . Dynamic profile of system variables after increasing DEA solution temperature from 35.12 to 37.4 is shown in Fig 3.18. The dynamic data in response to increasing reboiler duty from 10,986,810 to 12,634,832 kcal/hr. are shown in Fig 3.19. It can be noted that system disturbing variables are maintained unchanged at their fixed design values after increasing the values for manipulated variables.

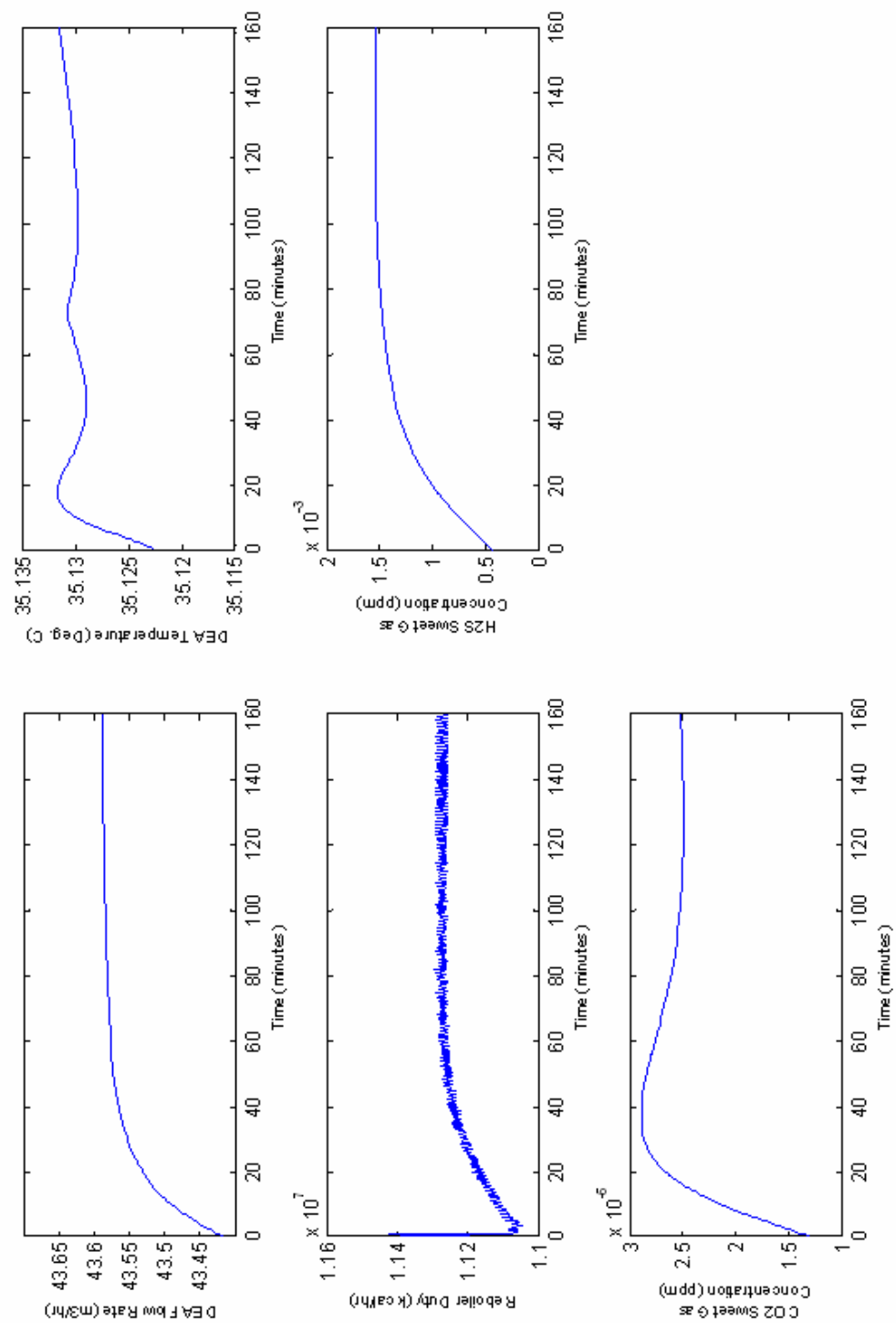


Figure 3.17 Dynamic data in response to increasing DEA solution flow rate from 43.4 to 49.9 m³/hr

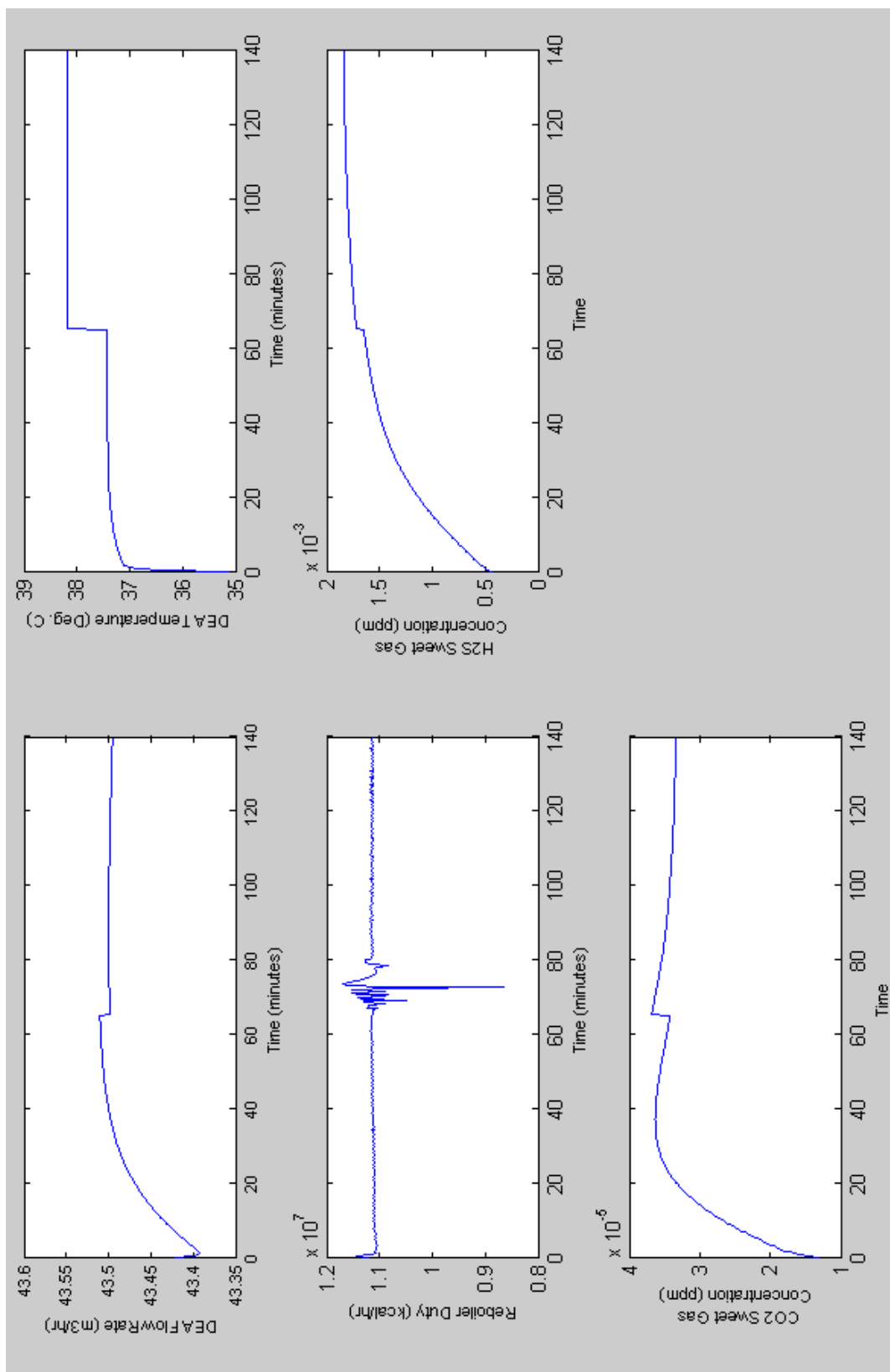


Figure 3.18 Dynamic data in response to increasing DEA solution temperature from 35.12 to 37.4 Deg. C

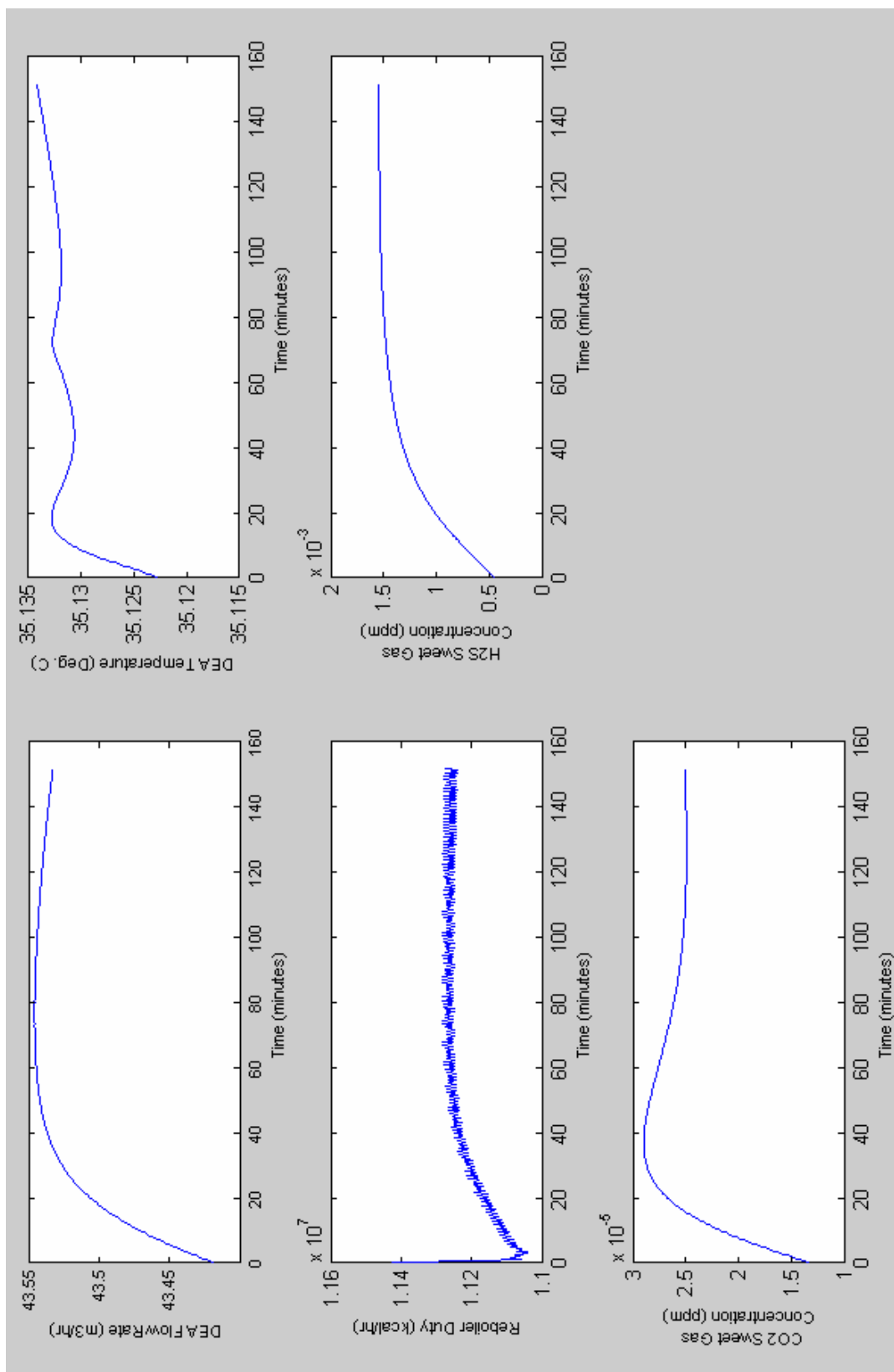


Figure 3.19 Dynamic data in response to increasing reboiler duty from 10,986,810 to 12,634,832 kcal/hr

3.4.3 Discussion of Dynamic Simulation:

Dynamic analysis is conducted on rigorous HYSYS model to obtain dynamic data necessary for ANN modeling and to prioritize the system controlling parameters as per their speed of response on sweet gas quality. The controlling variables, as has been mentioned earlier, are: DEA solution flow rate, DEA solution temperature, and reboiler duty.

If the objective is to meet a certain H_2S specification in the sweet gas, then increasing steam flow rate into regeneration reboiler is recommended. The other two alternatives would carry no capital investment but there will be an extra operational cost accompanied with them. These alternatives arranged as per their code of response as: the DEA solution temperature and DEA solution flow rate.

On the other hand, if the objective is to meet a certain CO_2 specification in the sweet gas, then the three controlling parameters could be used. Increasing DEA solution circulation would be at the top of the list due to its fast speed of response. Both DEA temperature and regeneration steam flow rate show almost similar dynamic responses. Subsequently, increasing DEA solution temperature is preferred because it is a cheaper option.

4.0 NEURAL NETWORK MODELING FOR AMINE SWEETENING UNIT

In this chapter a method of using Artificial Neural Networks (ANNs) to model the amine sweetening unit dynamics in a predictive way for the implementation of the model-based control strategy is proposed. First, an overview of neural networks is attained. Next, the learning methods available for training a neural network are given. Finally, the simulation results are presented and discussed.

4.1 Introduction:

Mechanistic models are difficult to establish using analytical methods. In a real application, obtaining accurate models using analytical methods is impractical for amine absorption unit trajectory tracking through MPC. When there are some parameter uncertainties in the prediction model or the structure of the prediction model is different from that of the real system, greater control errors or even system instability may be caused.

Since the late 1980's, artificial neural networks (ANNs) have found wide applications in the engineering field, because of the development in ANN's learning algorithms and computer technology. Most engineering researchers are interested in the following two properties of ANNs. The first is the ANNs' learning and universal approximation ability [18]; that is ANNs could be used to approximate any non-linear mapping relationship between the inputs and outputs. The second is ANNs parallel processing abilities [33].

Based on the above two properties, engineering researchers have successfully applied ANNs to many engineering areas, such as pattern recognition [2], non-linear system identification [4,5], and control [8,37].

4.2 Overview of Artificial Neural Networks (ANNs):

An artificial neural network is actually a network of interconnected elements. The models of these elements were inspired from the studies of the biological nervous systems so these elements are called neurons. Fig 4.1 depicts the schematic structure of a neuron. It is shown that a neuron receives n inputs $x_i=1, 2, \dots, n$, which can be either from the external source or the other neurons. Each input is manipulated by a scalar w_i ,

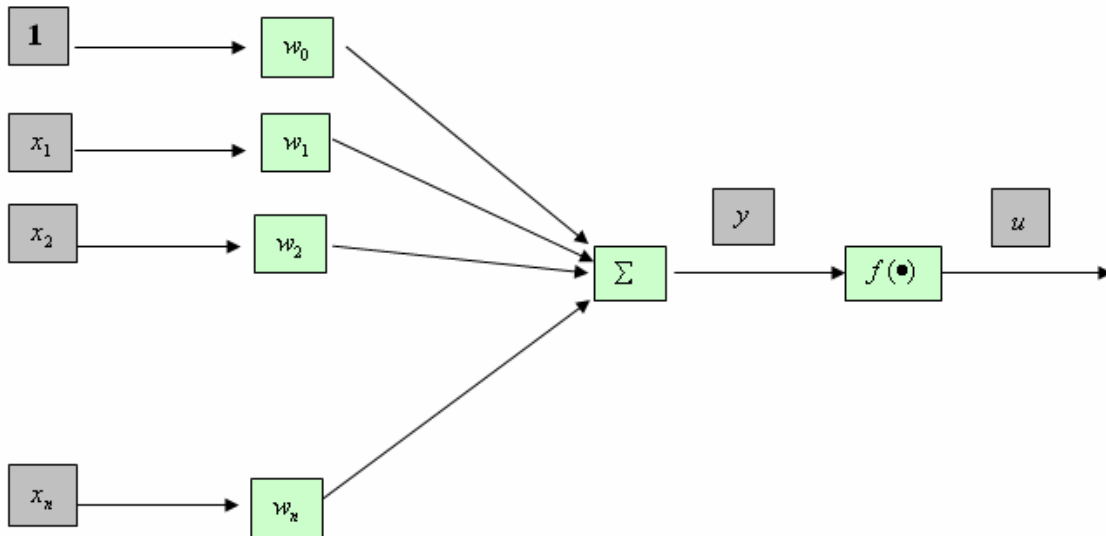


Figure 4.1 Structure of a neuron

. Each input is manipulated by a scalar w_i , known as the weight, and summed together with a bias w_o to form the intermediate value y . Finally, a non-linear transfer function $f(.)$ is applied to calculate the output of the neuron. The equation can be expressed as:

$$u = f(\sum w_i x_i + x_o) \quad (4.1)$$

To form a network structure, the inputs and outputs of the neurons are connected in some way. Due to its simplicity and successful implementation in other mass transfer processes, feed-forward neural network (FNNs) is to be used in this work

4.1.1 Feed-Forward Neural Networks (FNNs):

A general fully connected feed-forward multilayered neural network can be described in Fig 4.1, where the information propagates only in one direction (as indicated by the arrows). Each processing unit (denoted by a circle) is a neuron, and the interconnections between neurons are called synapses. The neuron first calculates the weighted sum of all synaptic signals from the previous layer plus a bias term, and then generates an output through its activation function. The input layer consists of only “fan-out” units. Each fan-out unit simply distributes an input to all neurons of the first hidden layer.

Fig 4.2 illustrates a one-hidden-layer FF network with inputs x_1, \dots, x_n and output \hat{y} . Each arrow in the figure symbolizes a parameter in the network. The network is divided into *layers*. The input layer consists of just the inputs to the network, followed by a hidden layer, which consists of any number of neurons, or hidden units placed in parallel.

Each neuron performs a weighted summation of the inputs, which then passes a nonlinear *activation function*, also called the *neuron function*.

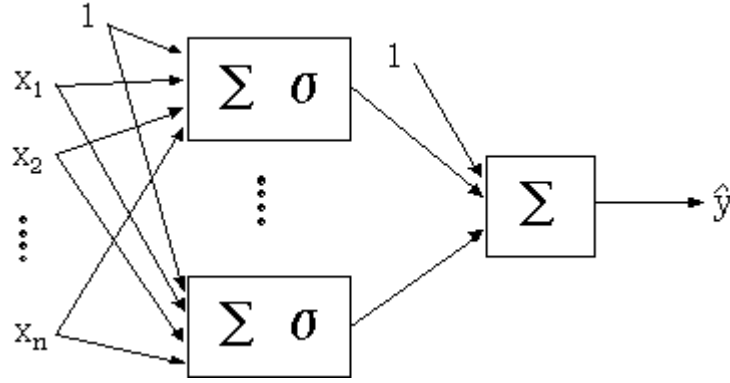


Figure 4.2 One Hidden Layer Feed-Forward Network

Mathematically the functionality of a hidden neuron is described by

$$\sigma \left(\sum_{j=1}^n w_j x_j + b_j \right) \quad (4.2)$$

, where the weights $\{w_j, b_j\}$ are symbolized with the arrows feeding into the neuron.

The network output is formed by another weighted summation of the outputs of the neurons in the hidden layer. This summation on the output is called the *output layer*. In the above figure, there is only one output in the output layer since it is a single-output problem. Generally, the number of output neurons equals the number of outputs of the approximation problem.

The neurons in the hidden layer of the network in Fig 4.2 are similar in structure to those of the perceptron, with the exception that their activation functions can be any differential function

The number of layers and the number of hidden neurons in each hidden layer are user design parameters. The general rule is to choose these design parameters so that the best possible model with as few parameters as possible is obtained. In practice, many experiments with different design have to be conducted in order to achieve the most suitable neural network.

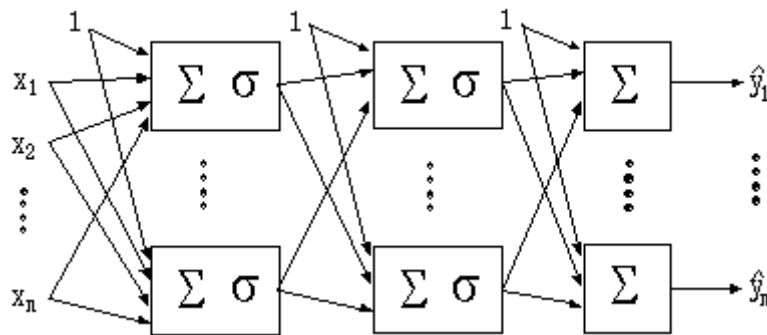


Figure 4.3 Multilayer Feed-Forward Network

As shown in Fig 4.3, a multilayer feed-forward neural network consists of several layers with different functions. The input layer is the one that receives inputs and typically performs no function other than buffering of the input signal. The outputs of the network are generated from the output layer. Any layer between the input and output layer is called a hidden layer because it is internal to the network and has no direct contact with the external environment. The neurons in a hidden layer and the output layer perform some activation functions. The most commonly-used activation functions can be found in

Table 4.1. Such a feed-forward neural network has been proven to have universal function approximation properties with only one hidden layer of sigmoid neurons [7]

Table 4.1 Commonly-used Activation Functions

Type of Functions	Functions
Linear	$f(x) = x$
Sigmoid	$f(x) = 1 / (1 + \exp(-x))$
Hyperboilc Tangent	$f(x) = (1 - \exp(-2x)) / (1 + \exp(2x))$

4.3 Training of a Neural Network:

It can be seen from section 4.2 that the output of the neuron, consequently the network, is determined by the values of the weights and biases of the network. To obtain the correct values of these parameters, a neural network has to go through a procedure, named learning (or training). There are three main categories of learning methods: supervised, reinforcement and unsupervised learning. In this thesis, only the supervised learning method is used.

To perform the supervised learning, samples, also called teacher, i.e. the correct relationship of the inputs and the outputs, must be provided. During the network training process, some learning algorithm should be used to adjust the weights and biases of the network to minimize the error between the outputs in the samples and the overall network outputs. The basic training algorithm is called the back-propagation. The feed-forward, back-propagation architecture was developed in the early 1970's by several independent sources [40]. This independent co-development was the result of a proliferation of

articles and talks at various conferences which stimulated the entire industry. Currently, this synergistically developed back-propagation architecture is the most popular, effective, and easy to learn model for complex, multi-layered networks. This architecture has spawned a large class of network types with many different topologies and training methods. Its greatest strength is in non-linear solutions to ill-defined problems.

The typical back-propagation network has an input layer, an output layer, and at least one hidden layer. There is no theoretical limit on the number of hidden layers but typically there is just one or two. The in and out layers indicate the flow of information during recall. Recall is the process of putting input data into a trained network and receiving the answer. Back-propagation is not used during recall, but only when the network is learning a training set.

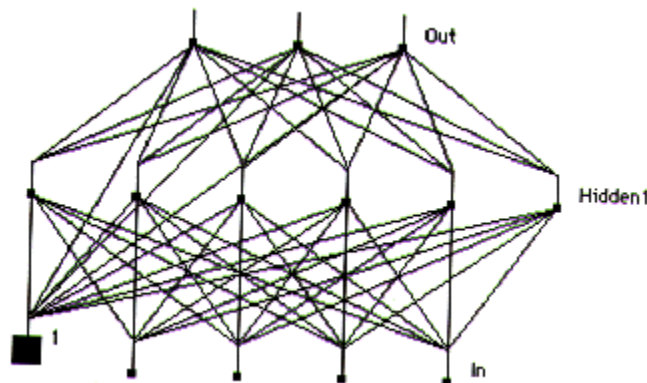


Figure 4.4 Feed-Forward Back-propagation Network

The number of layers and the number of processing element per layer are important decisions. These parameters to a feed-forward, back-propagation topology are also the most ethereal. There is no quantifiable, best answer to the layout of the network for any

particular application. There are only general rules picked up over time and followed by most researchers and engineers applying this architecture of their problems.

Rule One: As the complexity in the relationship between the input data and the desired output increases, then the number of the processing elements in the hidden layer should also increase.

Rule Two: If the process being modeled is separable into multiple stages, then additional hidden layer(s) may be required. If the process is not separable into stages, then additional layers may simply enable memorization and not a true general solution.

Rule Three: The amount of training data available sets an upper bound for the number of processing elements in the hidden layers. To calculate this upper bound, use the number of input output pair examples in the training set and divide that number by the total number of input and output processing elements in the network. Then divide that result again by a scaling factor between five and ten. Larger scaling factors are used for relatively noisy data. Extremely noisy data may require a factor of twenty or even fifty, while very clean input data with an exact relationship to the output might drop the factor to around two. It is important that the hidden layers have few processing elements. Too many artificial neurons and the training set will be memorized. If that happened then no generalization of the data trends will occur, making the network useless on new data sets.

Once the above rules have been used to create a network, the process of teaching begins. This teaching process for a feed-forward network normally uses some variant of the Delta Rule, which starts with the calculated difference between the actual outputs and the

desired outputs. Using this error, connection weights are increased in proportion to the error times a scaling factor for global accuracy. Doing this for an individual node means that the inputs, the output, and the desired output all have to be present at the same processing element. The complex part of this learning mechanism is for the system to determine which input contributed the most to an incorrect output and how does that element get changed to correct the error. An inactive node would not contribute to the error and would have no need to change its weights.

To solve this problem, training inputs are applied to the input layer of the network, and desired outputs are compared at the output layer. During the learning process, a forward sweep is made through the network, and the output of each element is computed layer by layer. The difference between the output of the final layer and the desired output is back-propagated to the previous layer(s), usually modified by the derivative of the transfer function, and the connection weights are normally adjusted using the Delta Rule. This process proceeds for the previous layer(s) until the input layer is reached.

There are many variations to the learning rules for back-propagation network. Different error functions, transfer functions, and even the modifying method of the derivative of the transfer function can be used. The concept of momentum error was introduced to allow for more prompt learning while minimizing unstable behavior. Here, the error function, or delta weight equation, is modified so that a portion of the previous delta weight is fed through to the current delta weight. This acts, in engineering terms, as a low-pass filter on the delta weight terms since general trends are reinforced whereas

oscillatory behavior is canceled out. This allows a low, normally slower, learning coefficient to be used, but creates faster learning.

Another technique that has an effect on convergence speed is to only update the weights after many pairs of inputs and their desired outputs are presented to the network, rather than after every presentation. This is referred to as cumulative back-propagation because the delta weights are not accumulated until the complete set of pairs is presented. The number of input-output pairs that are presented during the accumulation is referred to as an epoch. This epoch may correspond either to the complete set of training pairs or to a subset.

4.4 Training and Validation of ANN Models:

The scope of this thesis is to have the two constituents of the sweet gas stream, namely; H_2S and CO_2 , at desired specifications. The dynamic response of each constituent differs according to the kinematics and reaction rules controlling constituent's reaction with DEA. Subsequently, two neural network models are to be developed in correspondence with different dynamic behavior. To model the forward dynamics of each sweet gas component, a fully connected feed-forward neural network is used in this section. The NN model has a structure of 6 inputs subdivided equally into disturbing and controlling parameters. The disturbing parameters are the sour feed flow rate, the H_2S acid gas concentration, and the CO_2 acid gas concentration. The controlling parameters are the DEA flow rate, the DEA temperature, and the reboiler duty.

In modeling both feed-forward networks, the same structure is selected to characterize both networks. Each network has an input layer with 6 neurons, a hidden layer with 40 neurons and the output layer with one neuron representing the sweet gas constituent. The activation function used in each neuron in the input and hidden layers is the hyperbolic tangent sigmoid transfer function. The activation function used in each neuron in the output layer is the linear transfer function. The algorithm used to train the neural network model is the standard back-propagation. The back-propagation network training function is the Bayesian regularization back-propagation function. Moreover, the back-propagation learning function is selected to be the gradient descent with momentum weight and bias. The network's performance is measured according to the mean of squared errors.

The accuracy of the obtained NN model is viewed through the network active cost showing the squared error difference between actual and simulated output values. Secondly, the general performance of the network could be assessed via the plot of desired and simulated data sets. The higher the deviation between these two data sets the lower the fidelity of the model. Finally, the quality of the network training is checked by performing a linear regression between the network outputs and the targets.

Designing a model-based controller requires the availability of a dynamic model for system as well as neural networks setting the relationship between controlling & output parameters. Eight neural networks are to be viewed based on the above assessment framework to satisfy the controller design requirements. The neural network models for H_2S and CO_2 sweet gas concentrations are presented in this chapter. The remaining six

networks are establishing the relationship between controlling parameters and sweet gas composition. Modeling those networks is required before developing the model predictive controller. They will be addressed in details in Chapter 5.

- Neural network predictor for H₂S sweet gas concentration:

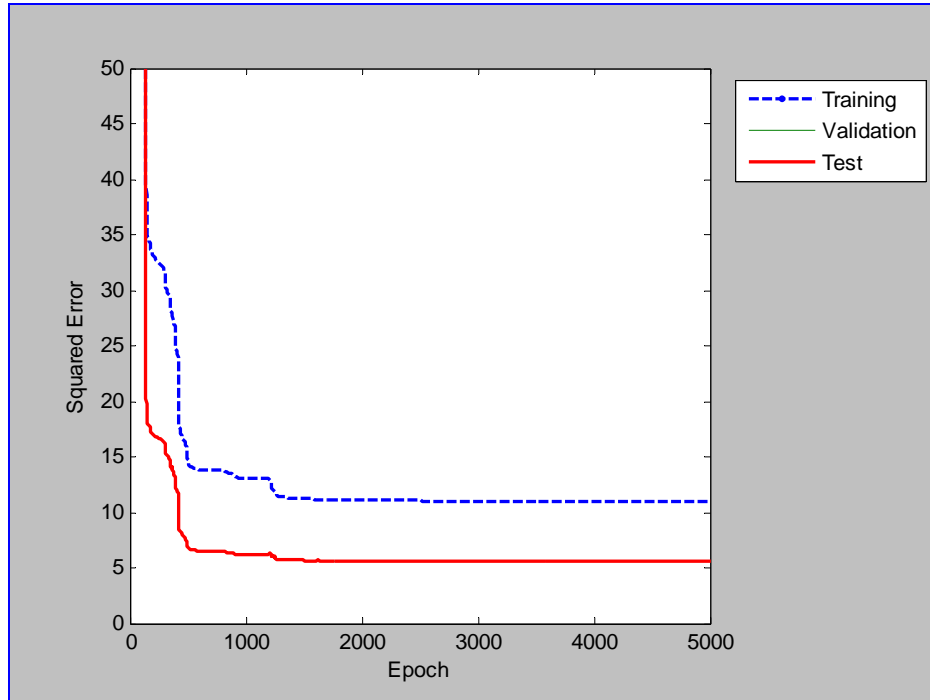


Figure 4.5 Learning Curve: NN model of 6 plant inputs and 1 plant output (H₂S)

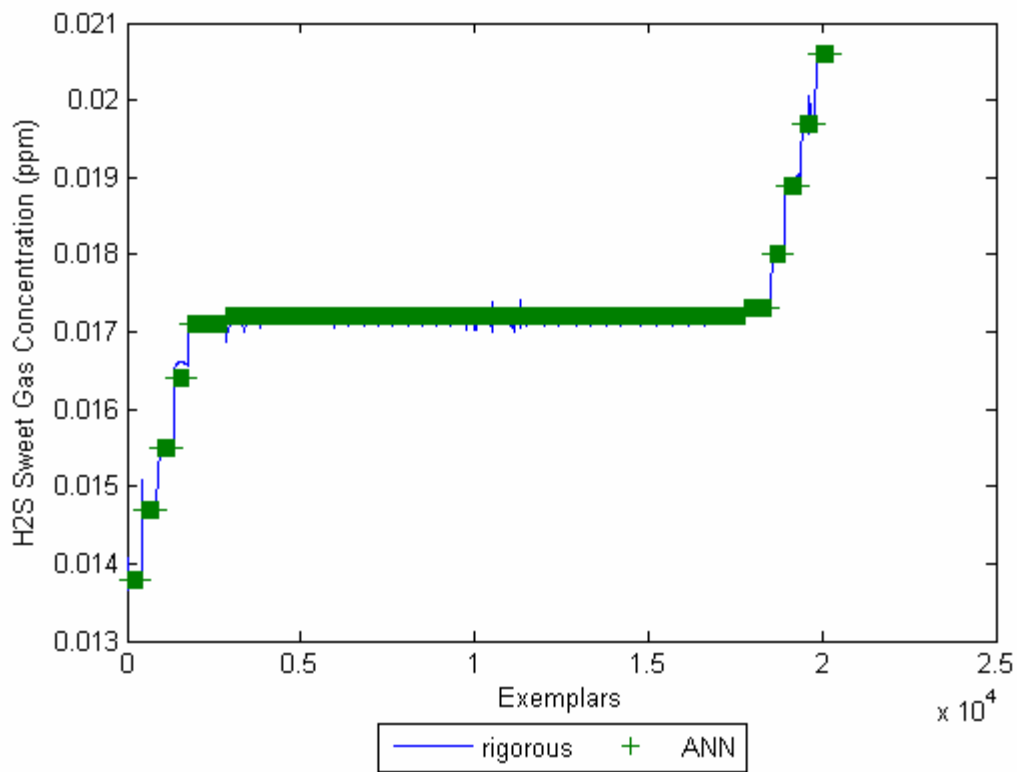


Figure 4.6 Rigorous Vs. ANN Plot: NN model of 6 plant inputs and 1 plant output (H2S)

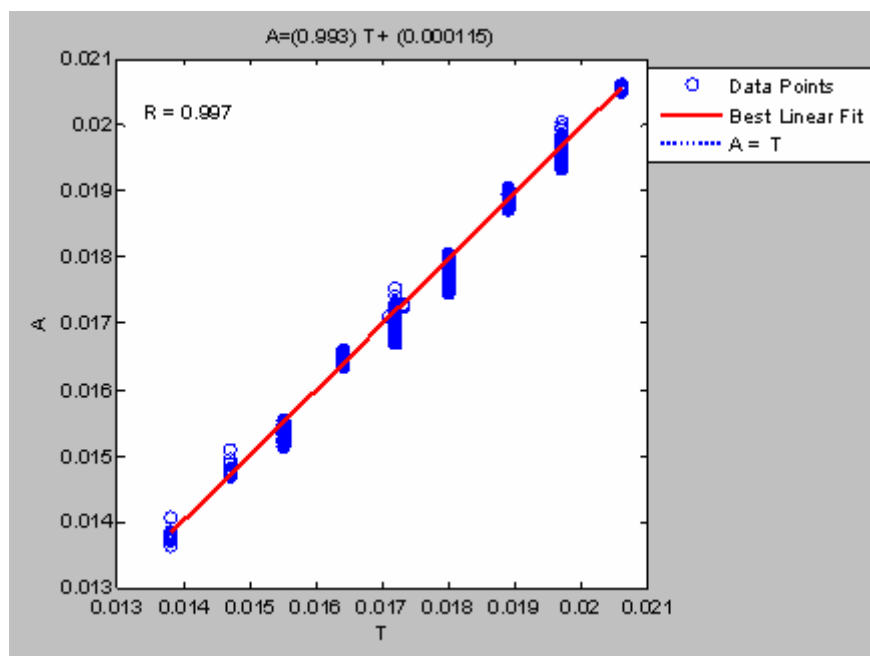


Figure 4.7 Best Linear Fit: NN model of 6 plant inputs and 1 plant output (H2S)

- Neural network predictor for CO₂ sweet gas concentration:

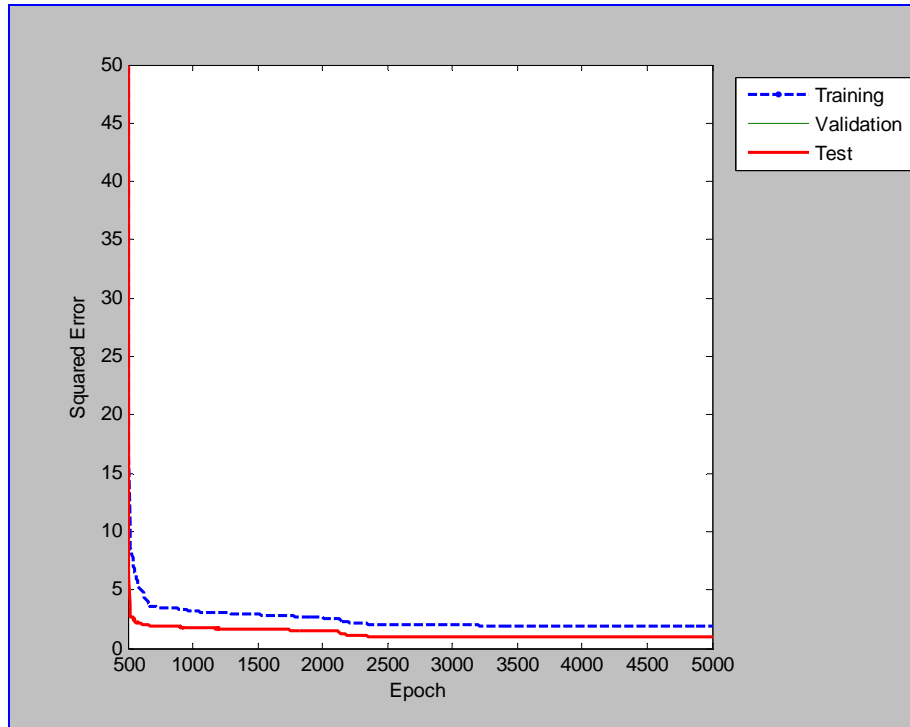


Figure 4.8 Learning Curve: NN model of 6 plant inputs and 1 plant output (CO₂)

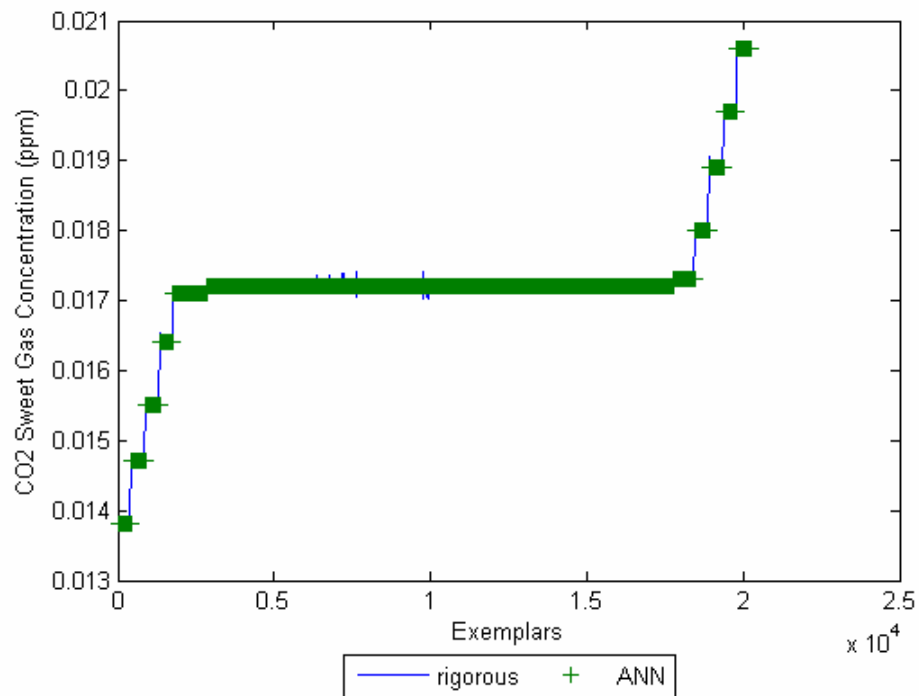


Figure 4.9 Rigorous Vs. ANN plot: NN model of 6 plant inputs and 1 plant output (CO₂)

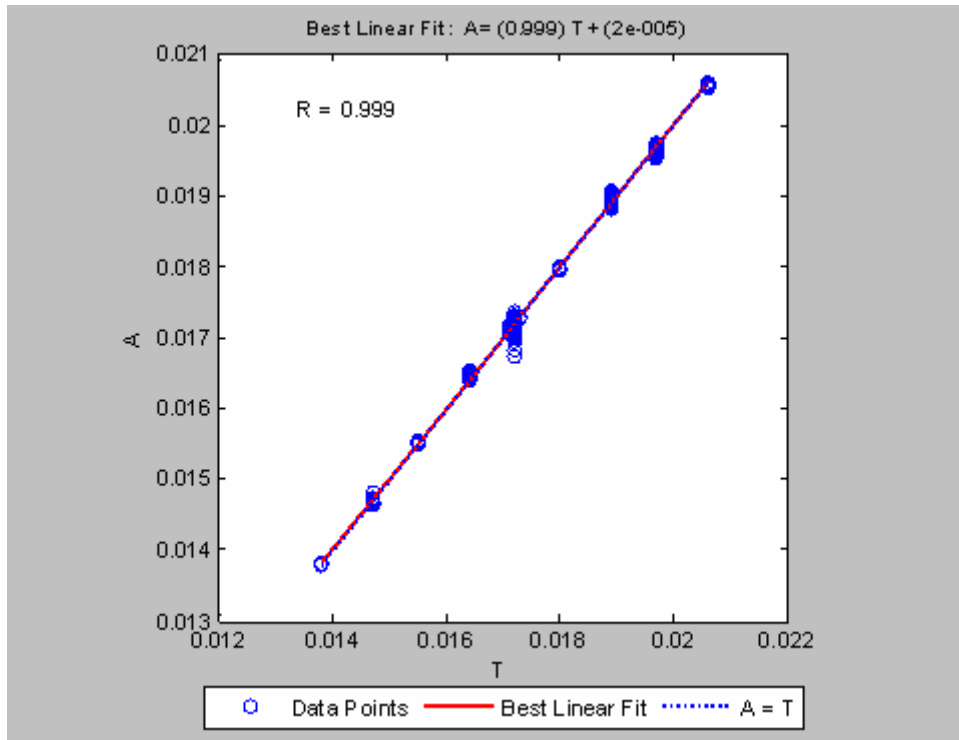


Figure 4.10 Best Linear Fit: NN model of 6 plant inputs and 1 plant output (CO2)

Neural networks prediction show a very good match with rigorous plant data. Obtaining the optimum performance indicated by the best fit line, shown in Figs 4.4 & 7, is possible with only 500 training epochs for the two above prediction models. It is to be emphasized that those training parameters specified in MATLAB m-file (please refer to appendix-1) are the best obtained after experimenting other alternatives available in the MATLAB Neural Network toolbox. The recurrent network is not a feasible option due to relatively huge data involved in this application. The Levenberg-Marquardt function could not be selected as a back-propagation training function due to high memory requirements by this function. Accordingly, the Bayesian regularization function was set as the training transfer function.

5.0 NEURO-MPC CONTROL OF AMINE SWEETENING UNIT MANIPULATOR

5.1 The principles of Non-linear Model Predictive Control:

In general, the model predictive control problem is formulated as solving on-line a finite horizon open-loop optimal control problem subject to system dynamics and constraints involving states and controls. Fig 5.1 shows the basic principle of model predictive control. Based on measurements obtained at time t , the controller predicts the future

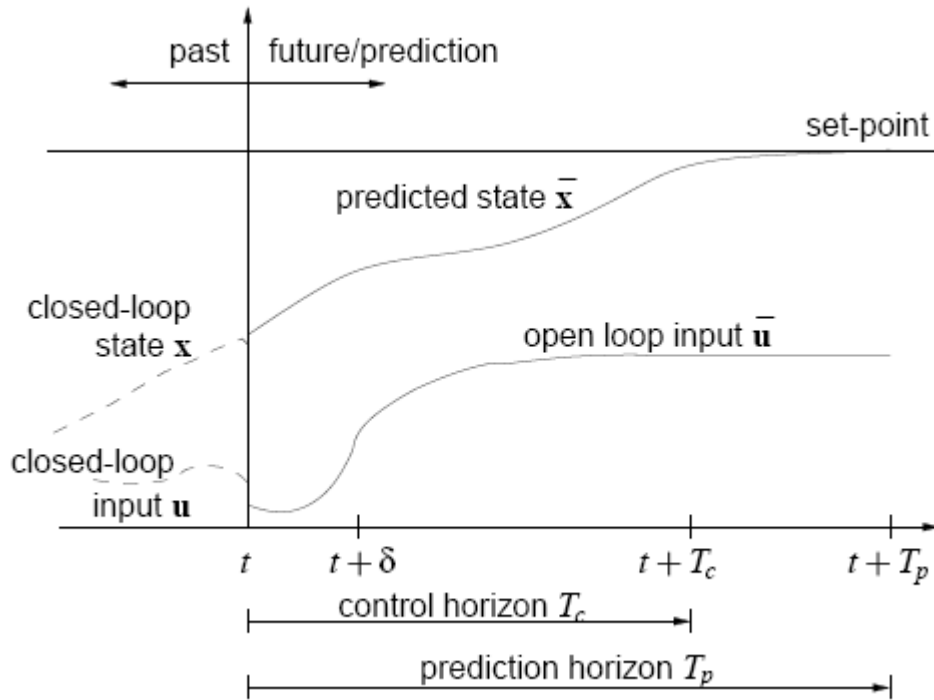


Figure 5.1 Basic Principle of MPC

dynamic behavior of the system over a prediction horizon T_p and determines (over a control horizon $T_c \leq T_p$) the input such that a predetermined open-loop performance objective functional is optimized. *If* there were no disturbances and no model-plant mismatch, and *if* the optimization problem could be solved for infinite horizons, then one

could apply the input function found at time $t = 0$ to the system for all times $t \geq 0$. However, this is not possible in general. Due to disturbances and model-plant mismatch, the true system behavior is different from the predicted behavior. In order to incorporate some feedback mechanism, the open-loop manipulated input function obtained will be implemented only until the next measurement becomes available.

The time difference between the recalculation/measurements can vary, however often it is assumed to be fixed, i.e the measurement will take place every d sampling time-units. Using the new measurement at time $t + \delta$, the whole procedure – prediction and optimization – is repeated to find a new input function with the control and prediction horizons moving forward.

It is to be noted that in the above figure, the input is depicted as arbitrary function of time. For numerical solutions of the open-loop optimal control problem it is often necessary to parameterize the input in an appropriate way. This is normally done by using a finite number of basis functions, e.g. the input could be approximated as piecewise constant over the sampling time δ .

5.2 Mathematical Formulation of Non-linear MPC:

The prediction algorithm uses the output of the plant's model to predict the plant's dynamics to an arbitrary input from the current time k to some future $k+n$. This is accomplished by time shifting equations for $y_n(k)$ and $net_j(k)$ by n resulting in

$$y_n(k+n) = \sum_{j=1}^{nh} w_j f_j(net_j(k+n)) + b \quad (5.1)$$

And

$$\begin{aligned} net_j(k+n) = & \sum_{i=0}^{nu} w_{j,i+1} \begin{cases} u(k+n-i), n - N_u < i \\ u(n+N_u), n - N_u \geq i \end{cases} + \sum_{i=1}^{\min(n,ny)} w_{j,nu+i+1} y_n(k+n-i) + \\ & + \sum_{i=n+1}^{ny} w_{j,nu+i+1} y(k+n-i) + b_j \end{aligned} \quad (5.2)$$

Where $f_j(\bullet)$ is the output function for the j^{th} node of the hidden layer, $net_j(n)$ is the activation level of the j^{th} node's output function, nh is the number of hidden nodes in hidden layer, w_j is the weight connecting the j^{th} hidden node to the output node, $w_{j,i}$ is the weight connecting the i^{th} input node to the j^{th} hidden node, b_j the bias on the j^{th} hidden node, b the bias on the output node. The first summation of (5.2) breaks the input into two parts.

Using quadratic cost function and the predictive model, it is possible to calculate the optimal control strategy for a non-linear model predicted by using NN. The cost function in predictive control is chosen as:

$$J = \sum_{j=N1}^{N2} [r(k+j) - y_n(k+j)]^2 + \sum_{j=1}^{Nu} \lambda(j) [\Delta u(k+j)]^2 \quad (5.3)$$

Where r is the required process output, y_n is the NN model output, u is the process input, N_1 and N_2 define the prediction horizon, N_u the control horizon and λ is a sequence of control weighting factors. A suitable choice for N_1 is to make it equal to the process delay between input and output. N_2 is then set to define the prediction horizon beyond this point and it represents the number of time-steps in the future for which the process response is recursively predicted as a result of the proposed control action sequence $u(k), \dots, u(k = N_u - 1)$ executed over the control horizon N_u . Control actions after the control horizon are held constant equal to the value $u(k + N_u - 1)$.

5.3 Simulink Model of the Amine Sweetening Unit:

Because H_2S and CO_2 react differently with DEA solution, two model predictive controllers are to be implemented in the amine sweetening plant. The Simulink NN predictive controller block is utilized in this regard. The FNN models of the plant, developed earlier in Chapter 4, are converted into Simulink models using MATLAB command *gensim*. Each model sets the relationship between the plant six inputting variables (disturbing and controlling) and a single plant output (i.e. H_2S). Fig 5.2 shows the first MPC to be implemented in the plant in order to control H_2S outlet. As shown in Fig 5.3, normalization is considered due to large scale of data used in this study. Three MPC blocks, as shown in Fig 5.4), are used and each block is responsible for sending a particular control signal (i.e. DEA solution flow rate) to the amine plant based on specified set-point of outlet variable. The embedded NN model in each MPC block determines the control signal value required to reduce the error between desired and

actual plant outlet values. Those models are FNN models developed before using the controller with network specifications specified in Table 5.1. The training and testing results in developing those models are presented in section 5.4. Fig 5.5 shows the second MPC scheme to be implemented in amine gas plant for controlling CO_2 sweet gas concentration.

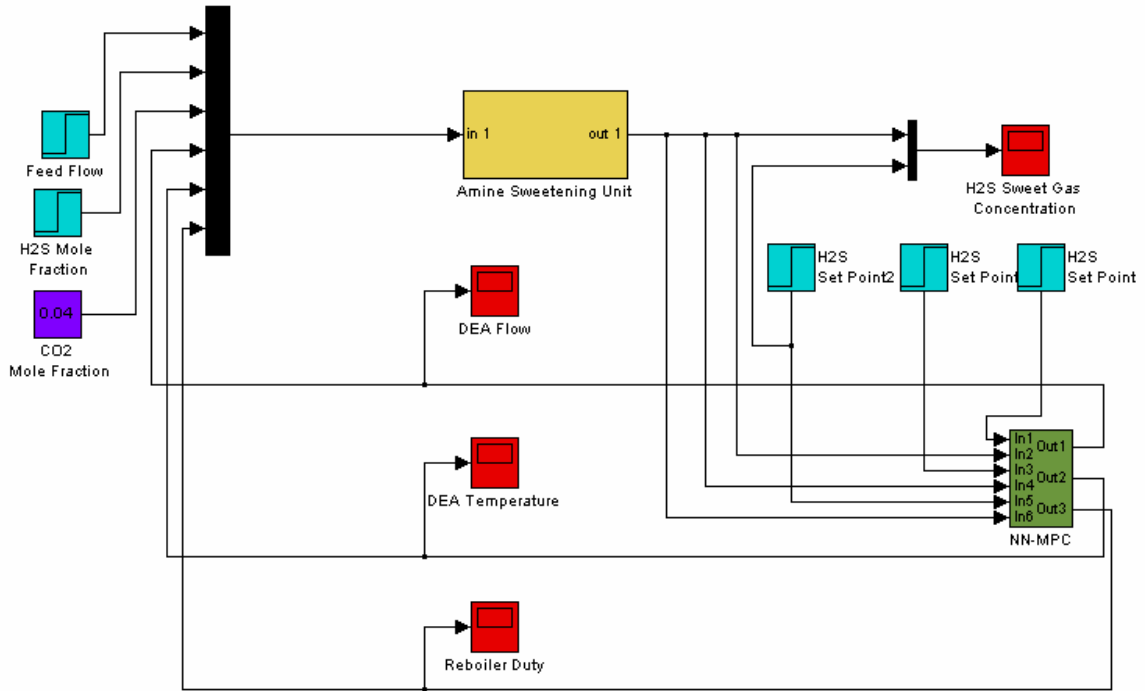


Figure 5.2 Simulink Model of Proposed MPC controlling H2S outlet

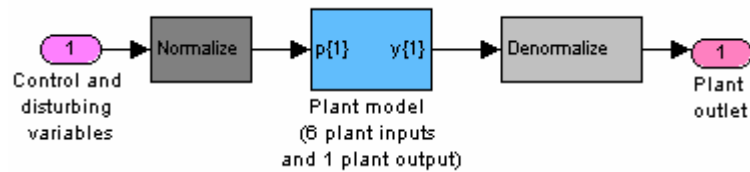


Figure 5.3 Sub-block of amine sweetening unit

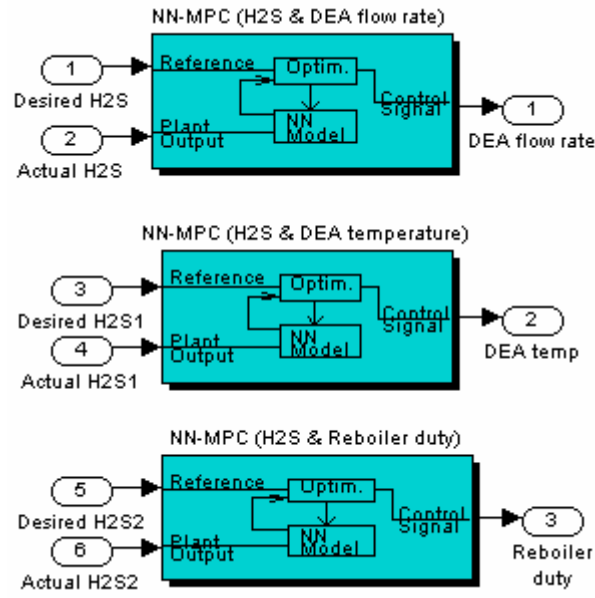


Figure 5.4 Sub-block of NN-MPC

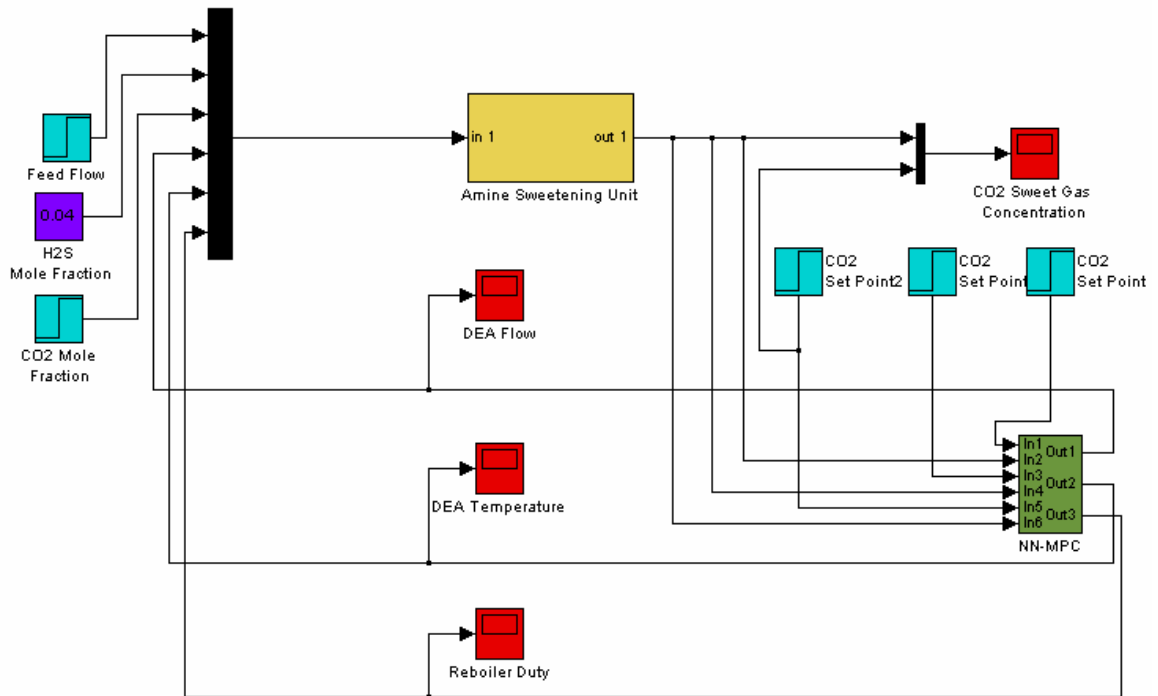


Figure 5.5 Simulink model of proposed MPC controlling CO₂ outlet

Table 5.1 Characteristics of NN-MPC models

Type of network	FNN
Size of hidden layer	10
No. Delayed plant inputs	2
No. Delayed plant outputs	2
Training Samples	10,000
Validation Samples	10,000
Training Epochs	200
Training Function	trainlm

5.4 Training of the NN Predictive Model:

This part discusses the training of the three FNN prediction models for each MPC controller. Here the training data for each FNN prediction model are obtained by recording the controlling variables and the plant output concentrations during the running of the amine sweetening unit dynamic model. To develop those data driven input-output relationships, a fully connected feed-forward neural network is used in the plant identification sub-block in the NN Predictive Controller Simulink block.

- NN model relating controlling variable (DEA flow) and plant output (H2S):

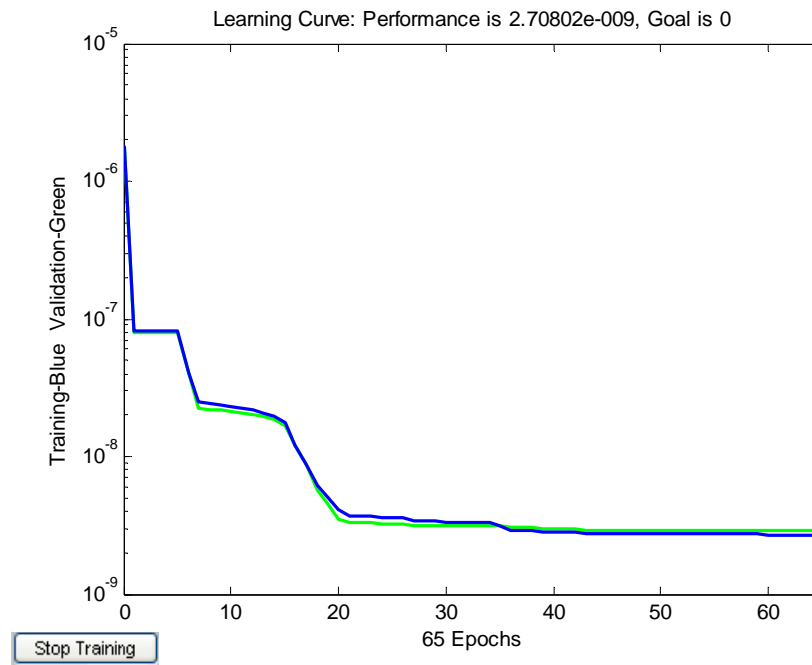


Figure 5.6 Learning Curve: NN model relating DEA flow & H2S

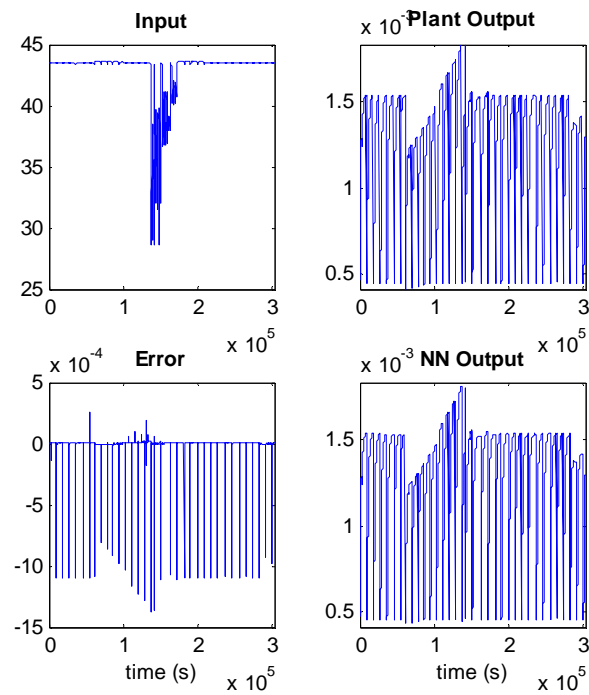


Figure 5.7 Training Data: NN model relating DEA flow & H2S

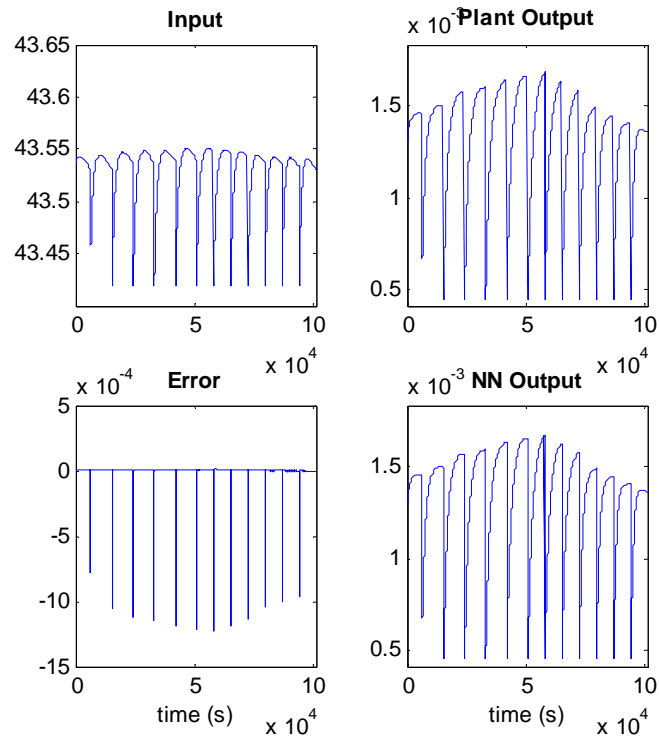


Figure 5.8 Validation Data: NN model relating DEA flow & H2S

- NN model relating controlling variable (DEA temperature) and plant output (H2S):

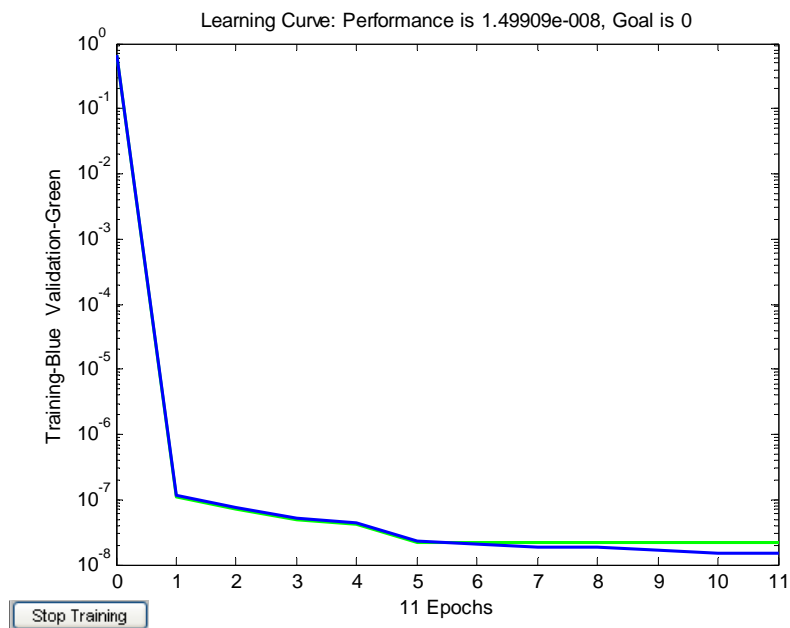


Figure 5.9 NN Model relating DEA temperature & H2S

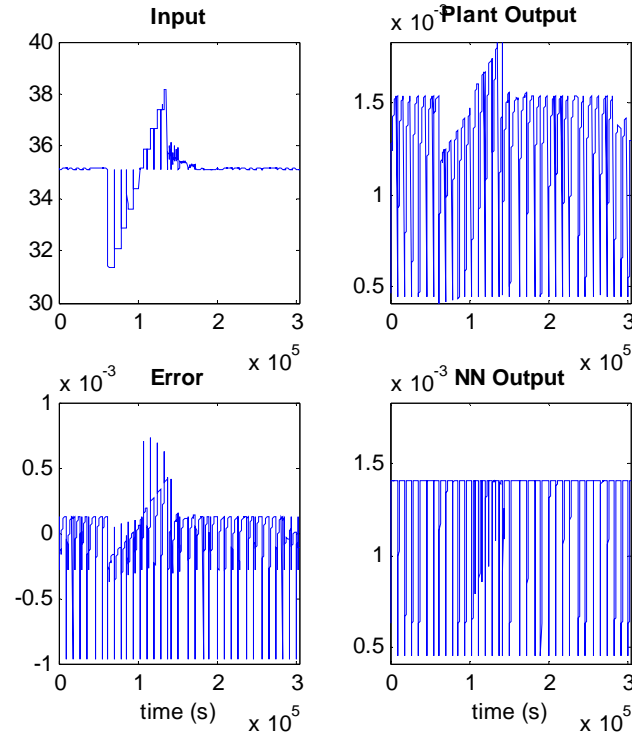


Figure 5.10 Training Data: NN model relating DEA Temp & H2S

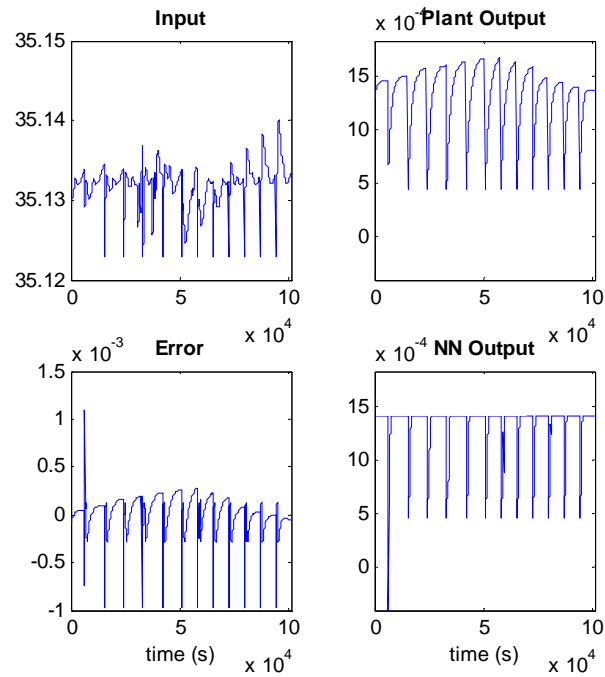


Figure 5.11 Validation Data: NN model relating DEA temp & H2S

- NN model relating controlling variable (reboiler duty) and plant output (H2S):

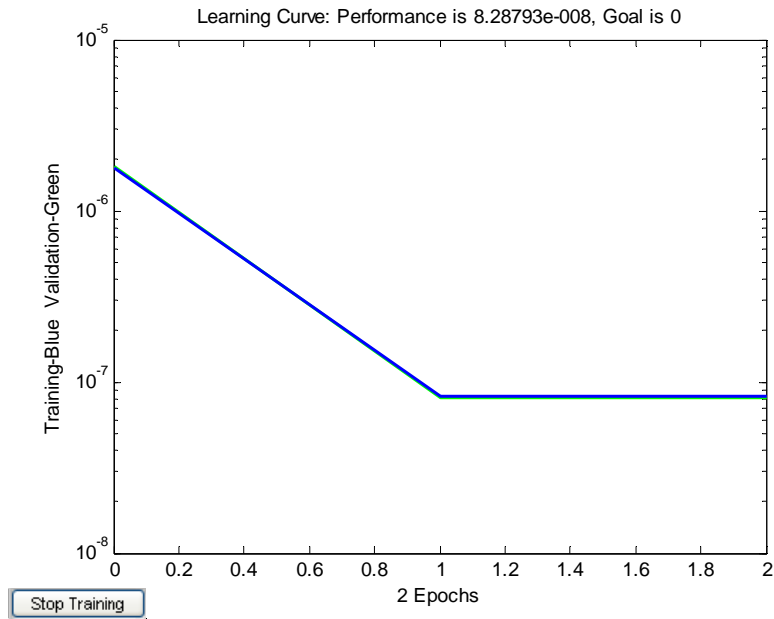


Figure 5.12 Learning Curve: NN model relating reboiler duty & H2S

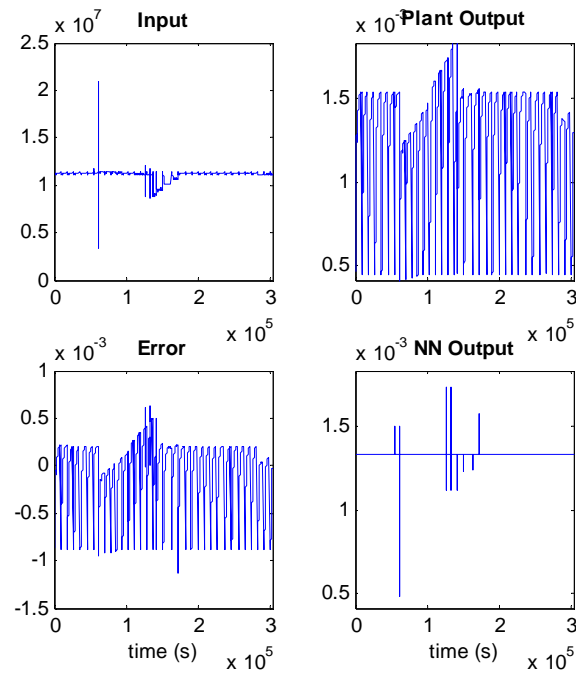


Figure 5.13 Training Data: NN model relating reboiler duty & H2S

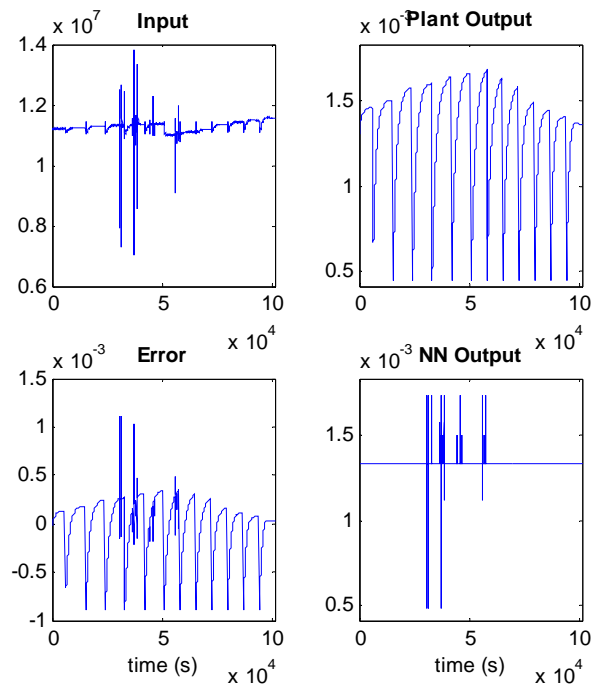


Figure 5.14 Validation Data: NN model relating reboiler duty & H2S

- NN model relating controlling variable (DEA flow) and plant output (CO2):

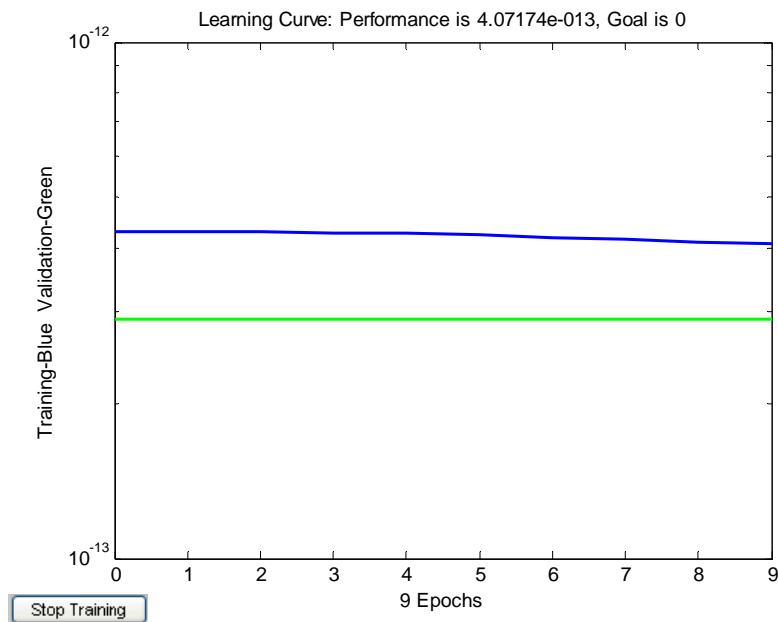


Figure 5.15 Learning Curve: NN model relating DEA flow & CO2

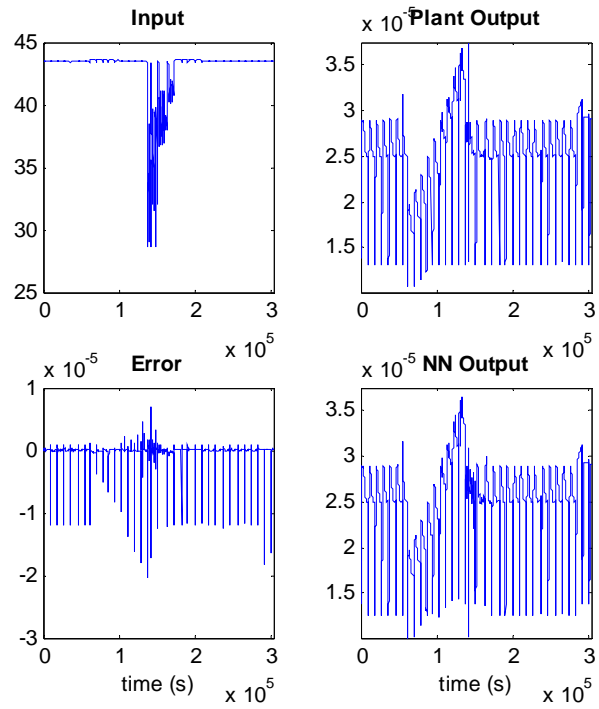


Figure 5.16 Training Data: NN model relating DEA flow & CO₂

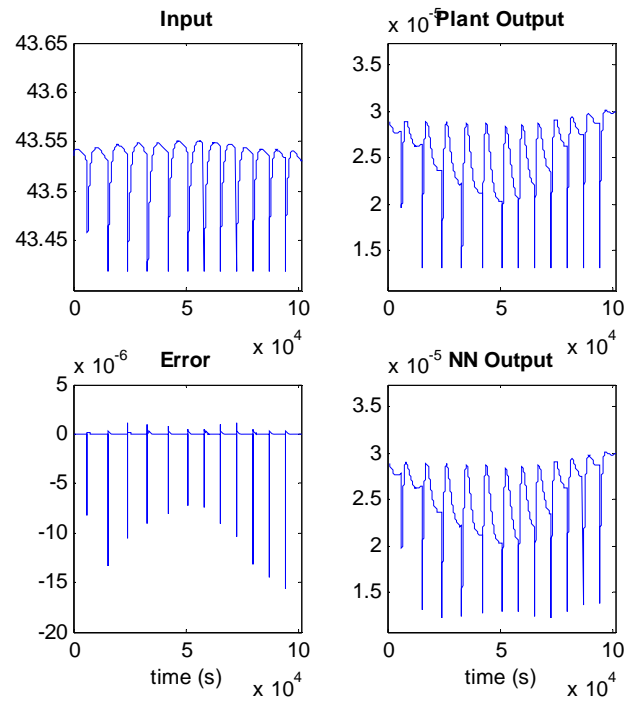


Figure 5.17 Validation Data: NN model relating DEA flow & CO₂

- NN model relating controlling variable (DEA temperature) and plant output (CO2):

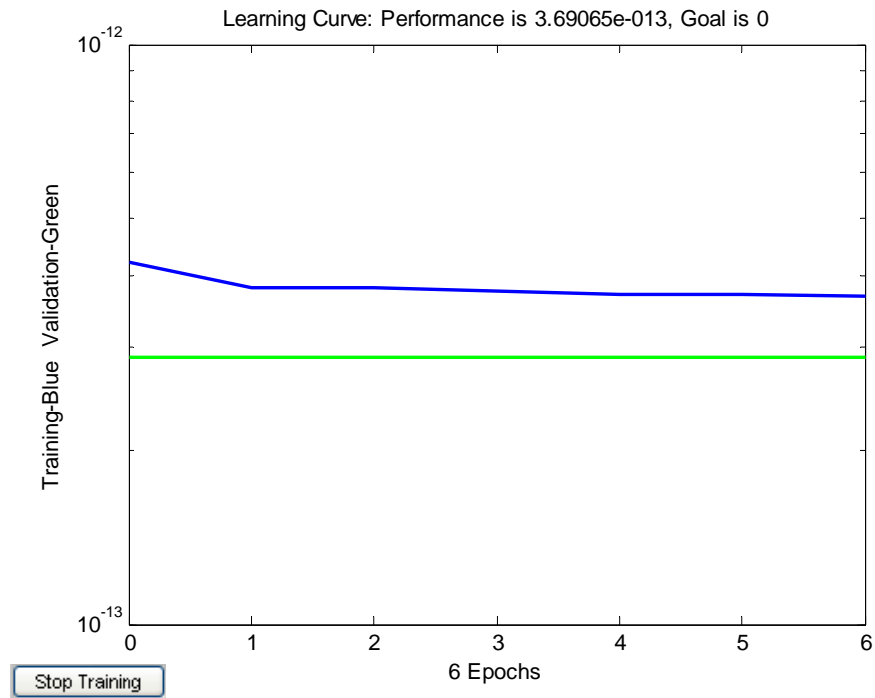


Figure 5.18 Learning Curve: NN model relating DEA temperature & CO2

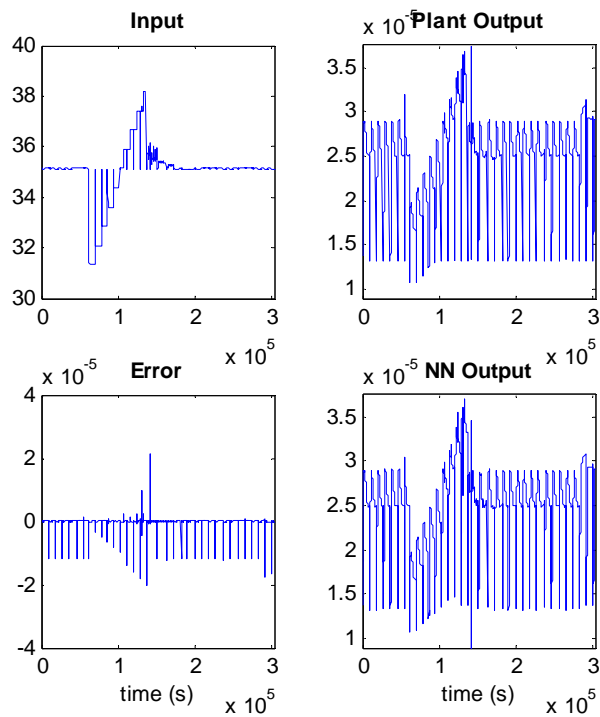


Figure 5.19 Training Data: NN model relating DEA temperature & CO2

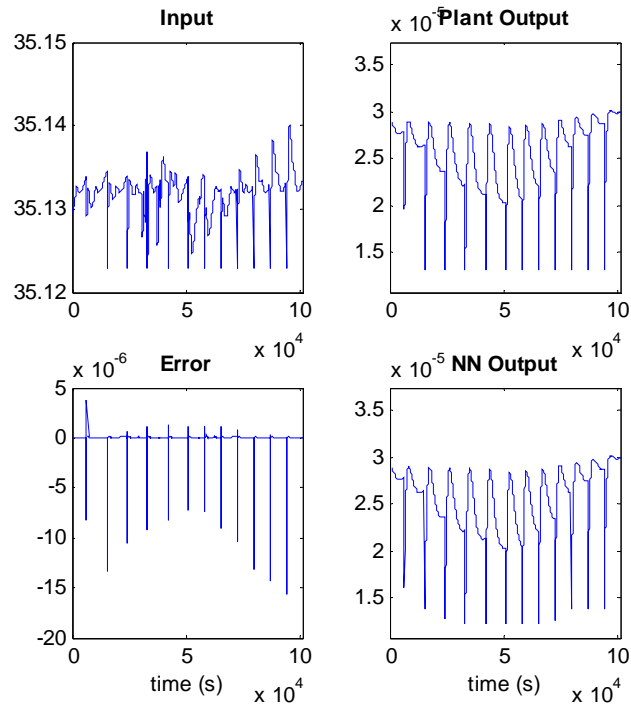


Figure 5.20 Validation Data: NN model relating DEA temp & CO2

- NN model relating controlling variable (reboiler duty) and plant output (CO2):

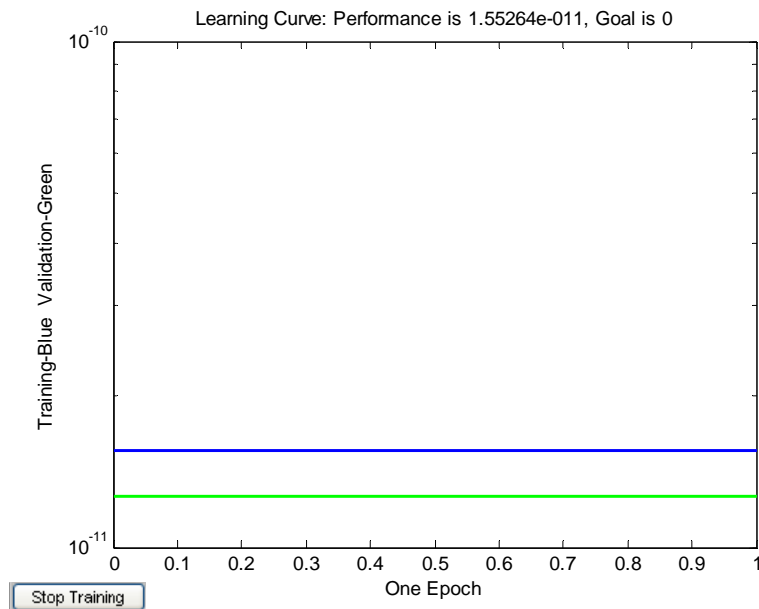


Figure 5.21 Learning Curve: NN model relating reboiler duty & CO2

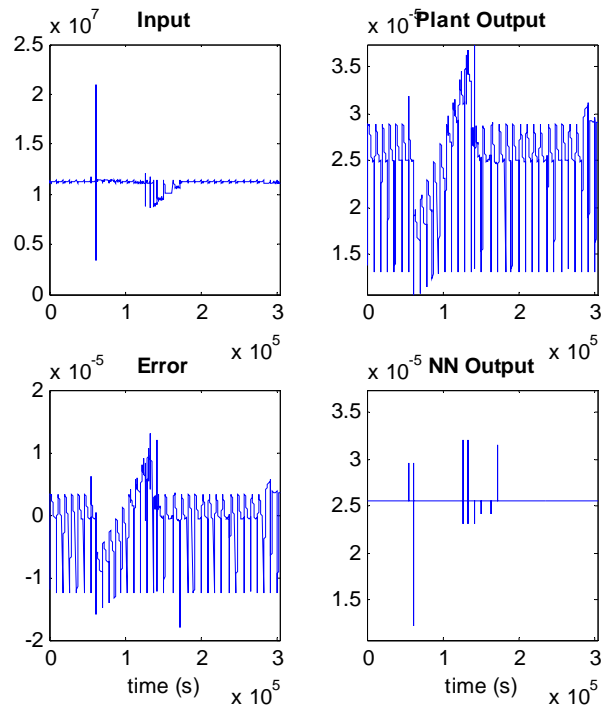


Figure 5.22 Training Data: NN model relating reboiler duty & CO2

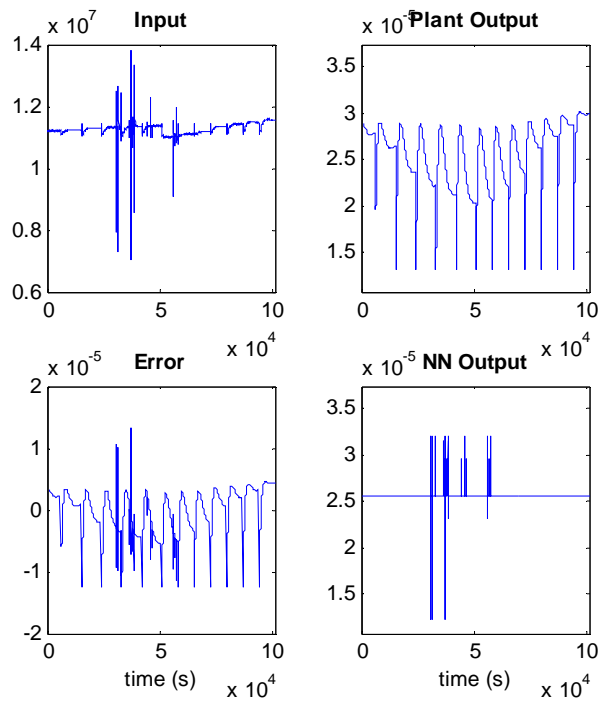


Figure 5.23 Validation Data: NN model relating reboiler duty & CO2

To model the dynamic behavior of the amine sweetening unit, six fully connected feed-forward neural networks are used in this section. Each FFN model has a structure of 1 input and 1 output as per the requirement of the Simulink block. One hidden layer with 40 neurons is used in the six concerned networks. The algorithm used to train the network is the standard back-propagation.

5.5 Simulation Results of NN-MPC:

There are three factors to be considered prior to implementing the proposed NN-MPC scheme in the amine absorption plant, namely; closed loop performance, stability, and computational efficiency. In general, using an infinite control and prediction horizon, i.e. T_c and T_p is desired to minimize the performance objective determined by the cost functional [28]. However, the open-loop control problem that must be solved on-line, is often formulated in a finite horizon manner and the input function is parameterized finitely, in order to allow a real-time numerical solution of the non-linear optimal control problem. Thus, it is desirable from a computational point of view to implement NN-MPC schemes using short horizons, but when a finite prediction horizon is used, the actual closed-loop actual trajectory will differ from the predicted open-loop trajectory, even if no model plant mismatch and no disturbances are present [23,28]. Accordingly, the computational power will determine the prediction horizon length required to avoid sacrificing stability and performance of NN-MPC scheme.

Using the optimization toolbox in MATLAB, two different prediction horizons are used in order to demonstrate the effect of horizon length on controller performance. This is conducted on the proposed NN-MPC scheme, shown in Fig 5.2, used to control H_2S

sweet gas concentration. The NN-MPC design parameters for short and long horizons are listed in Tables 5.2 and 5.3, respectively.

Table 5.2 Design Parameters for NN-MPC with short horizon

Prediction Horizon (T_p)	7
Control Horizon (T_c)	2
Control Weighting Factor	0.05
Searching Parameter	0.001

Table 5.3 Design Parameters for NN-MPC with long horizons

Prediction Horizon (T_p)	280
Control Horizon (T_c)	260
Control Weighting Factor	0.05
Searching Parameter	0.001

To test the performance of the proposed model predictive control strategy, the desired trajectories of plant outputs are generated by inputting the system a group of step excitations.

Table 5.3 shows the step changes carried out on the plant in order to monitor the tracking error of controlling H_2S sweet gas concentration. The tracking error represents the difference between the actual and desired concentrations.

Table 5.4 Step excitations for test case

Variable	Unit	Initial Value	Final Value
Feed Flow Rate	kgmoles/hr	1220	1240
H ₂ S Mole Fraction in Feed Gas	weight percent	0.014	0.018
CO ₂ Mole Fraction in Feed Gas	weight percent		

Table 5.5 Desired values for H₂S and CO₂ in the sweet gas stream

Variable	Unit	Initial Value	Final Value
Desired H ₂ S	ppm	0.0018	
Desired CO ₂	ppm	0.000037	

It is to be noted that CO_2 mole fraction in the feed gas was set unchanged in evaluating NN-MPC performance for H_2S control because it was concluded from Chapter 3 that it is not a main factor contributing to H_2S sweet gas concentration. On the other side, H_2S mole fraction in the feed gas was fixed in testing the performance of NN-MPC for CO_2 control in the sweet gas

5.5.1 Performance Test for NN-MPC Scheme Controlling H₂S Sweet Gas Concentration:

- Feed Flow Rate:

Figs 5.24-26 show the dynamic behavior of the system controlling parameters is presented in response to a step change in feed flow rate carried out on NN-MPC scheme with short horizon

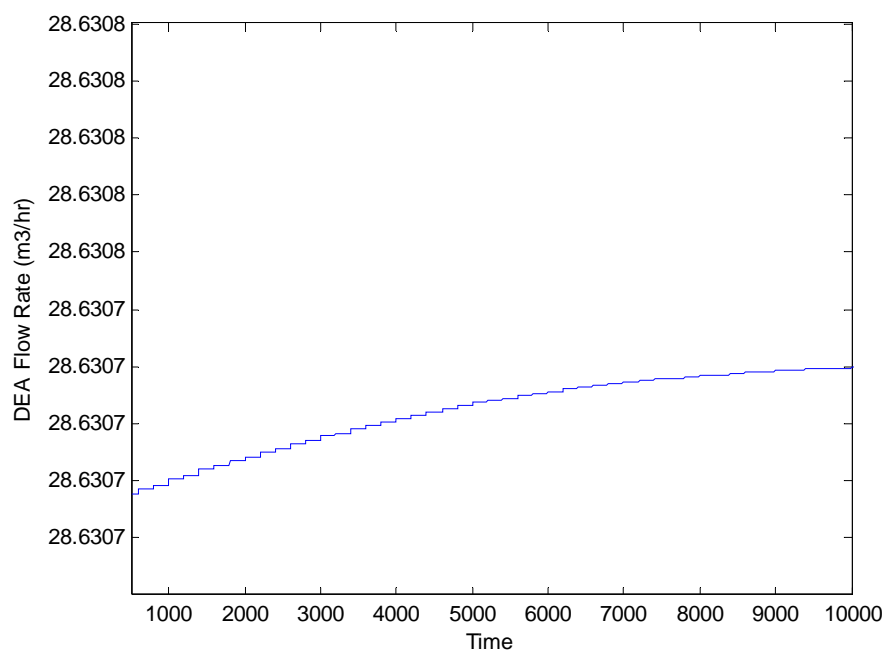


Figure 5.24 Dynamic profile of DEA flow rate in response to step change in feed flow rate (short horizon of H2S NN-MPC)

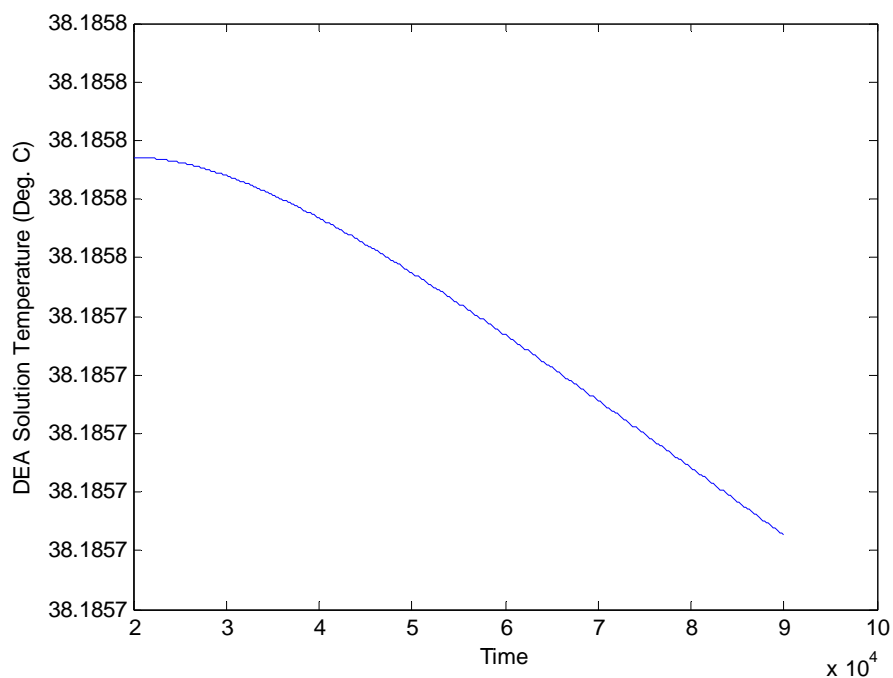


Figure 5.25 Dynamic profile of DEA temperature in response to step change in feed flow rate (short horizon of H2S NN-MPC)

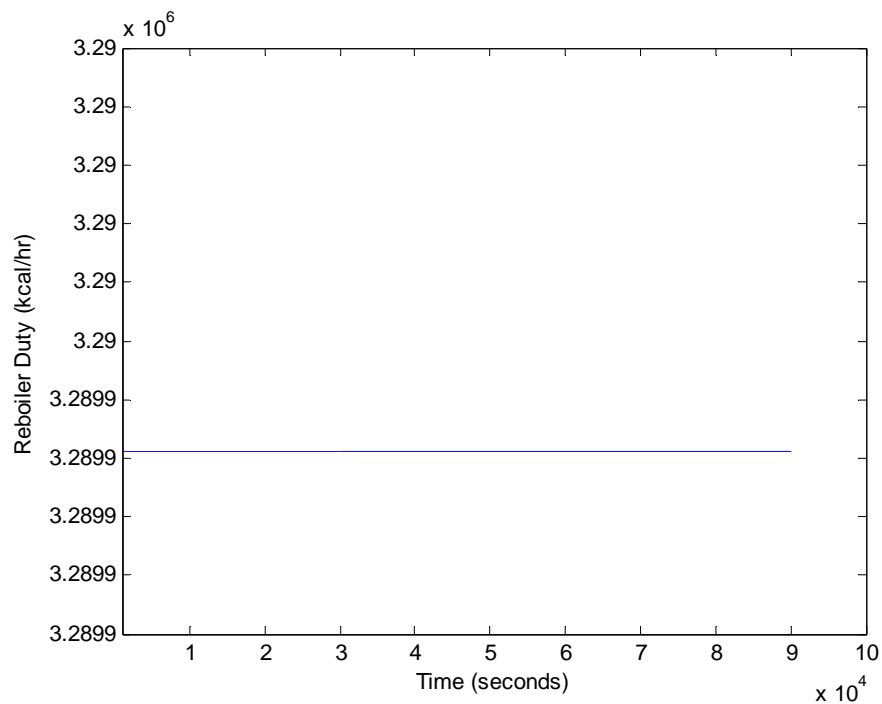


Figure 5.26 Dynamic profile of reboiler duty in response to step change in feed flow rate (short horizon of H₂S NN-MPC)

The dynamic behavior of H_2S sweet gas concentration, associated with a short horizon specification, in response to above mentioned step change in feed flow rate is shown in

Fig. 27

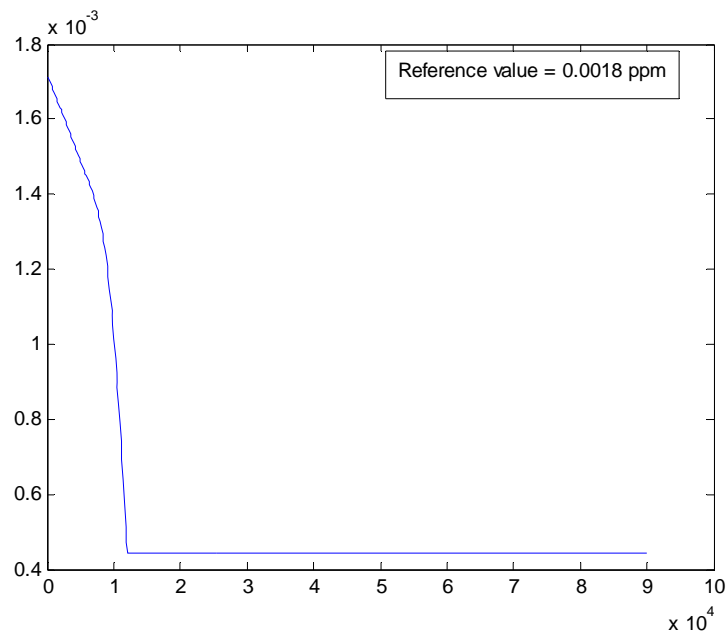


Figure 5.27 Dynamic profile of H₂S sweet gas concentration in response to step change in feed flow rate for NN-MPC with short horizon

The dynamic profile of system controlling parameters after increasing the length of prediction and control horizons are presented in Figs 5. 28-30

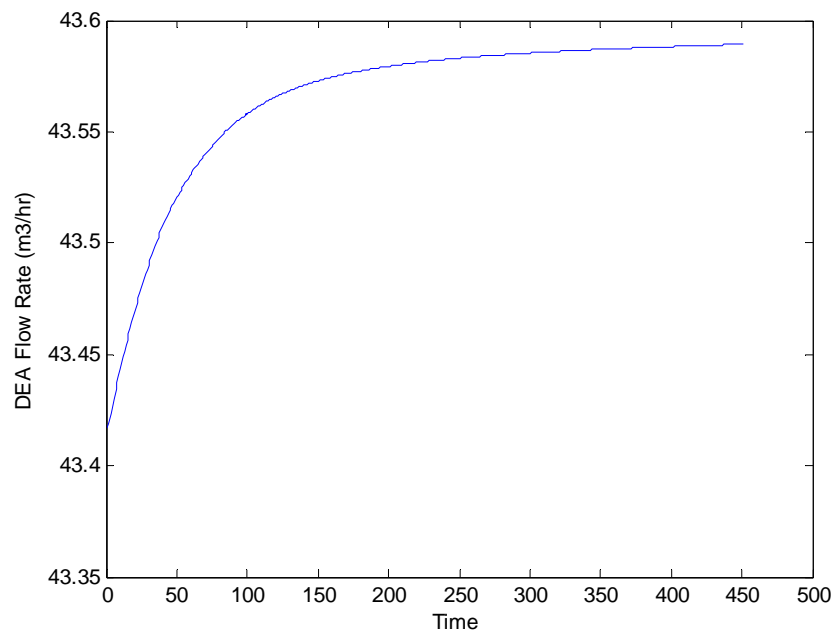


Figure 5.28 Dynamic profile of DEA flow rate in response to step change in feed flow rate (long horizon of H₂S NN-MPC)

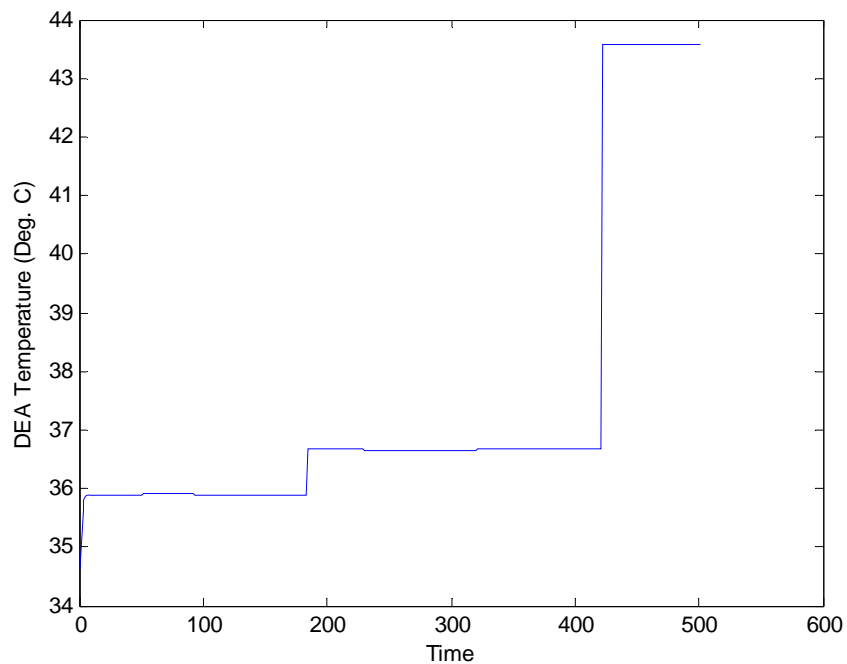


Figure 5.29 Dynamic profile of DEA temperature in response to step change in feed flow rate (long horizon of H₂S NN-MPC)

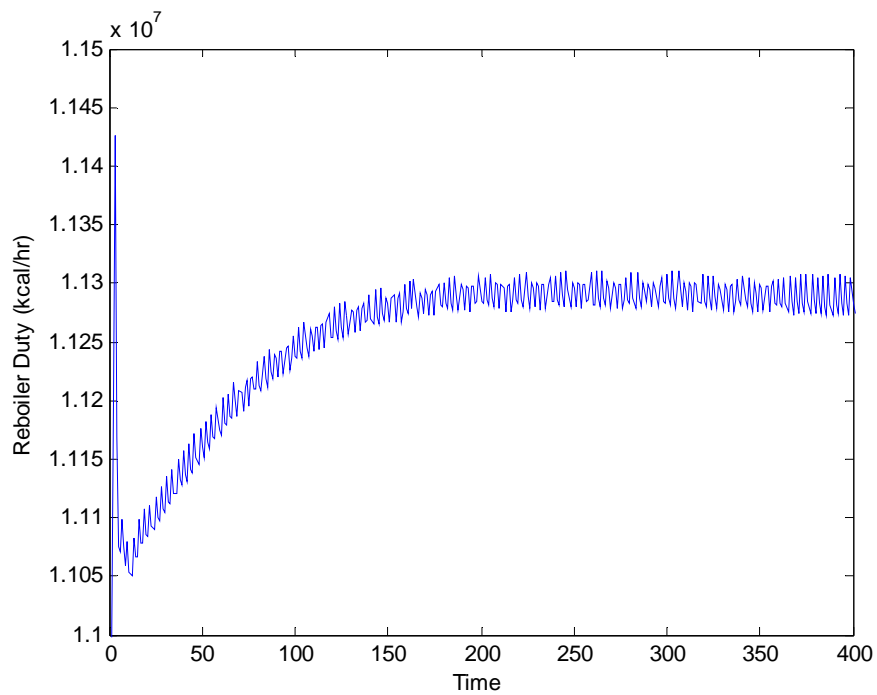


Figure 5.30 Dynamic profile of reboiler duty in response to step change in feed flow rate (long horizon of H₂S NN-MPC)

The improvement in tracking error reduction between actual and desired H_2S can be seen in Fig 5.31

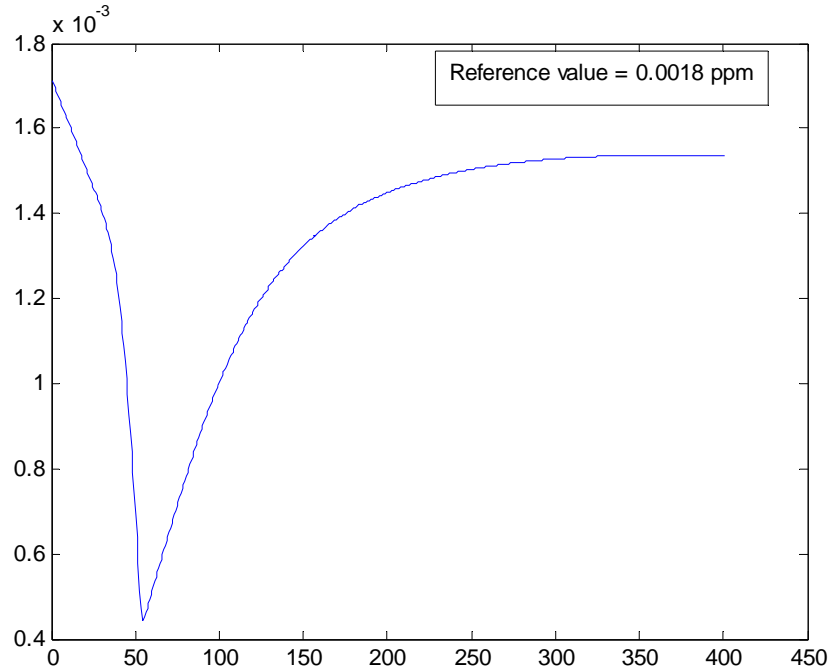


Figure 5.31 Dynamic profile H_2S sweet gas concentration in response to step change in feed flow rate for NN-MPC with long horizon

- H_2S Mole Fraction in Feed Gas:

The dynamic behavior of amine plant controlling variables with response to a step change in H_2S mole fraction in the feed gas from 0.0172 to 0.01972 weight percent is demonstrated in Figs 5.32-34. Those dynamic responses are for short prediction and control horizons of NN-MPC

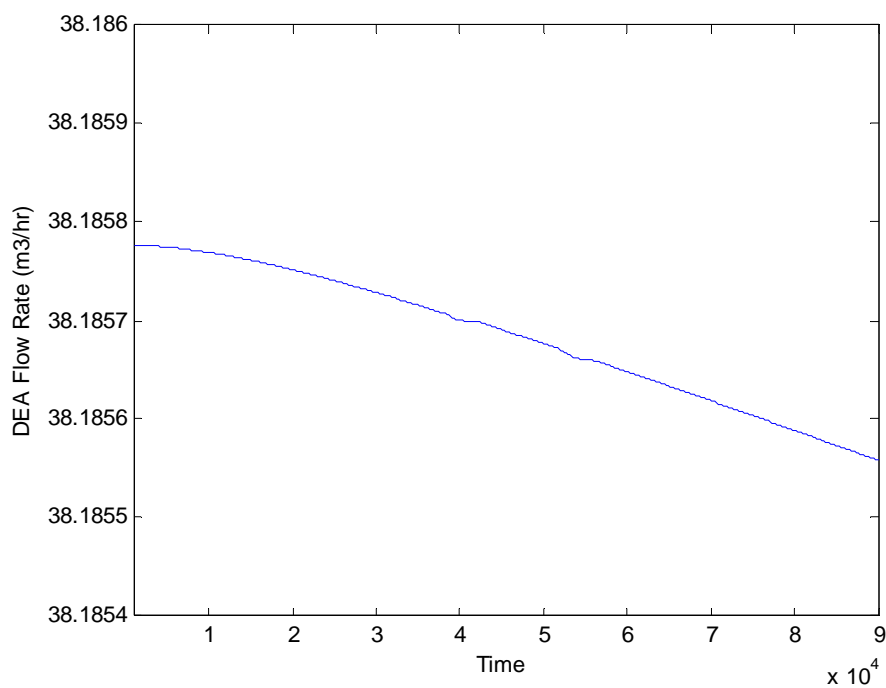


Figure 5.32 Dynamic profile of DEA flow rate in response to step change in H2S feed mole fraction (short horizon of H2S NN-MPC)

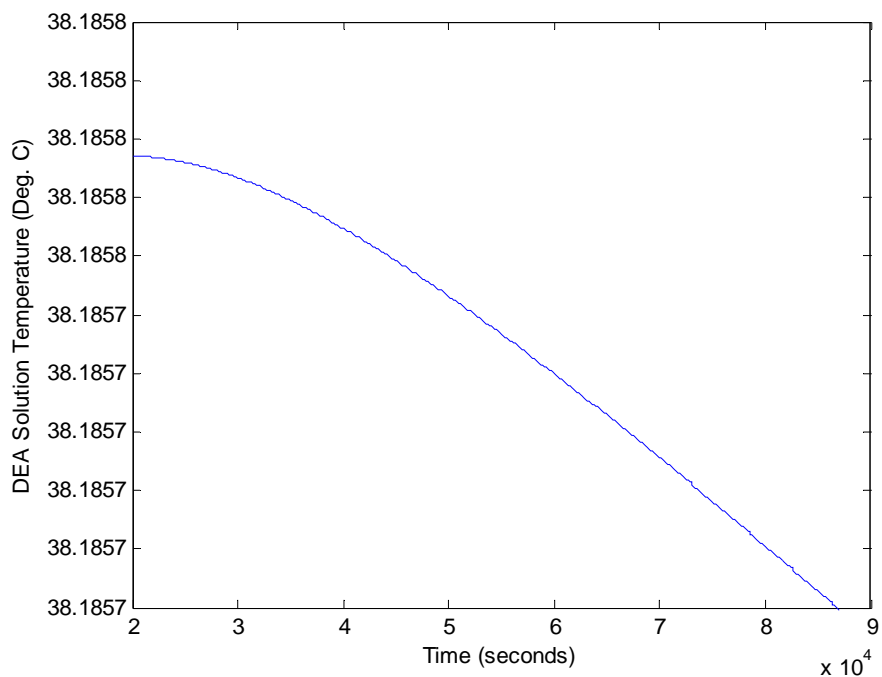


Figure 5.33 Dynamic profile of DEA temperature in response to step change in H2S feed mole fraction (short horizon of H2S NN-MPC)

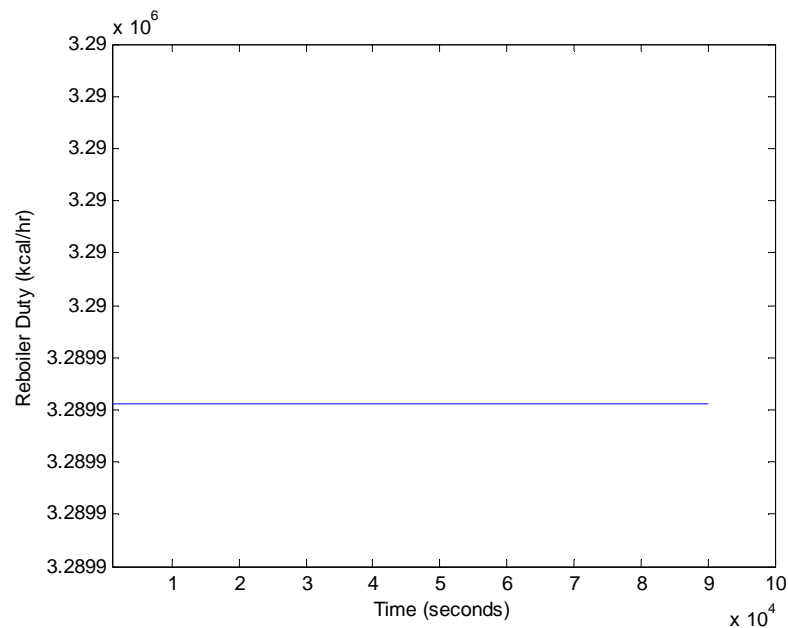


Figure 5.34 Dynamic profile of reboiler duty in response to step change in H2S feed mole fraction (short horizon of H2S NN-MPC)

The high tracking error, shown in Fig 5.35, indicated that the length of the specified horizon is not adequate

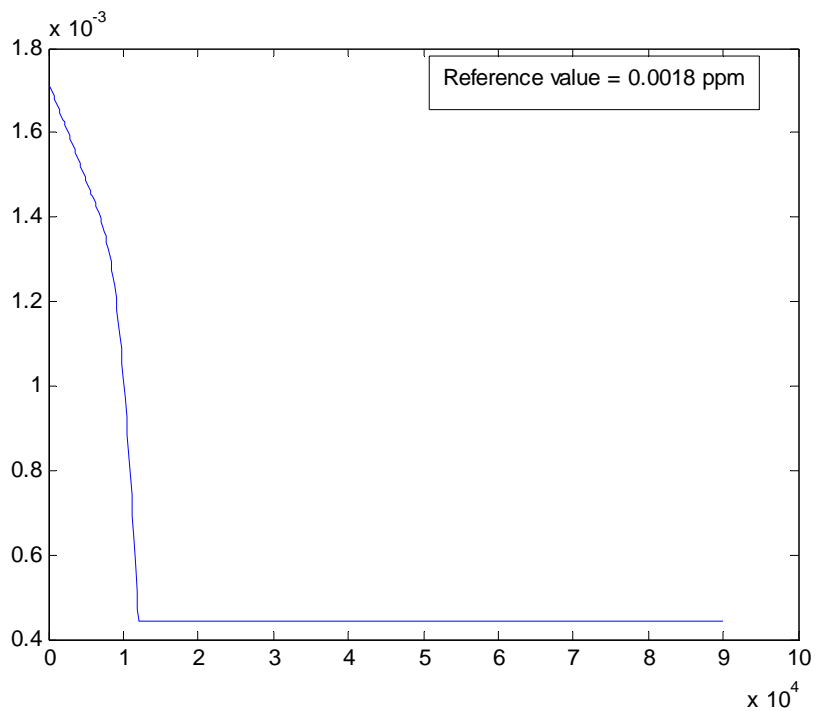


Figure 5.35 Dynamic profile of H2S sweet gas concentration in response to step change in H2S feed mole fraction (short horizon of H2S NN-MPC)

Subsequent to resetting the prediction and control horizons to 280 and 260, respectively, the tracking error has dropped significantly. Figs 5.36-38 show the dynamic behavior of the system controlling variables and Fig 5.39 shows the corresponding H_2S sweet gas concentration

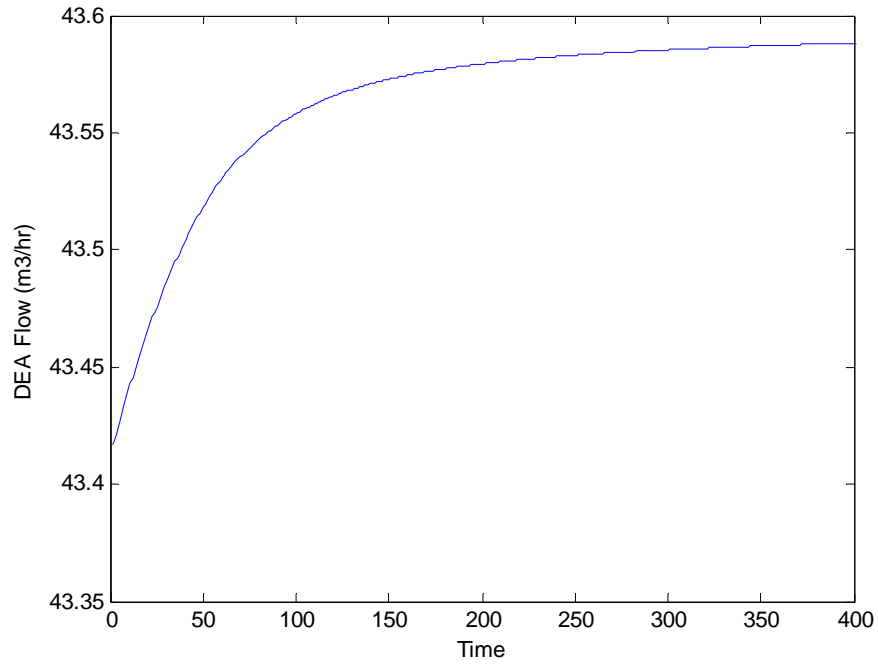


Figure 5.36 Dynamic profile of DEA flow rate in response to step change in H_2S feed mole fraction (long horizon of H_2S NN-MPC)

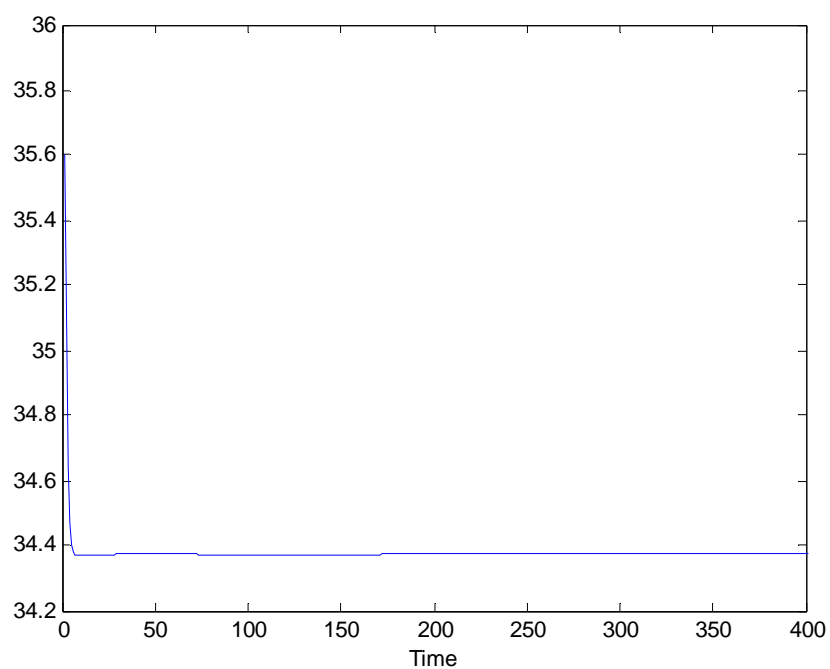


Figure 5.37 Dynamic profile of DEA temperature in response to step change in H₂S feed mole fraction (long horizon of H₂S NN-MPC)

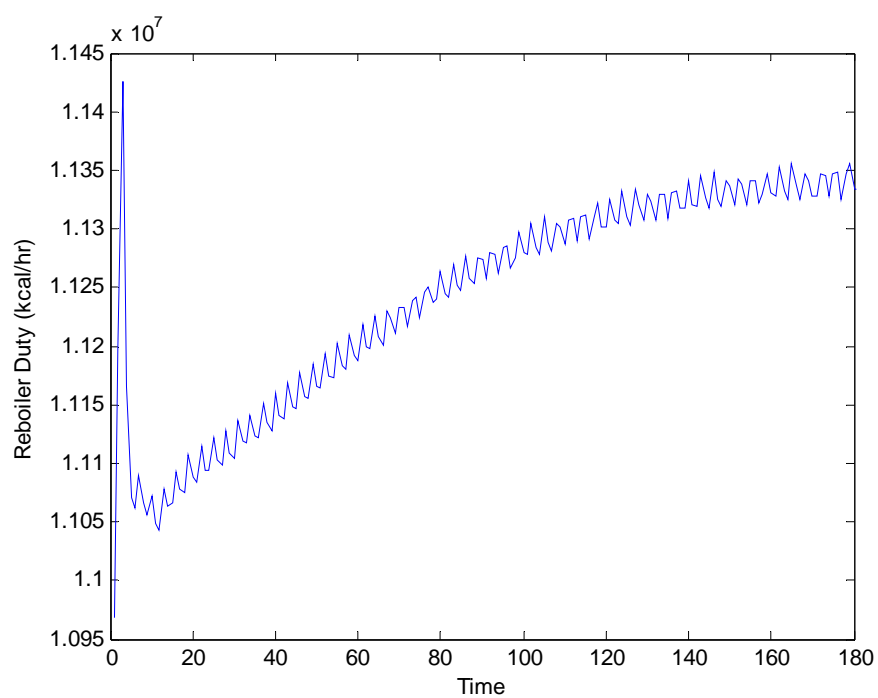


Figure 5.38 Dynamic profile of reboiler duty in response to step change in H₂S feed mole fraction (long horizon of H₂S NN-MPC)

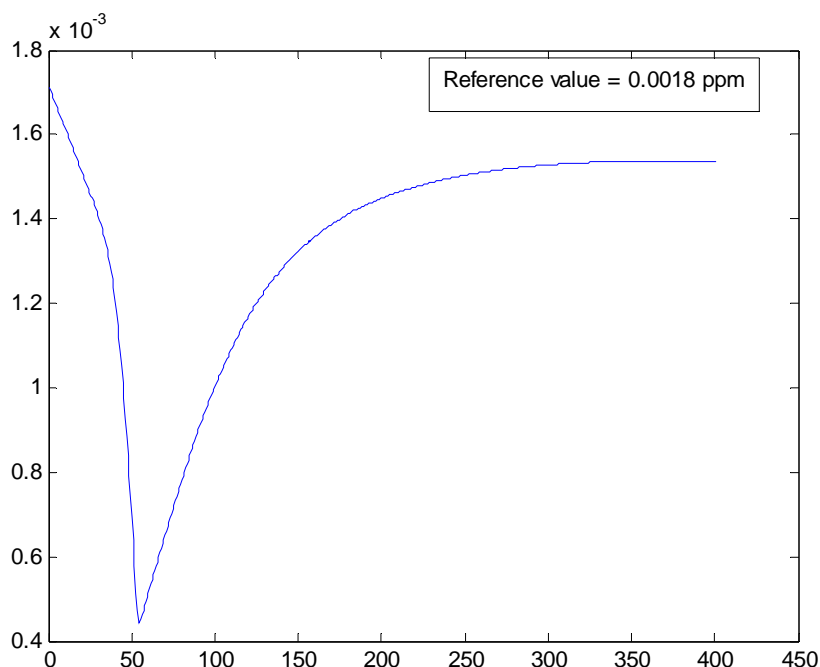


Figure 5.39 Dynamic profile of H₂S sweet gas concentration in response to step change in H₂S feed mole fraction (long horizon of H₂S NN-MPC)

5.5.2 Performance Test for NN-MPC Scheme Controlling CO₂ Sweet Gas Concentration:

Next, the performance of NN-MPC controlling CO₂ composition in sweet gas is evaluated by applying step changes, listed in Table 5.4, in feed flow rate and CO₂ mole fraction in the feed gas. The lengths of prediction and control horizons utilized in this performance test are those in Tables 5.2 and 5.3 for short and long horizons, respectively. The dynamic behavior of amine sweetening unit controlling variables, with short horizon specification, in response to step change in feed flow rate are shown in Figs 5.40-42

• Feed Flow Rate:

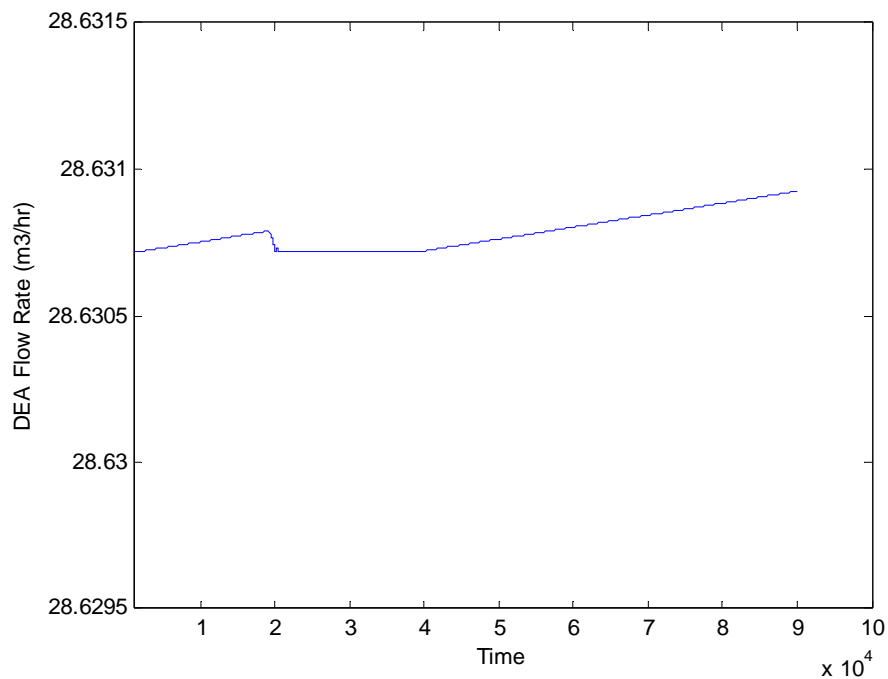


Figure 5.40 Dynamic profile of DEA flow rate in response to step change in feed flow rate (short horizon of CO₂ NN-MPC)

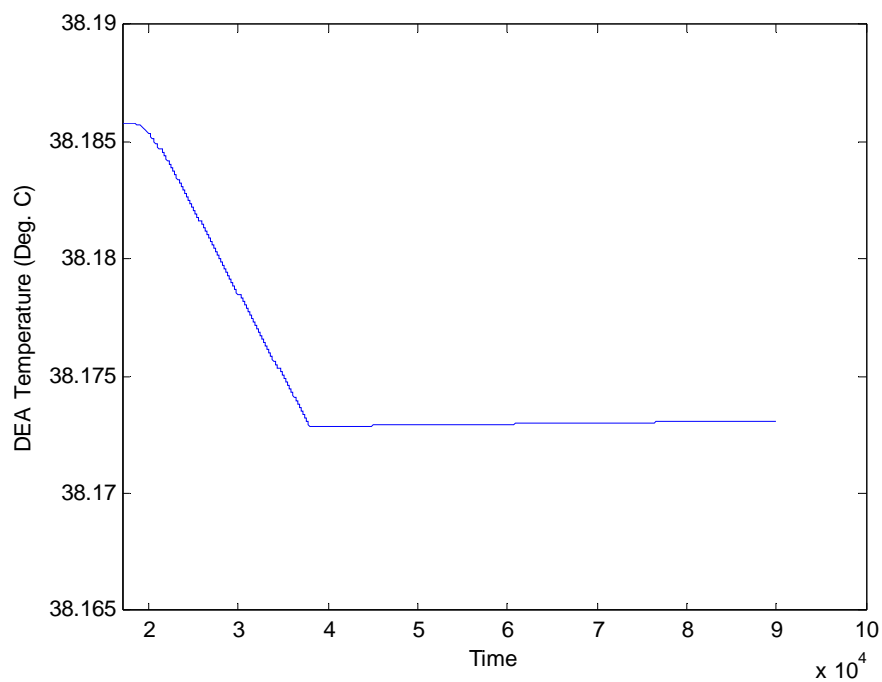


Figure 5.41 Dynamic profile of DEA temperature in response to step change in feed flow rate (short horizon of CO₂ NN-MPC)

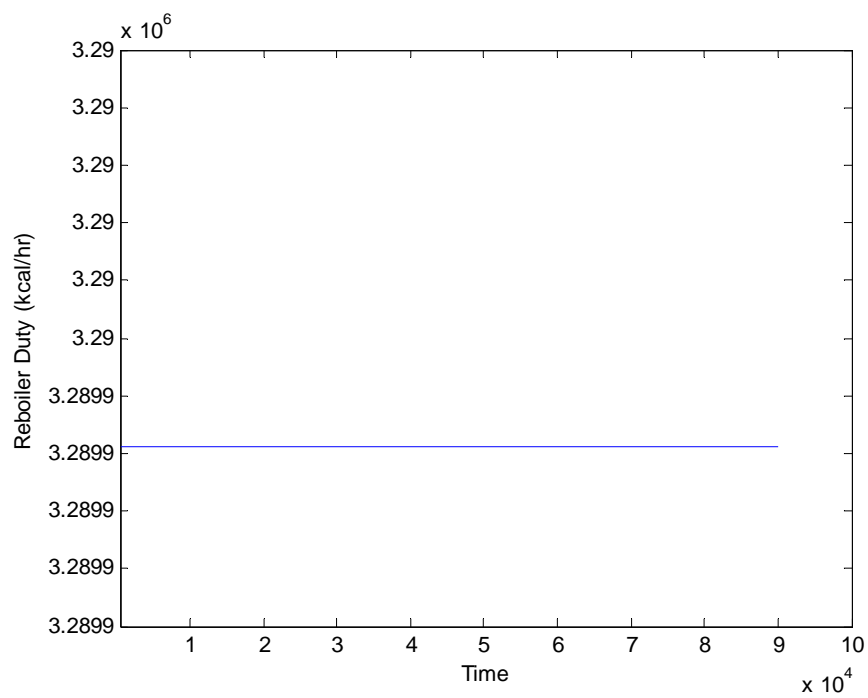


Figure 5.42 Dynamic profile of reboiler duty in response to step change in feed flow rate (short horizon of CO₂ NN-MPC)

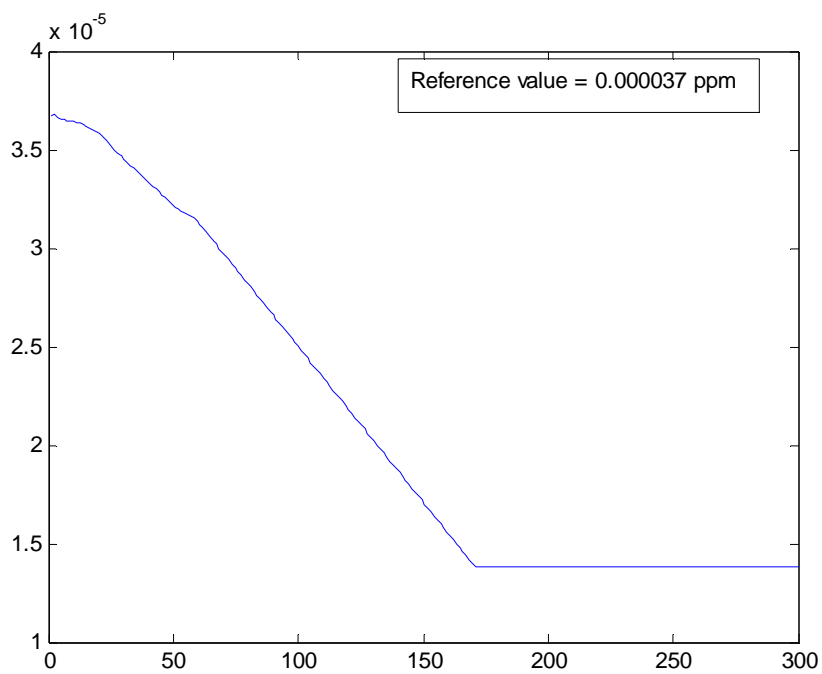


Figure 5.43 Dynamic profile of CO₂ sweet gas concentration in response to step change in feed flow rate (short horizon of CO₂ NN-MPC)

In order to overcome the NN-MPC mal-performance, shown in Fig 5.43, longer prediction and control horizons were used. Figs 5.44-46 show the dynamic behavior of amine plant control variables in response to the same step change applied earlier on feed flow rate. The CO_2 sweet gas composition is shown in Fig 5.47

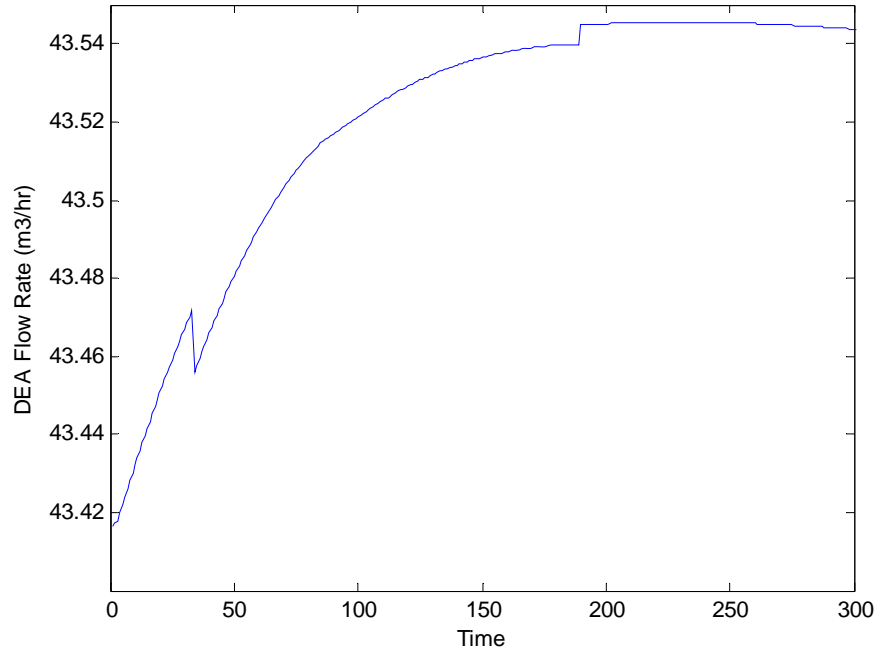


Figure 5.44 Dynamic profile of DEA flow rate in response to step change in feed flow rate (long horizon of CO_2 NN-MPC)

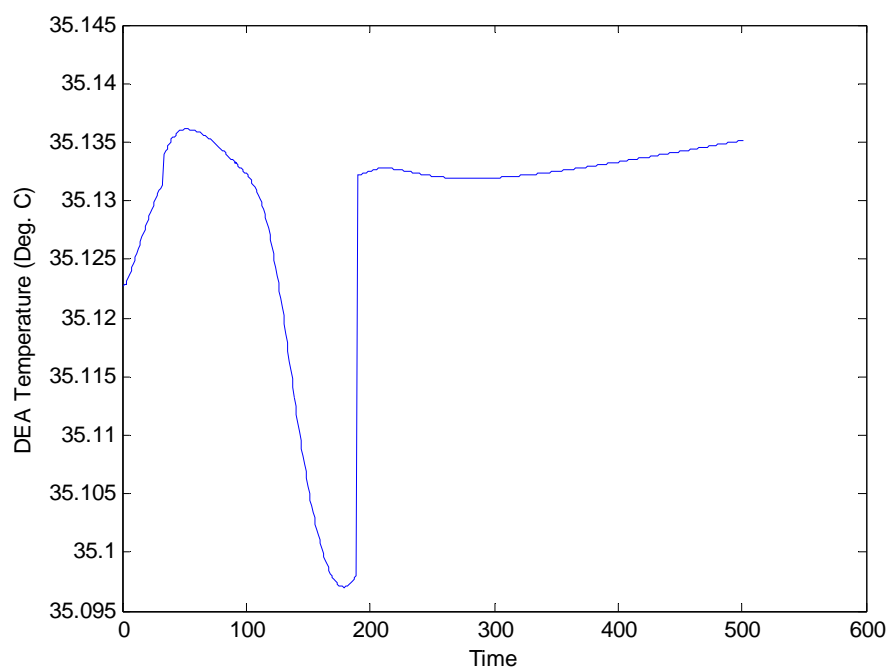


Figure 5.45 Dynamic profile of DEA temperature in response to step change in feed flow rate (long horizon of CO₂ NN-MPC)

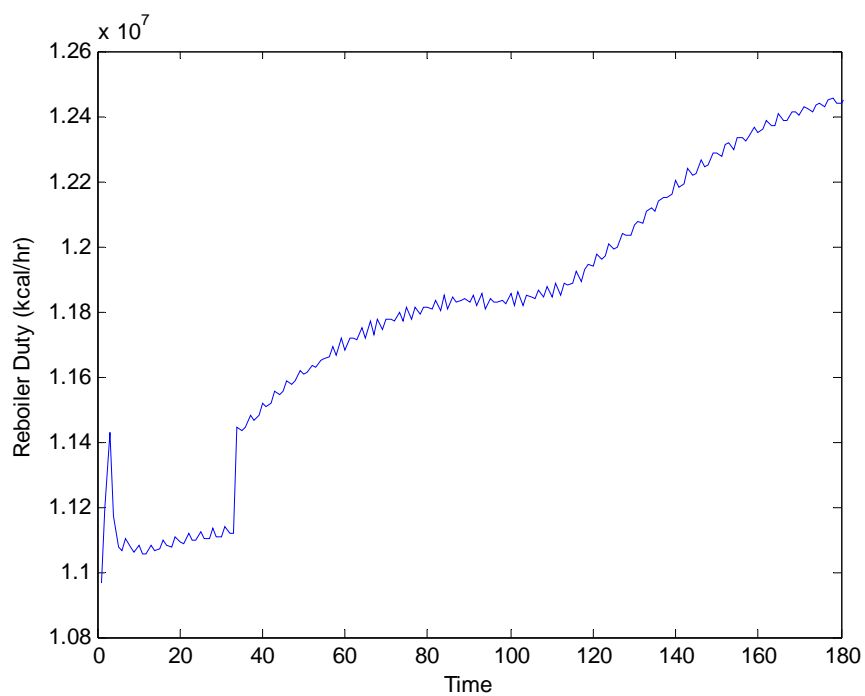


Figure 5.46 Dynamic profile of reboiler duty in response to step change in feed flow rate (long horizon of CO₂ NN-MPC)

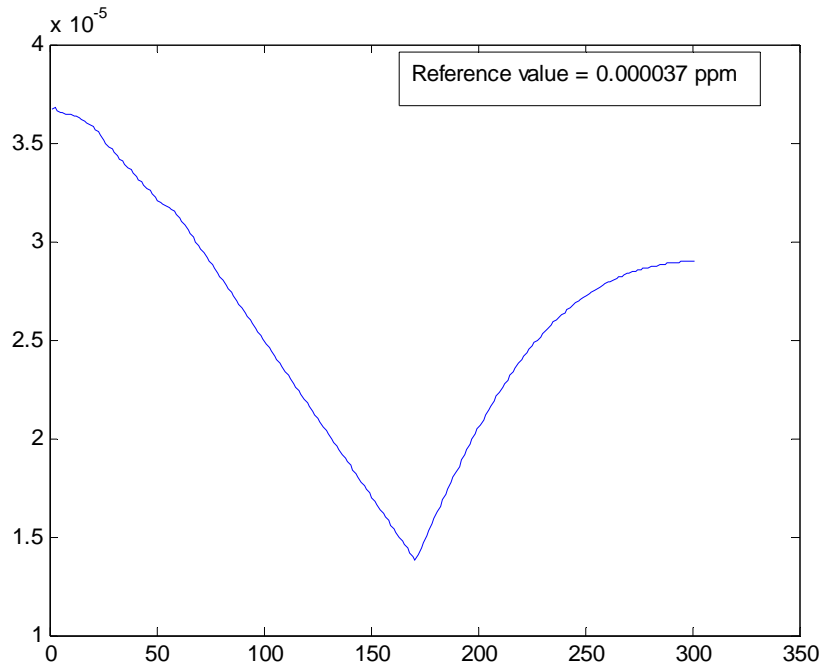


Figure 5.47 Dynamic profile of CO₂ sweet gas concentration in response to step change in feed flow rate (long horizon of CO₂ NN-MPC)

• CO₂ Mole Fraction in Feed Gas:

Figs 5.48-50 show the dynamic responses of system control variables in response to a step change in CO₂ mole fraction in the feed gas with short horizons specified for NN-MPC and Fig 5.51 shows the CO₂ sweet gas concentration.

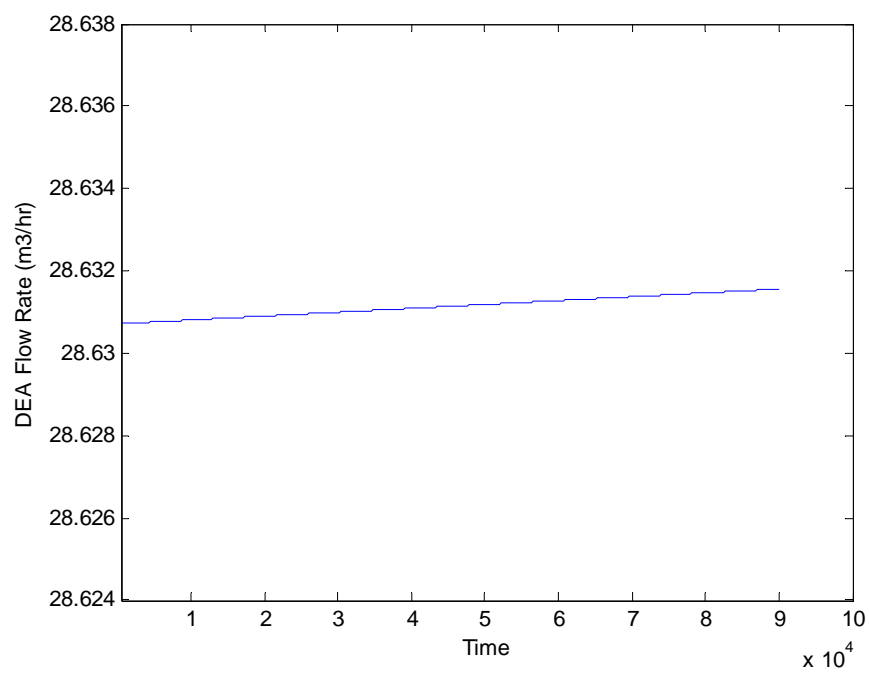


Figure 5.48 Dynamic profile of DEA flow rate in response to step change in CO₂ feed mole fraction (short horizon of CO₂ NN-MPC)

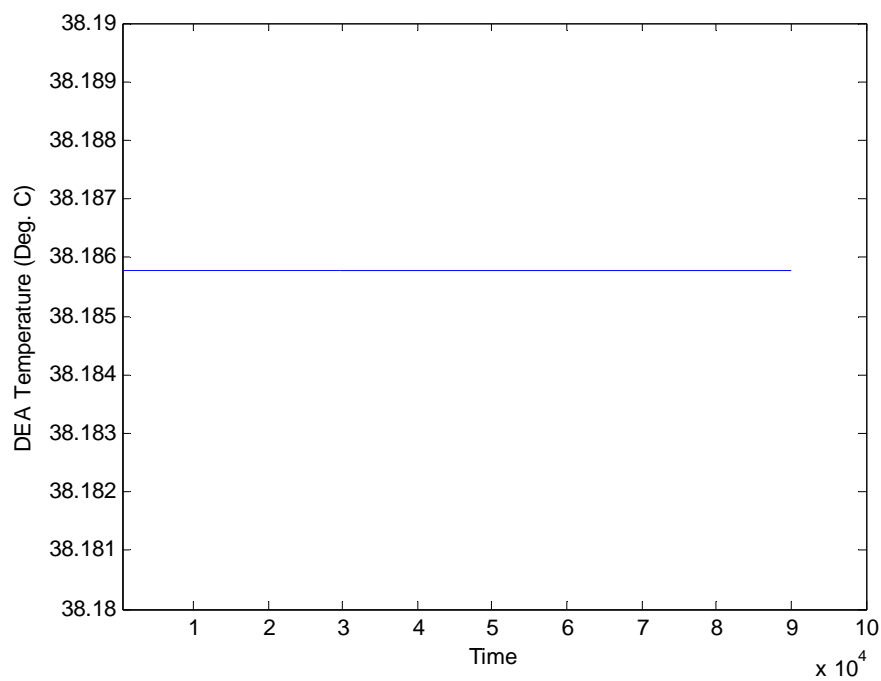


Figure 5.49 Dynamic profile of DEA temperature in response to step change in CO₂ feed mole fraction (short horizon of CO₂ NN-MPC)

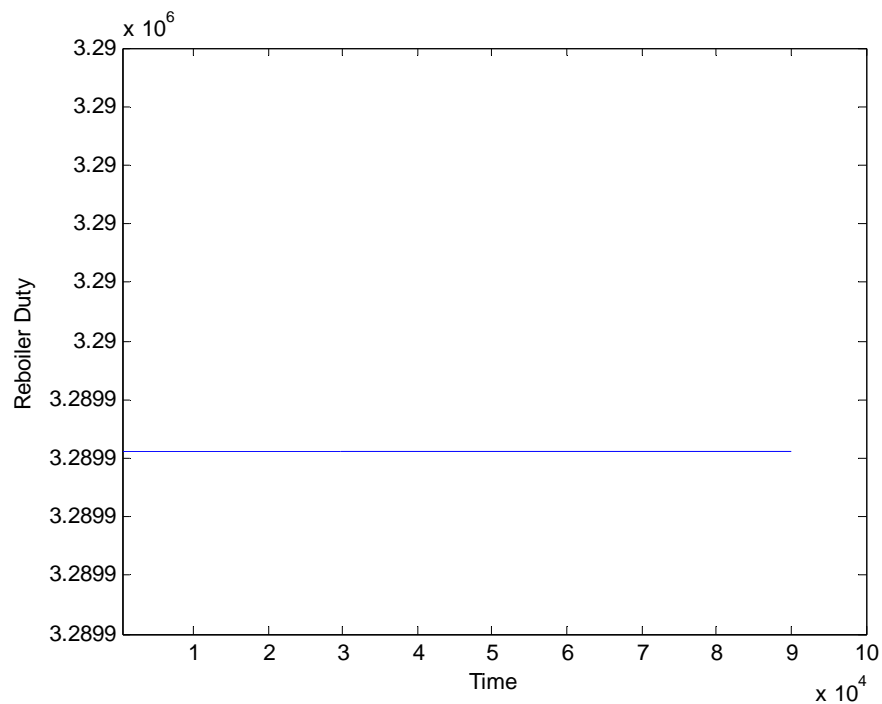


Figure 5.50 Dynamic profile of reboiler duty in response to step change in CO₂ feed mole fraction (short horizon of CO₂ NN-MPC)

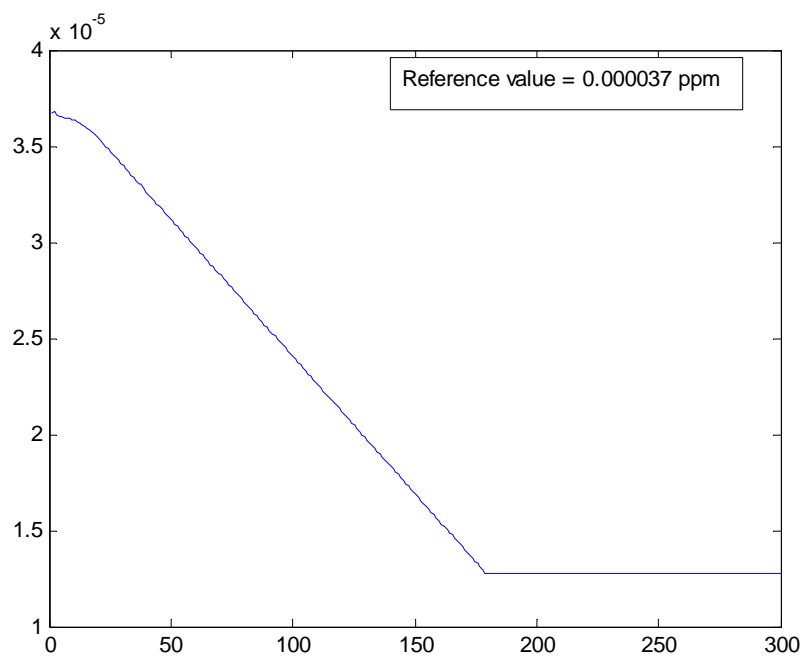


Figure 5.51 Dynamic profile of CO₂ sweet gas concentration in response to step change in CO₂ feed mole fraction (short horizon of CO₂ NN-MPC)

Next, longer horizons are used to increase the efficiency of CO_2 NN-MPC. The prediction and control horizons are set to 280 and 260, respectively.

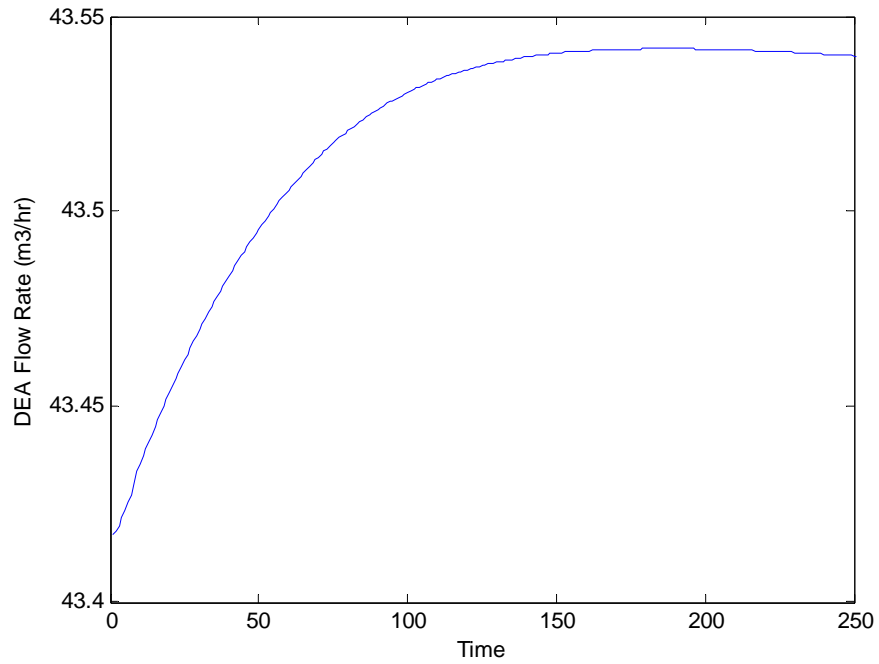


Figure 5.52 Dynamic profile of DEA flow rate in response to step change in CO_2 feed mole fraction (long horizon of CO_2 NN-MPC)

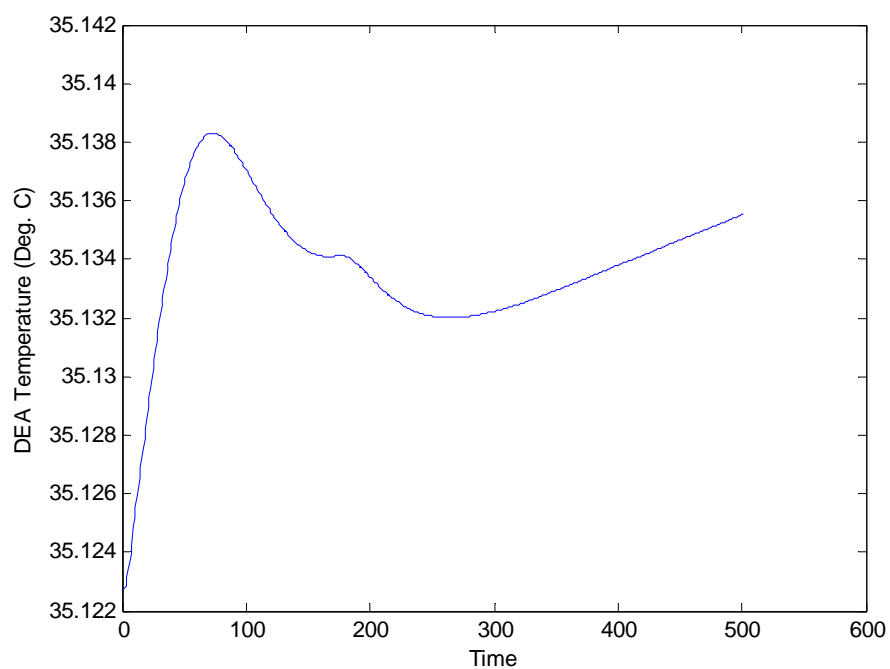


Figure 5.53 Dynamic profile of DEA temperature in response to step change in CO₂ feed mole fraction (long horizon of CO₂ NN-MPC)

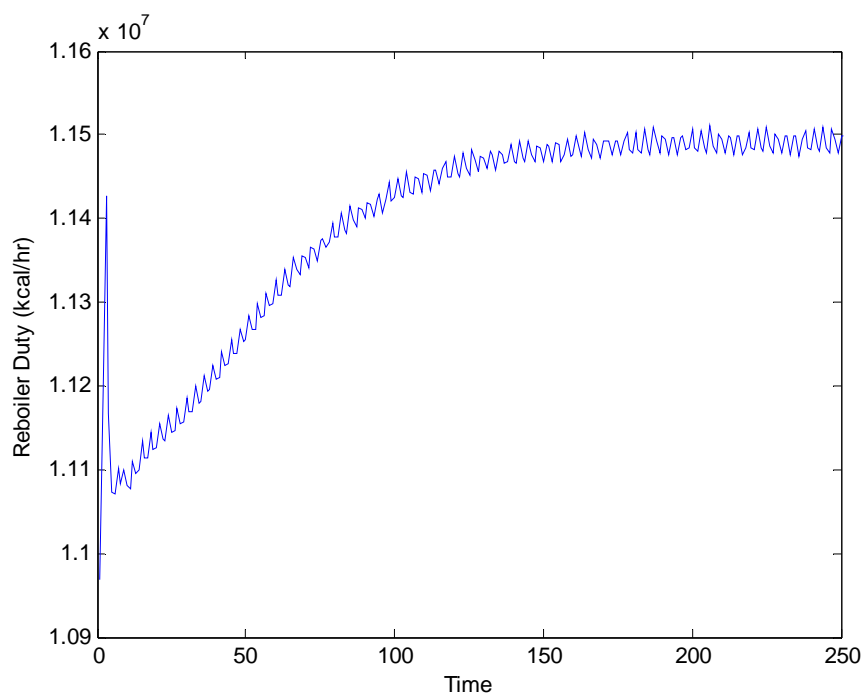


Figure 5.54 Dynamic profile of reboiler duty in response to step change in CO₂ feed mole fraction (long horizon of CO₂ NN-MPC)

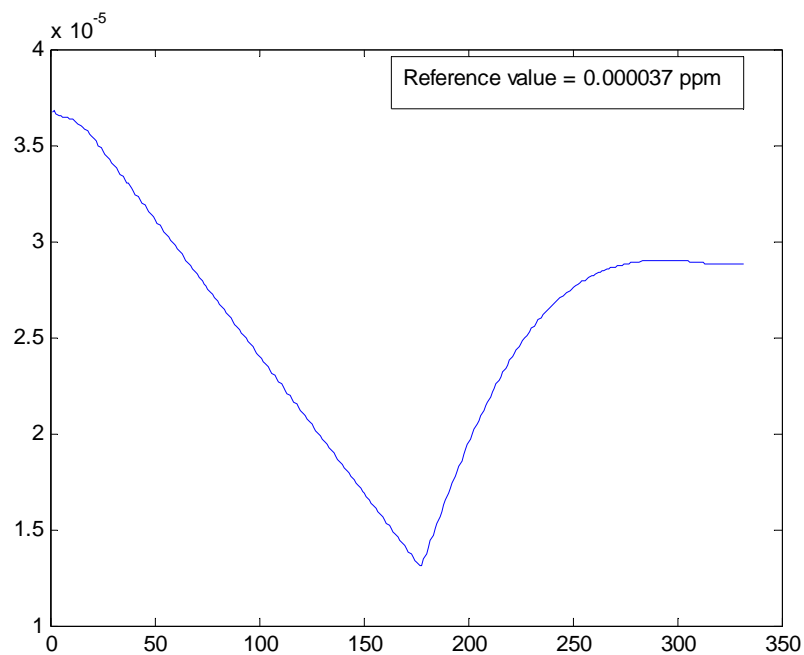


Figure 5.55 Dynamic profile of CO₂ sweet gas concentration in response to step change in CO₂ feed mole fraction (long horizon of NN-MPC)

6.0 Conclusion and Recommendations

6.1 Summary and Conclusions:

In this thesis a dynamic rigorous model of amine sweetening unit was built using HYSYS. This simulation model was treated as the “real” plant after it had been validated. Steady state and dynamic analysis and control system design were carried out utilizing this simulation model.

The MPC model based control strategy was applied to amine absorption plant with view to control H_2S and CO_2 composition in sweet gas. Process modeling is required for MPC control. However, rigorous mechanistic model can not be used for implementation of MPC because of computational limitation. Therefore, neural network technique for modeling has been developed for amine sweetening plant. Feed-forward neural network (FNN) has been employed for deriving input-output prediction model. The input-output data to train this FNN model were extracted from the dynamic responses calculated by HYSYS dynamic simulation. Obtaining a Recurrent Neural Network (RNN) model was not a feasible option in this application because of its long computational time. Moreover, the large scale of data and high number of system parameters limited the choice of NN modeling dynamics. The FNN is augmented in the MPC control structure as the plant model leads to NN-MPC.

The performance of the proposed MPC structure under different model uncertainties has been investigated. It was found that closed-loop performance and stability of the

proposed NN-MPC depend on setting prediction and control horizons. It is desirable to minimize the performance objective determined by the cost functional using long horizons. However, from computational point of view using short horizons is preferred. The shorter the horizon, the less costly the solution of the on-line optimization problem. MPC shows good performance in terms of both regulatory (disturb rejection) and servo (set point tracking) control actions. The multivariable nonlinear nature of the proposed NN-MPC makes it a good candidate to replace the existing conventional single loop PID linear controllers. However, real-time implementation of NN-MPC is feasible if the computational load is manageable without sacrificing stability and performance.

6.2 Recommendations:

Based on the results of the sensitivity analysis conducted on steady state and dynamic models of amine sweetening unit, the control parameters were prioritized as per their speed of response on sweet gas specifications. Maintaining H_2S , on fast-track basis, could be achieved by increasing steam flow rate into regeneration reboiler. On the other side, increasing DEA solution flow rate would be preferred over increasing DEA solution temperature or reboiler duty because of its fast response. This selection offers a zero-investment choice for ADGAS in marinating plant throughput across their facilities at a fixed rate.

The main problem with the NN-MPC controller is its long computational time and thus it is difficult to implement in real time. Therefore the real time application of the NN-MPC should be the future research topic. Advancements in computer technology and future

development of fast and efficient numerical solution methods will enable real-time implementation of MPC on large scale plants.

REFERENCES

1. Albus, J.S., "A New Approach to Manipulator Control: Cerebellar Model Articulation Control (CMAC)." *Trans. ASME, Journal of Dynamics. System and Control*, Vol.97, 1975. pp 220-227
2. Bishop, C.M., *Neural Networks for Pattern Recognition*. Clarendon, 1995
3. C.A. Ruiz, M.S. Basualdo, N.J. Scenna, Reactive distillation Dynamic simulation, *Trans. Inst. Chem. Eng. A* 73 (1995) 363_ 378
4. Chen, S. and Billings. S. A., "Neural Networks for Non-linear Dynamic System Modeling and Identification." *International Journal of Control*, Vol. 56, 1992, pp 319-346
5. Chen, S. and Billings. S. A., "Neural Networks for Non-linear Dynamic System Modeling and Identification." *International Journal of Control*, Vol. 56, 1990, pp 1191-1214
6. Cutler, C.R. and Ramaker, B.C., "Dynamic Matrix Control-a computer control algorithm ". *Automatic Control* ('Onference, San Fransisco, 1980)
7. Draeger, A, Engell, S. and Ranke, H., "Model Predictive Control Using Neural Networks." *IEEE Control Systems Magazine*, Vol. 15, No.5, Oct., 1995, pp 61-66
8. Elliot, D.L., *Neural Systems for Control*, Academic Press, San Diego, 1997
9. E.E.Meadow and J.B.Rawlings, "Model Predictive Control,"*In Nonlinear Process Control*, M. Henson and D. Seborg> Englewood Cliffs, NJ; Prentice-Hall, 1997, pp 233-310
10. E.Y. Kenig, R. Schneider, A. Go'rak, Rigorous dynamic modeling Of complex reactive absorption processes, *Chem. Eng. Sci.* 54 (1999) 5195_ 5203.
11. Fang, G. and Dissanayke, M.W.M.G., "A Neural Network-based Method for Time-optimal Trajectory Planning." *Robotica*, Vol. 16, Part 2, 1998, pp 143-158
12. F. Allgower, T.A. Badgwell, J. S. Qin, J. B. Rawlings, and S. J. Wright. Nonlinear predictive control and moving horizon estimation-An introductory overview. In P.

- M. Frank, editor, *Advances in Control, Highlights of ECC'99*, pages 391-449, Springer, 1999
13. Garcia, C.E., Prett, D.M, and Morai, "Model Predictive Control: Theory and Practice-a survey", *Automatica*, Vol.25, No.3, 1989, pp 335-348
 14. Gurney, K., *An Introduction to Neural Networks*, UCL Press, London, 1997
 15. Hassoun, M.H., *Fundamentals of Artificial Neural Networks*, MIT Press, 1995
 16. Hopfield. J.J., "Neural Networks and Physical Systems with Emergent Collective Computational Abilities ", *Proceedings of the National Academy of Sciences*, Vol. 79, 1982, pp 2554-2558
 17. Hornik, K., Strinchcombe, M. and White, H., " Multilayer Feedforward Networks Are Universal Approximators." *Neural Networks*, Vol.2, 1989. pp 359-366
 18. Hornik, K., Strinchcombe, M. and White, H., "Multilayer Feedforward Networks Are Universal Approximators." *Neural Networks*, Vol. 2, 1989, pp 359-366
 19. Hoskins J. C. and D. M. Himmelblau, Artificial neural network models of knowledge representation in chemical engineering. *Computers Chem. Engineering* 55(1993)
 20. Hunt, KJ, and Sbarbaro, D., " Neural Networks for Non-linear Internal Model Control", *Proc. IEEE*, pt.D, Vol. 138, 1991, pp 431-438
 21. Jordan, M.I., "Attractor Dynamics and Parallelism in a Connectionist Sequential Machines." *Proceedings of the 8th Annual Conference of the Cognitive Science Society*, 1986, pp 531-456
 22. Joseph, B., Jang. S. and Mukai, H., "Integrated Model Based Control of Multivariable Non-linear Systems." *Proc. IFAC Workshop on Process Model Based Control*, Atlanta. 1998
 23. L. Biegler. Efficient solution of dynamic optimization and NMPC problems. In F. Allgower and A. Zheng, editors, *Nonlinear Predictive Control*, pages 219-244, Birkhauser, 2000
 24. MacKenzie et al., 1987

25. Omidvar, O., *Neural Systems for Robotics*, Academic Press, San Diego, 1997
26. Psaltis, D., Sideris, A., and Yamamura, Y.Y., “A multilayered Neural Network Controller”. *IEEE Control System Magazine*, 8, 1998, pp. 17-21
27. Richalet, J. Raault, Testud, J.L., and Papon, J., “Model Predictive Heuristic Control: Application to Industry Processes”. *Automatica*, Vol. 14, No.2, 1978, pp 413-428
28. R. Findeisen, F. Allgower, M. Diehl, H. G. Bock, J. P. Schlöder, and Z. Nagy. Efficient nonlinear model predictive control. In 6th International Conference on Chemical Process Control-CPC VI, pages 454-460, 2000
29. R. R. Bitmead, M. Gevers, and V. Wertz, 1990
30. R. Schneider, A. Go' rak, Model optimization for the dynamic Simulation of reactive absorption processes, *Chem. Eng. Technology* 24 (2001) 979_ 989.
31. R. Schneider, E.Y. Kenig, A. Go' rak, Dynamic modelling of Reactive absorption with the Maxwell_ Stefan Approach, *Trans Inst. Chem. Eng. A* 77 (1999) 633_ 638
32. R. Taylor, R. Krishna, Modelling reactive distillation, *Chem. Eng. Sci.* 55 (2000) 5183_ 5229
33. Rumelhart, D. and McClelland, J., *Parallel Distributed Processing Exploitations in the Micro-structure of Cognition*, Volume 1 and 2, Cambridge. MIT Press, 1986
34. R. Vas Bhat, 1998, W. P. M. Van Swaaij and G. F. Versteeg, 1992
35. S. J. Qin and T. A. Badgwell, An overview of industrial model predictive control technology, in *Chemical Process Control-AICHE Symposium Series*, J. Kantor, C. Garela, and B. Carnahan, Eds. New York; AICHE, 1997, pp, 232-256
36. Su, H.T., McAvoy, T.J., “Applications of Neural Network Long-range Predictive Models for Non-linear Model Predictive Control.” *Journal of Process Control*, 1993

37. Suykens, J.A.K., Vandewalle, J.P.L. and De Moor, B.L.R., *Artificial Neural Networks for Modeling and Control of Non-linear Systems*. Kluwer Academic Publishers. 1996

38. S. Valerio, M. Vanni, Interfacial mass transfer and chemical Reaction in non-ideal multicomponent systems, *Chem. Eng. Sci.* 49 (1994) 3297_ 3305.

39. Wenzhi Gao and Rastko R. Selmic, Neural Network Control of a Class of a Non-linear Systems With Actuator Saturation, *IEEE Transactions on Neural networks* (2003)
40. Werbor; Parker; Rumelhart, Hinton and Williams. *Parallel Distributed Processing Exploitations in the Micro-structure of Cognition*, Volume 1, MIT Press, 1986

41. Werbos, P.J., “Generalization of Back-propagation with application to a Recurrent Gas Market Model”, *Neural Networks*, 1998. Vol. 1, pp 339-356

42. Wide, P.D., *Neural Network Models: Theory and Projects*, Springer-Verlag, New York, 1997

43. W.J. DeCoursey, Enhancement factors for gas absorption with reversible reaction, *Chem. Eng. Sci.* 37 (1982) 1483_ 1489.

44. Z. Nagy, R. Findeisen, M. Diehl, F. Allgower, H. G. Bock, S. Agachi, J. P. Schloder, and D. Leineweber, Real-time feasibility of nonlinear predictive control for large scale processes- a case study. In *Proc. Amer. Contr. Conf.*, pages 4249-4254, Chicago, 2000. ACC.

APPENDICES

MATLAB Code for FNN Modeling

```
clc
clear
% Load data
data=dlmread('test1.txt');
X1=data(:,1); X2=data(:,2);X3=data(:,3);
X4=data(:,4);X5=data(:,5);X6=data(:,6);
Y1=data(:,7);
X1=[X1 X2 X3 X4 X5 X6]; Y1=[Y1];
[sample,c]=size(X1');
% Prepare Inputs and Targets
abc=sortrows([X1 X2 X3 X4 X5 X6 Y1 ],2);
p=abc(:,1:6)';
t=abc(:,7)';
%Normalizing data

[pn,minp,maxp,tn,mint,maxt] = premnmx(p,t);
%pn=p; tn=t;
%Principal compoent analysis
[R,Q] = size(pn)
n=1:1:Q;
% Divide data into Training, Validation and Testing sets
iitr = 1:1:Q;
iitst= 1:2:Q;
iiival= 1:2:Q;

ptr = pn(:,iitr); ttr = tn(:,iitr);
val.P = pn(:,iiival); val.T = tn(:,iiival);
test.P = pn(:,iitst); test.T = tn(:,iitst);

% Create the feedforward Network
Net=newff(minmax(ptr),[1 40 1],{ 'tansig' 'tansig' 'purelin'},
'trainbr');

% Set training parameters
Net.trainParam.epochs=1500;           % Maximum number of epochs
Net.trainParam.show=50;               % Period of showing calculation
progress
Net.trainParam.lr=0.1;                % Algorithm learning rate
Net.trainParam.goal=1e-10;            % Optimisation goal
Net.trainParam.min_grad=1e-10;        % Minimum gradient
Net.trainParam.mem_reduc=1;           % Memory reduction parameter
Net.trainParam.max_fail=550;
Net.performFcn = 'msereg';
Net.performParam.ratio = 0.5;
```

```

% Train the network
time0 = cputime;
[Net,tr]=train(Net,ptr,ttr,[],[], val,test);
time = cputime-time0;
[str,errmsg] = sprintf('The CPU time = %d sec',time); disp(str);

% Plot errors
figure(1)
plot(tr.epoch,tr.perf,tr.epoch,tr.vperf,tr.epoch,tr.tperf)
legend('Training','Validation','Test',-1);
ylabel('Squared Error'); xlabel('Epoch')

% Simulate the network
an = sim(Net,pn);

% Un-normalize the data
a = postmnmx(an,mint,maxt);

figure(2)
plot(n,a,n,t,'+')

% Perform a linear regression between the network outputs
(unnormalized) and the targets
% to check the quality of the network training.
for i=1:l
figure(i+2)
[m(i),b(i),r(i)] = postreg(a(i,:),t(i,:));
end

```


VITA

The author, Jasim Mohamed AL Hammadi, was born in Dubai, United Arab Emirates in November 20th, 1977. He got his high school diploma in 1995 from emirate of Sharjah. After being awarded with a scholarship from ADNOC, he received his bachelor degree in Chemical Engineering in December, 1999 from University of Tulsa in United States of America. He joined Abu Dhabi Gas Liquefaction Company (ADGAS) in April, 2000 as a process engineer. In May 2001, he was attached to the Projects Division in ADGAS as a project coordinator based in Japan for one year.

The author issued a paper on Environmental Effect of Sulfur Recovery in the gas processing symposium held in Qatar in 2004. In addition, he participated in the second Mechatronics symposium held in April, 2005 at the American University of Sharjah by presenting a paper on Modeling and Control of Amine Sweetening Units. He joined the Mechatronics program in the American University of Sharjah in Feb, 2003 as a part time student and received Master of Science degree in Mechatronics in June, 2005